INFORMATION TO USERS

This manuscript has been reproduced from the microfilm master. UMI films the text directly from the original or copy submitted. Thus, some thesis and dissertation copies are in typewriter face, while others may be from any type of computer printer.

The quality of this reproduction is dependent upon the quality of the copy submitted. Broken or indistinct print, colored or poor quality illustrations and photographs, print bleedthrough, substandard margins, and improper alignment can adversely affect reproduction.

In the unlikely event that the author did not send UMI a complete manuscript and there are missing pages, these will be noted. Also, if unauthorized copyright material had to be removed, a note will indicate the deletion.

Oversize materials (e.g., maps, drawings, charts) are reproduced by sectioning the original, beginning at the upper left-hand corner and continuing from left to right in equal sections with small overlaps.

ProQuest Information and Learning
300 North Zeeb Road, Ann Arbor, MI 48106-1346 USA
800-521-0600

The Effect of Varying the Sieve Tray Perforation Size on Liquid-Phase Controlled Absorption

by

Harry A. Laudie

A thesis submitted in partial fulfillment

of the requirements for the degree of

Master of Applied Science

in the

DEPARTMENT OF CHEMICAL ENGINEERING

UNIVERSITY OF OTTAWA

Ottawa, Canada March, 1969

Research Director

Candidate

ABSTRACT

A pilot plant sieve plate absorption column was used to study the effect of varying the perforation size in liquid phase controlled absorption. Four separate test trays were utilized which had hole diameters of 0.125, 0.250, 0.500, and 1.000 inches but which, at the same time had equal total gas flow areas. The gas-liquid systems used were carbon dioxide with water and carbon dioxide with aqueous glycol solution. Test runs were performed at 77°F. and at a pressure of approximately 830 mm. of mercury. Liquid flow rates ranged from 0.1 to 4.0 gpm. while gas flow rates ranged from 0.0 to 1.0 cu. ft./sec.. Experiments included the measurement of dry plate pressure drops, wet plate pressure drops, clear liquid depths and froth heights, the determination of Murphree liquid efficiencies, and also the determination of concentration profiles within the liquid froth for carbon dioxide and water.

The Murphree liquid efficiencies were found to be almost independent of the hole diameter, and unexpectedly almost independent of liquid flow rates and also of gas flow rates. That is, the Murphree liquid efficiency was found to be approximately constant (70-90 percent). Murphree liquid efficiencies were found to be dependent on liquid viscosity and solute gas diffusivity. The wet plate pressure drops and depths of clear liquid were both found to be almost independent of hole diameter. The froth heights were found to be somewhat dependent on the hole diameter, smaller holes yielding greater froth heights. The concentration profiles showed that the major

concentration gradient of the liquid in the froth occurred in the region below the weir height. From the results obtained by the integration of the concentration profiles, it was concluded that the mixing of the liquid on the tray could be adequately described by the "plug flow" mixing model.

TABLE OF CONTENTS

LIST OF FIGURES

LIST OF TABLES

ACKNOWLEDGEMENTS

The author wishes to thank Dr. W. Hayduk for his advice and guidance throughout the course of this project. The author is also indebted to Mr. G. Gasperetti and Mr. B. Kelly for constructing the equipment, Mr. J. Auns and Mr. B. Dick for photographic services, and the National Research Council of Canada for financial aid.

NOMENCLATURE

A_c	Cross sectional area of column	sq. ft.
A_f	Free area, percent hole area to tray area	sq. ft.
C	Orifice plate coefficient	-
D_h	Hole diameter	inches
E_L	Point efficiency	-
E_{ML}	Murphree liquid efficiency	-
F	F-factor, $F = V_c \sqrt{G}$	ft./sec.$(lb./cu.ft.)^{\frac{1}{2}}$
L	Liquid flow rate	gpm.
	Liquid flow velocity in equations 29-36	ft./hr.
L'	Liquid flow rate	lb.moles/(hr.sq.ft.)
	Liquid flow rate in equation 28	lbs./(hr.sq.ft.)
N_L	Number of point liquid phase transfer units	-
N_{tL}	Number of liquid phase mass transfer units	-
P	Pitch, centre to centre distance between holes	inches
Q	Gas flow rate at column conditions	cu. ft./hr.
S	Tray spacing	inches
T	Plate thickness	inches
V_c	Superficial gas velocity	ft./sec.
V_h	Average gas velocity through perforations	ft./sec.
W	Weir height	inches
Z	Average distance across tray	inches
a	Interfacial area	sq.ft./cu.ft.
	Constant in equation 14	-
b	Constant in equation 15	-

c	Concentration of gas in liquid	gm.moles/litre
	Constant in equation 23	-
c_{in}	Inlet concentration of gas in liquid	gm.moles/litre
c_{out}	Outlet concentration of gas in liquid	gm.moles/litre
c^*	Equilibrium concentration of gas	gm.moles/litre
d	Average liquid flow path width	inches
	Constant in equation 23	-
e	Entrainment	lbs.liquid/lbs.gas
	Constant in equation 23	-
f	Fanning friction factor, equation 18	-
g	Acceleration due to gravity	ft./sq.sec.
h	Vertical distance from tray floor	inches
h_c	Equivalent clear liquid depth	inches of water
h'_c	Pressure drop in equation 16	inches of water
h_D	Dry plate pressure drop	inches of water
h'_e	Pressure drop in equation 17	inches of water
h_f	Froth height	inches
h'_f	Pressure drop in equation 18	inches of water
h_L	Length of a transfer unit	1/inches
h_R	Residual pressure drop	inches of water
h_w	Wet plate pressure drop	inches of water
k_L	Liquid phase mass transfer coefficient	ft./hr.
k'_L	Liquid phase mass transfer coefficient	lb./(hr.ft.^{2})
k_x	Liquid film coefficient	lb.moles/(hr.sq.ft.)
l	Average distance travelled by liquid	inches
v_l	Liquid velocity, equation 7	ft./sec.

x	Concentration of gas in liquid	mole fraction
	Cartesian co-ordinate	-
x^*	Equilibrium concentration of gas	mole fraction
y	Cartesian co-ordinate	-
z	Horizontal distance along the tray floor	inches
α	Conversion factor from lb.moles/cu.ft. to gm.moles/litre	
$\mathcal{D}$	Diffusivity of dissolved gas in liquid	sq.cm./sec.
μ	Viscosity of fluid	centipoises
σ	Surface tension of fluid	dynes/cm.
ρ	Density of fluid	lbs./cu.ft.
ρ_M	Density of fluid	lb.moles/cu.ft.

SUBSCRIPTS

c	clear, column
D	dry
f	froth, free
G	gas
h	hole
L	liquid
M	molar
w	wet

INTRODUCTION

Industrial equipment for performing countercurrent gas absorption or stripping can be classified as one of four types, spray towers, aerated-tank absorbers, packed towers, or plate towers. Although each has its own particular advantages, plate towers are commonly used because they are efficient and can be operated over a wide range of conditions. Intimate mixing is obtained when gas is forced through holes or slots into a shallow pool of liquid. A large part of the interphase transfer occurs as the gas bubbles are formed and as they rise through the agitated liquid. Additional transfer takes place above the liquid surface, when the spray and froth are thrown up by the gas as it passes through the liquid (1). There are several tray designs, each with its own devices for gas dispersion, such as the bubble caps, slots, valves, or simply perforations. The simplest in design is the sieve tray.

In recent years, there has been an increased interest in sieve trays for gas-liquid contacting because of their advantages when compared with competitive trays. When compared with bubble cap trays, sieve trays have a lower initial cost because they are easier and cheaper to manufacture (2,3,4), have higher vapour throughputs (4), a lower gas pressure drop (3,5), a lower liquid hydraulic resistance (3,4,5) and produce a lower liquid entrainment (4). Moreover, sieve trays seem to give a higher rate of mass transfer (6,7) and an efficiency equal to or greater than that of bubble cap trays (3,4,8). Sieve trays have been thought to suffer from a limited operating range(9,10) but

this has been largely disproved (6,11,12). Depending on the hole size, they can be sensititive to corrosion and plugging (4) and they require exact horizontal alignment to prevent large liquid hydraulic gradients, especially in towers of large diameter.

Trays are installed horizontally one above the other in a column and are separated by some optimum distance usually depending on the construction and maintenance requirements. For a non-foaming system this is typically 18 to 24 inches (4,13,14). A non-foaming system is one in which the froth formed is not dependent on the liquid properties but only exists as a result of the gas flow. Sieve trays have been designed without downcomers (15). With downcomerless trays the liquid as well as the gas pass through the same perforations (but in opposite directions) and the liquid holdup on the trays is usually small. More often liquid is conducted from one tray to the tray below by means of a downcomer. Large columns usually have segmental downcomers, but small columns frequently use a pipe passing through the plate as a downcomer. Gas-liquid disengagement is sometimes considered to be poor in circular downcomers (16) but this depends to a large extent on the cross-sectional area. To increase the liquid holdup in a downcomer-plate arrangement a weir is constructed to keep a required minimum depth of liquid on the tray.

This research project was undertaken to determine first what effect large diameter holes had on the pressure drop and efficiency of sieve tray absorbers. In addition concentration profiles were obtained in an attempt to clarify the mechanism of

absorption. Finally experiments were performed to determine the effect of using a viscous solvent in which the diffusivity of the dissolved gas was inherently low.

The absorption column was of pilot plant size utilizing circular plates because of its similarity to industrial columns and the ease of construction. A pipe downcomer was chosen because of its simple construction. To eliminate some of the column mechanical effects on efficiencies, the weir height, tray spacing, free area, downcomer area, and tray thickness were kept constant for all the absorption experiments.

Most published absorption results were obtained with sieve trays having small hole sizes, in the range of 1/16 to 1/4 inches in diameter. For their hole sizes the efficiencies were similar. The authors then postulated (without verification) that larger hole sizes should result in decreased efficiencies because larger holes might be expected to result in a lower interfacial area (2,3,17,18,19). A few authors (20,21,22) recommended large holes, in the range of 1/2 to 1.0 inch in diameter, but did not give any supporting experimental data. The prime advantage of large hole sizes might be expected in fouling services. For a constant fouling rate, the period of time before some particular fraction of the hole area became fouled would be directly proportional to the hole size.

The absorption system studied, carbon dioxide and water, was chosen for several reasons. Because it has been used often, a comparison of results was possible. The equilibrium solubilities were readily available (23,24), and the physical

properties of the dilute aqueous solutions of carbon dioxide could be considered to be the same as for pure water. Pure carbon dioxide was used so that gas phase resistances were eliminated thereby insuring that the resistance to mass transfer lay entirely in the liquid phase. The concentration of carbon dioxide in water could be easily determined by titration. The aqueous solution was acidic but only mildly corrosive, non-foaming and non-toxic. To show the combined effect of viscosity and diffusivity on efficiency, experiments were also performed using carbon dioxide and an aqueous solution of ethylene glycol. All experiments were performed at 77°F. and a pressure of approximately 830 mm. of mercury.

Murphree liquid phase efficiencies were calculated. Gas flow rates ranged from 0.0 to 1.0 cu. ft./sec.. Absorption experiments were conducted with liquid flow rates of 0.1, 0.2, 0.5, 1.0, 2.0, and 4.0 gpm. for each of the four trays having respectively hole sizes of 0.125, 0.250, 0.500, and 1.000 inches in diameter. For the aqueous glycol experiments, carbon dioxide flow rates ranged from 0.0 to 1.0 cu. ft./sec., liquid flow rates were 0.5, 1.0, and 2.0 gpm., and the tray hole size was 0.250 inches in diameter. Values for dry plate pressure drop, wet plate pressure drop, equivalent clear liquid depths, and froth heights were measured. Point concentrations of carbon dioxide in the liquid were measured for water and also for the aqueous glycol solvent using the tray having 0.250-inch diameter holes. Based on the point or local concentrations, a mixing model was proposed. Finally, emperical correlations for the

Murphree liquid efficiency, the wet plate pressure drop, the clear liquid depth, and the froth height were attempted.

THEORY AND LITERATURE REVIEW

A. Absorption Theory and Definitions

Gas absorption is a unit operation in which a gas is contacted with a liquid for the purpose of preferentially dissolving one or more components of the gas. When a slightly soluble gas dissolves in a pure liquid, most of the resistance to mass transfer lies in the liquid, and the system is said to be liquid phase controlled. Although derived for packed columns the transfer unit concept can be applied to trays. If the gas bubbles rise at a nearly uniform rate through the froth, then the mass transfer coefficient and interfacial area per unit volume of froth would be of the same order of magnitude throughout. If it is also assumed that the liquid moves across the tray at essentially a constant velocity regardless of the height above the tray surface, the rate of mass transfer would depend only on the concentration driving force.

A component balance on a vertical element of fluid, dz in thickness, results in the differential equation:

$$d(xL') = k_x a(x^*-x)dz \tag{1}$$

If L' is assumed constant across the tray

$$L'(dx) = k_x a(x^*-x)dz \tag{2}$$

This can be integrated to give the number of transfer units

$$N_{tL} = \int \frac{dx}{x^*-x} = \int \frac{k_x a}{L'} dz \tag{3}$$

For dilute solutions it can be assumed that

$$c = x\rho_M \alpha \tag{4}$$

Hence, substituting equation 4 into equation 3

$$N_{tL} = \int \frac{dc}{c^*-c} = \int \frac{k_L a}{v_l} dz \qquad (5)$$

If at the inlet of the tray, z=0, the gas concentration in the liquid is c_{in}, and at the outlet of the tray, z=Z, the gas concentration in the liquid is c_{out}, then:

$$N_{tL} = \int_{c_{in}}^{c_{out}} \frac{dc}{c^*-c} = \frac{k_L a Z}{v_l} \qquad (6)$$

The average width of the liquid flow path, d, on a circular tray can be considered as the width of a rectangle which has a length equal to the tray diameter and an area equal to the cross-sectional area of the tray (10). If h_c is the equivalent clear liquid depth, then

$$v_l = \frac{0.321\ L}{d\ h_c} \qquad (7)$$

The numerical constant has the units of ft. sq. in./gpm. sec.. It was found experimentally that the largest concentration gradient existed in the liquid which was below the weir height. If it is considered that the weir height is the characteristic dimension in equation 6, then

$$N_{tL} = \frac{k_L a W}{v_L} \qquad (8)$$

If the equilibrium concentration is constant across the tray, and the mixing occurs only in the direction perpendicular to the liquid flow, equation 6 can be integrated to give

$$N_{tL} = -\ln\left(1-\frac{c_{out}-c_{in}}{c^*-c_{in}}\right) \qquad (9)$$

The Murphree liquid efficiency is

$$E_{ML} = \frac{c_{out}-c_{in}}{c^*-c_{in}} \tag{10}$$

Combining equations 8,9, and 10; the relationship between the Murphree liquid efficiency and the mass transfer coefficient is

$$E_{ML} = 1.0 - \exp\left(\frac{k_L a\, W}{v_l}\right) \tag{11}$$

In an analogous manner to that for packed absorption columns, Sherwood and Pigford (1) have defined a length of a transfer unit for tray columns. It is defined as

$$h_L = \frac{l}{N_{tL}} \tag{12}$$

The parameter l is the average distance travelled by the liquid.

B. Sieve Tray Efficiencies

To describe the effectiveness of contacting in liquid phase controlled absorption processes, a Murphree liquid efficiency is defined as the ratio of actual change in a liquid concentration to the change which would have occurred if the liquid was in equilibrium with the gas. These efficiencies are functions of the structural parameters of the column and the physical properties of the fluids. A high liquid residence time on the tray is usually considered to result in efficient contacting for liquid phase controlled systems (3). An increase in weir height (13,25,26), length of liquid flow path (25), or tray width (27) would tend to increase the tray efficiencies since the liquid residence time would be increased. The percent free area of a sieve tray is defined as the percentage ratio of

hole area to tray area. A large free area should be conducive to high efficiencies (22) because more bubbles can be formed enabling, even at low gas velocity, an increase in the contacting time between gas and liquid. The optimal free area should be between 5 and 15 percent of the total tray area (4). Efficiencies tend to decrease for trays having excessively large free areas because of weeping (28).

With small holes the degree of mixing and interfacial area in the froth might be expected to be greater than that obtainable with large holes and consequently one might predict that smaller holes would give a higher efficiency. Experiments reported in the literature were performed with small-holed sieve trays. Ellis and Moyade (2) desorbed oxygen from an aqueous solvent using air in a column equipped with plates having hole sizes of 1/8, 3/16, and 1/4 inches in diameter. Umholtz and Van Winkle (26) performed hydrocarbon distillations with plates having hole sizes of 1/16, 1/8, 5/32, and 3/16 inches in diameter. Van Winkle (25) absorbed methyl alcohol vapour into water and used hole diameters of 1/8 to 1/4 inches. Calderbank Evans and Rennie (29) and Hellums (19) observed the effect of small-holed sieve plates on binary distillation systems. Hay and Johnson (18) experimented with methanol-water distillation with plates having hole sizes of 1/8, 3/16, and 1/4 inches in diameter. These authors verified that hole diameter had no appreciable effect on efficiency for hole sizes within the ranges they studied.

It has been concluded that efficiency decreases with an increasing liquid flow rate (3,13,28) because of the decreased

contacting time of liquid and gas. When the gas flow rate was increased the degree of mixing and interfacial area were increased. On the other hand, the contact time between gas and liquid was decreased. The two effects would tend to cancel one another so that there was little effect of gas flow rate on efficiency except in the weeping region (4,26,30).

Studies of the effect of liquid physical properties have been scarce. Efficiencies have been found to decrease with an increase in liquid viscosity (13,31) or a decrease in solute diffusivity (13,29,32). Highly viscous liquids were reported to form froths having a lower interfacial area. Low solute diffusivities reduced the rate of mass transfer.

Experiments in which carbon dioxide was desorbed from water using air, in laboratory tray columns, have been reported to have low efficiencies (28,33,34). Low efficiencies were also reported in experiments in which carbon dioxide was selectively absorbed from air and carbon dioxide mixtures (6,35,36). When pure carbon dioxide was absorbed by water, however, efficiencies in excess of 70% were obtained. It appeared possible that in the former experiments a significant gas phase resistance reduced the overall tray efficiency in spite of the authors' claims to the contrary. West Gilbert and Shimiza (31), Eden and Pigford (37), and Walter and Sherwood (30) noted that with trays designed for low liquid flow rates (less than 2.0 gpm.) for a pure carbon dioxide and water system, the water was almost saturated in all cases and the efficiencies were very high.

C. Dry and Wet Plate Hydraulics

It is convenient to use the diagram shown in Figure 1 for defining the equipment and operating variables.

Gas flow through a dry plate is similar to flow through an orifice. There are expansion, contraction, and friction losses which result in a permanent pressure loss. Because of their simplicity, dry plate pressure drop relationships are highly developed. In an analogy to flow through an orifice, some authors (38,39) have correlated their data using the simple orifice equation

$$h_D = cV_c^2 \tag{13}$$

Others (11,20) have assumed a simple equation

$$h_D = cV_c^a \tag{14}$$

The constant a is approximately 1.8. Some authors (3,26,35) have used the F-factor in their correlations to obtain

$$h_D = cF^b \tag{15}$$

Here b is approximately 2.0 and c is an emperical constant.

McAllister (5) derived a theoritical correlation for dry plate pressure drops involving pressure losses. The contraction, expansion, and friction losses, respectively, can be expressed as

$$h_c' = 0.4\left(1.25 - \frac{A_h}{A_c}\right)\frac{V_h^2}{2g} \tag{16}$$

$$h_e' = \left(1.0 - \frac{A_h}{A_c}\right)^2 \frac{V_h^2}{2g} \tag{17}$$

$$h_f' = \frac{4fTV_h^2}{2gD_h} \tag{18}$$

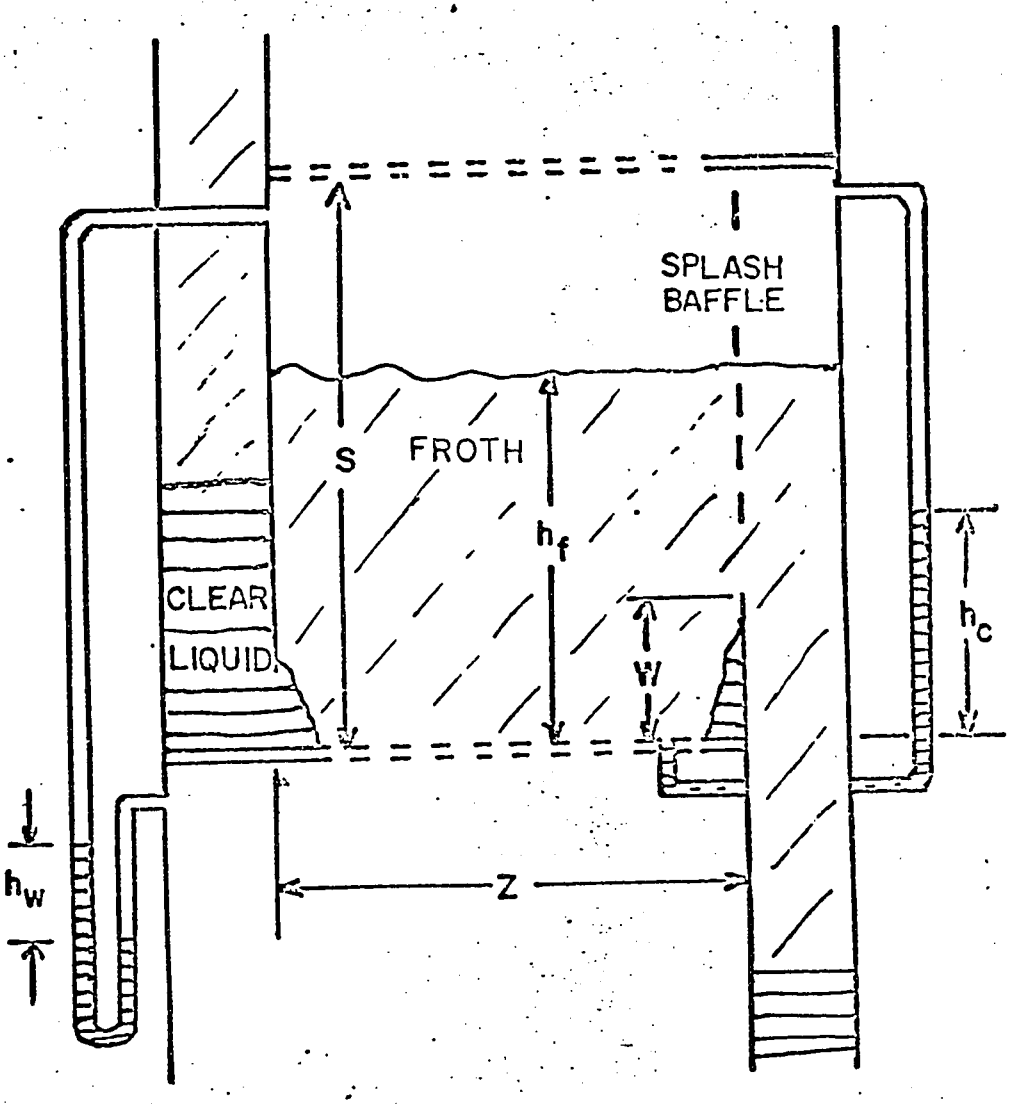

Figure 1. Schematic Diagram of Tray Dynamics

These can be combined to give

$$h_D = K\left[0.4\left(1.25-\frac{A_h}{A_c}\right) + 4f\left(\frac{T}{D_h}\right) + \left(1-\frac{A_h}{A_c}\right)^2\right]\frac{V_h^2}{2g} \qquad (19)$$

The coefficient K which accounts for hole interaction, is a function of hole diameter, D_h, and plate thickness, T. The coefficient has been correlated by a K versus T/D_h curve over an extremely wide range of conditions as shown in Figure 19. Recently Harada (40) and Sterbacek (38) have verified this equation experimentally and Madigan (41) has correlated the coefficient by

$$K = 1.09(D_h/T)^{0.25} \qquad (20)$$

for a range of T/D_h from 0.2 to 2.0.

There is a two-phase mixture of liquid and gas above an operating tray. This adds an extra hydraulic resistance to the gas flow. This extra pressure drop has been found experimentally to be equal to the equivalent clear liquid depth. The clear liquid depth is that which would occur if all the liquid in the froth collapsed and formed a pool of liquid. Although not as theoretically well developed as dry plate pressure drops, wet plate pressure drops show similar trends with respect to hole diameter. An increase in wet plate pressure drop occurs with an increase in gas flow rate (25,42), a decrease in free area (40), an increase in plate thickness (5) and tray length (25), an increase in liquid flow rate (35,43), and an increase in weir height (25.32) because these factors tended to increase the equivalent clear liquid depth, h_c. The most common wet plate pressure drop correlation (3,6,10,26,38) is

$$h_w = h_D + h_c + h_R \tag{21}$$

where h_R is the residual pressure drop as a result of bubble formation and is a function of the liquid surface tension. The residual pressure drop can be calculated (14,39,40) by

$$h_R = 0.06\, \sigma/\rho_L D_h \tag{22}$$

Wet plate pressure drops were found to be almost independent of liquid viscosity and density (16,44).

The clear liquid depth was measured by means of a side tube as shown in Figure 1. The gas blown through the holes causes the clear liquid to expand and form froth. Both the clear liquid depth and the froth height normally increase with an increasing liquid flow rate, with an increasing gas flow rate, and also an increasing weir height (18,35). Froth height is almost independent of hole diameter (2,18) but tends to diminish with increasing liquid density and viscosity (13,44). The clear liquid depth is a measure of the liquid residence time. Huang (4) recommended clear liquid depths between 2 and 4 inches as an optimum operating range. Correlations for clear liquid depths (6,17) are of the type

$$h_c = a + bF + cL + dW + eD_h \tag{23}$$

Similar correlations are used for the froth heights (17,35).

Entrainment is the carry-over of liquid from one tray to the tray above. Entrainment tends to lower the tray efficiency (11,45) and it can be estimated from nomograms (4,46) which relate the amount of entrainment to the column structural parameters.

Weeping is defined as the falling of liquid through the

sieve plate holes. It decreases efficiency because liquid by-passes the plate without contacting the gas. The weep point is defined as the minimum gas flow rate at which liquid is just prevented from draining through the tray perforations. Weeping tends to start at a lower gas flow rate when either the free area or hole diameter are decreased (10,40). It also tends to start at lower gas flow rates with solvents of higher surface tension (5). Correlations have been proposed to predict the point of incipient weeping (5,9,45).

D. Mixing Models and Concentration Profiles

Numerous mixing models have been used in an attempt to describe the mass transfer mechanism on sieve trays. The plug flow model (equation 9) has been used often (18,27,30,31,34) because of a lack of local concentration and liquid velocity data. Other models proposed have been complete mixing (36), partial mixing (47), liquid splashing (48), moving froth layer (40), chain bubbling (49), pool mixing (13), penetration theory (37), and eddy diffusion model (13,19,40). These models have been only partially successful in explaining the transfer mechanism.

In this research the concentration profiles were measured and a mixing model based on it is proposed. Consider the diagram of the n^{th} plate in a column as shown in Figure 2. The liquid enters at composition x_{n-1} and immediately after leaving the inlet downcomer the liquid rises vertically and reaches a composition x_i which is a function of position h. The liquid can be considered to flow in layers horizontally across the tray. Each liquid layer then travels horizontally across the tray and reaches

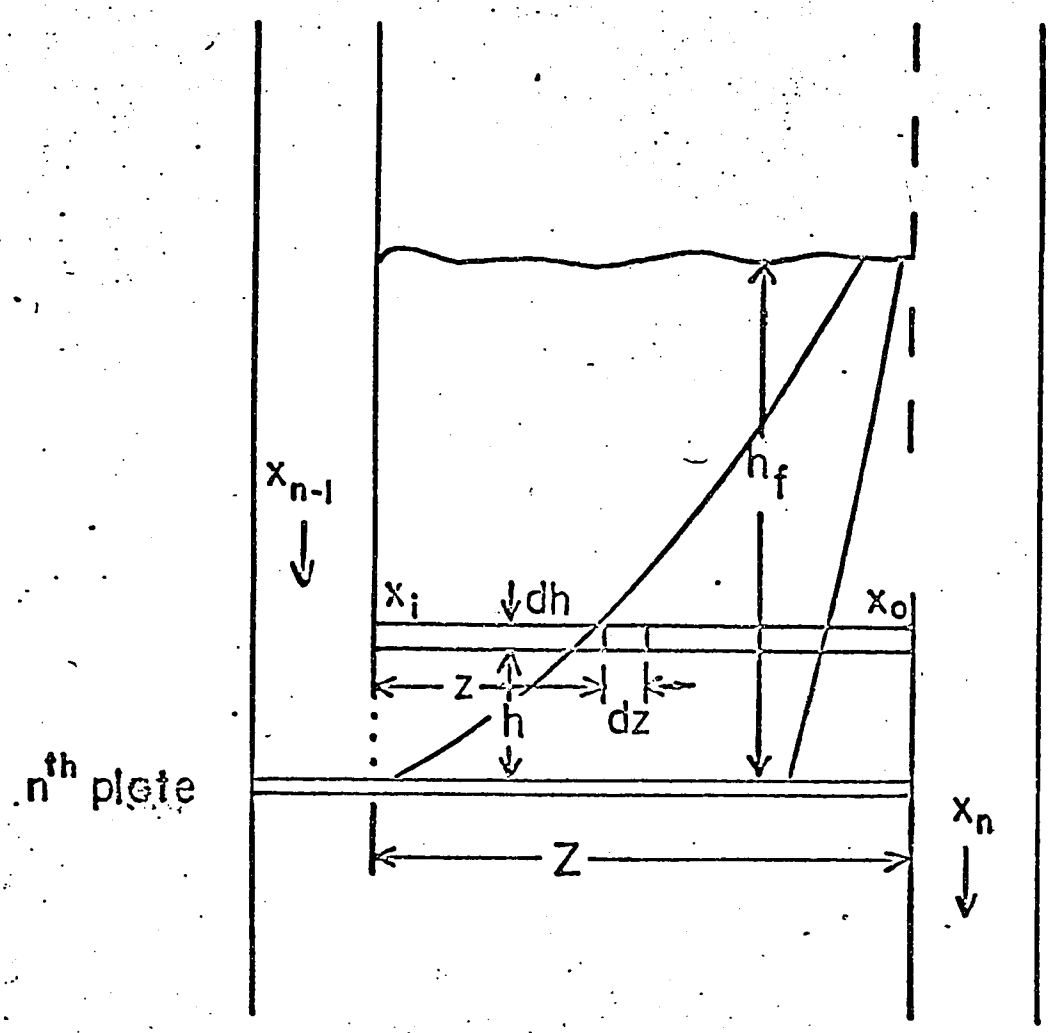

Figure 2. Theoretical Mixing Model

a composition x_o. Then the liquid layers near the outlet downcomer (each of which has a composition x_o based on position, h) combine and leave the tray having a composition x_n.

For uniform gas composition on the tray, then in the horizontal slab, the number of point liquid phase transfer units are given by

$$N_L = \int_{x_i}^{x_o} \frac{dx}{x^*-x} \tag{24}$$

which can be integrated and rearranged to give

$$x^*-x_i = (x^*-x_o)e^{N_L} \tag{25}$$

The point efficiency in the horizontal direction can be defined as

$$E_L = \frac{x_o-x_i}{x^*-x_i} \tag{26}$$

A combination of equations 25 and 26 yields

$$1-E_L = e^{-N_L} \tag{27}$$

From equation 6, N_L can be expressed as a function of the horizontal distance across the tray

$$N_L = \frac{k_L'a\ z}{L'} \tag{28}$$

A mass balance on an element of fluid near the inlet downcomer yields

$$Ldx = k_La(x^*-x)dh \tag{29}$$

This can be integrated in the vertical direction to obtain

$$\int_{x_{n-1}}^{x_i} \frac{dx}{x^*-x} = \frac{k_La}{L}\int_0^h dh \tag{30}$$

Assuming that $k_L'a/L'$ and k_La/L are not functions of position, equation 30 can be integrated to give upon rearranging

$$x^*-x_i = (x^*-x_{n-1})e^{-\frac{k_La}{L}h} \tag{31}$$

Equating and rearranging equations 25 and 31 one obtains

$$x_o = x^* - (x^*-x_{n-1})\exp(-N_L)\exp(-\frac{k_La}{L}h) \tag{32}$$

If one assumes that x_n is the average composition of a mixture from the tray floor to the froth height, then

$$x_n = \bar{x}_o = \frac{\int_0^{h_f} x_o\,dh}{\int_0^{h_f} dh} \tag{33}$$

Substituting equation 32 into 33 and integrating one obtains upon rearranging

$$\frac{x^*-x_n}{x^*-x_{n-1}} = e^{-N_L}\ \frac{L}{k_La\ h_f}\left[1 - \exp(-\frac{k_La}{L}h_f)\right] \tag{34}$$

The overall Murphree liquid efficiency is

$$E_{ML} = \frac{x_n-x_{n-1}}{x^*-x_{n-1}} \tag{35}$$

Combining equations 27, 34, and 35 yields

$$\frac{1-E_{ML}}{1-E_L} = \frac{L}{k_La\ h_f}\ \left[1 - \exp(-\frac{k_La}{L}\ h_f)\right] \tag{36}$$

Equation 36 is the relationship between Murphree liquid efficiency and point efficiency.

APPARATUS

The experimental equipment consisted of an absorption column, a stripper, storage tanks, a heat exchanger, and auxiliaries such as a pump, gas blower, and a vacuum pump. Liquid in the storage tanks was drawn up into the stripper by vacuum. The liquid then entered a circulation pump. Part of the liquid from the discharge of the pump was returned to the stripper. The remaining liquid was metered by one of two rotameters and was pumped to the inlet of the absorption column. The partially saturated liquid collected at the bottom of the column was returned to the storage tanks. The carbon dioxide was circulated by a gas blower. A process flow diagram is shown in Figure 3.

The absorption column consisted of three QVF glass sections, 18 inches in length and 6 inches in internal diameter. These were separated by brass sieve plates and secured by standard flanged fittings. Each plate was supported on either side by a brass ring 1/4-inch in thickness, 1/2-inch in width, and 6 inches in internal diameter. These rings were used for installing pressure taps and sampling tubes. Butyl rubber gaskets were installed on either side of each of the rings to provide a gas-tight seal. The ends of the column were 1/4-inch thick brass plates. Column details are shown in Figures 4 and 5.

Gas was introduced into the bottom of the column by means of a 2-inch diameter copper tube which was partially hooded to prevent liquid from entering the blower. At the top of the column the gas flowed through a 2-inch copper tube, and through a straight section of pipe approximately 50 pipe diameters in

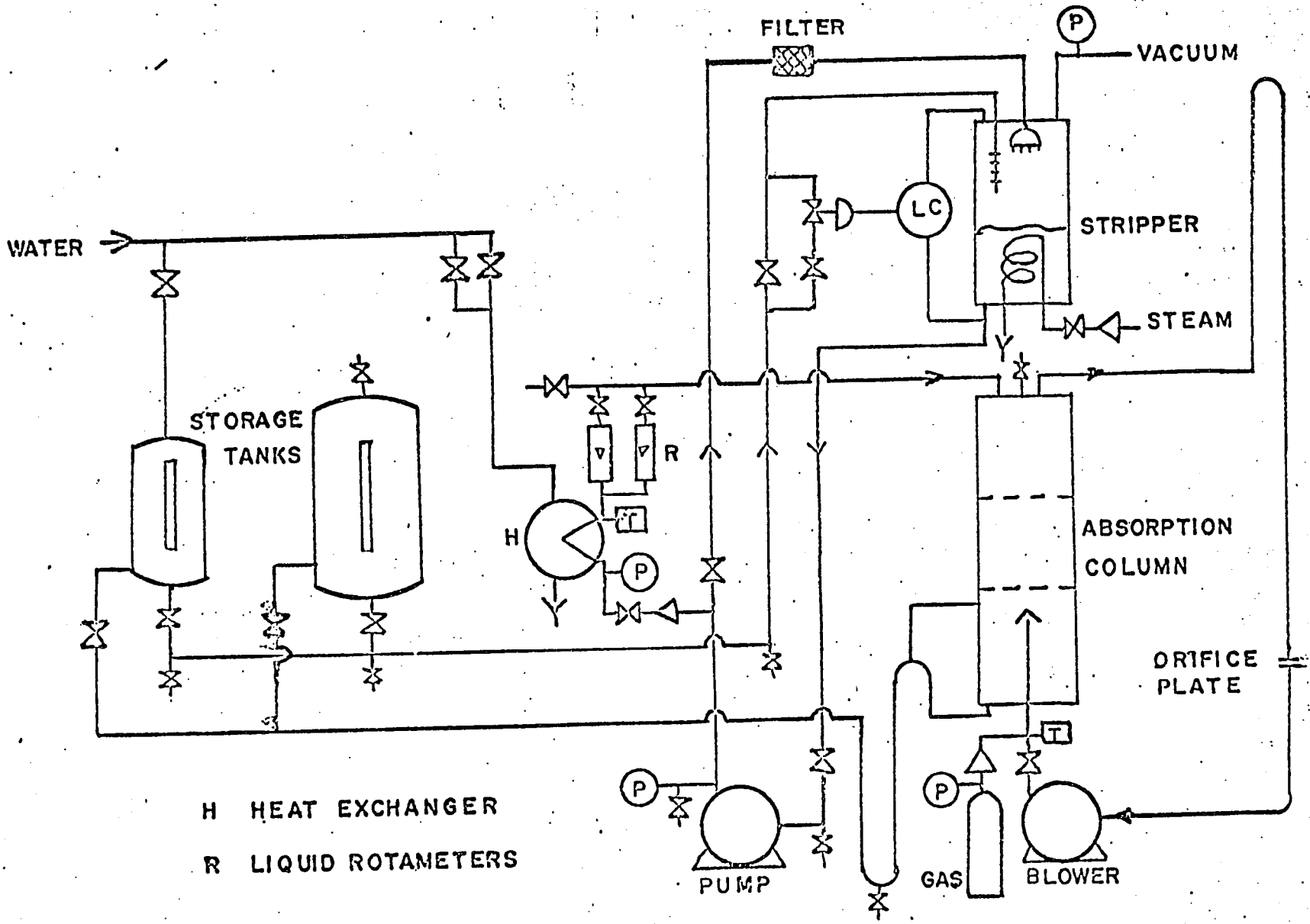

Figure 3. Process Flow Diagram of Experimental Equipment

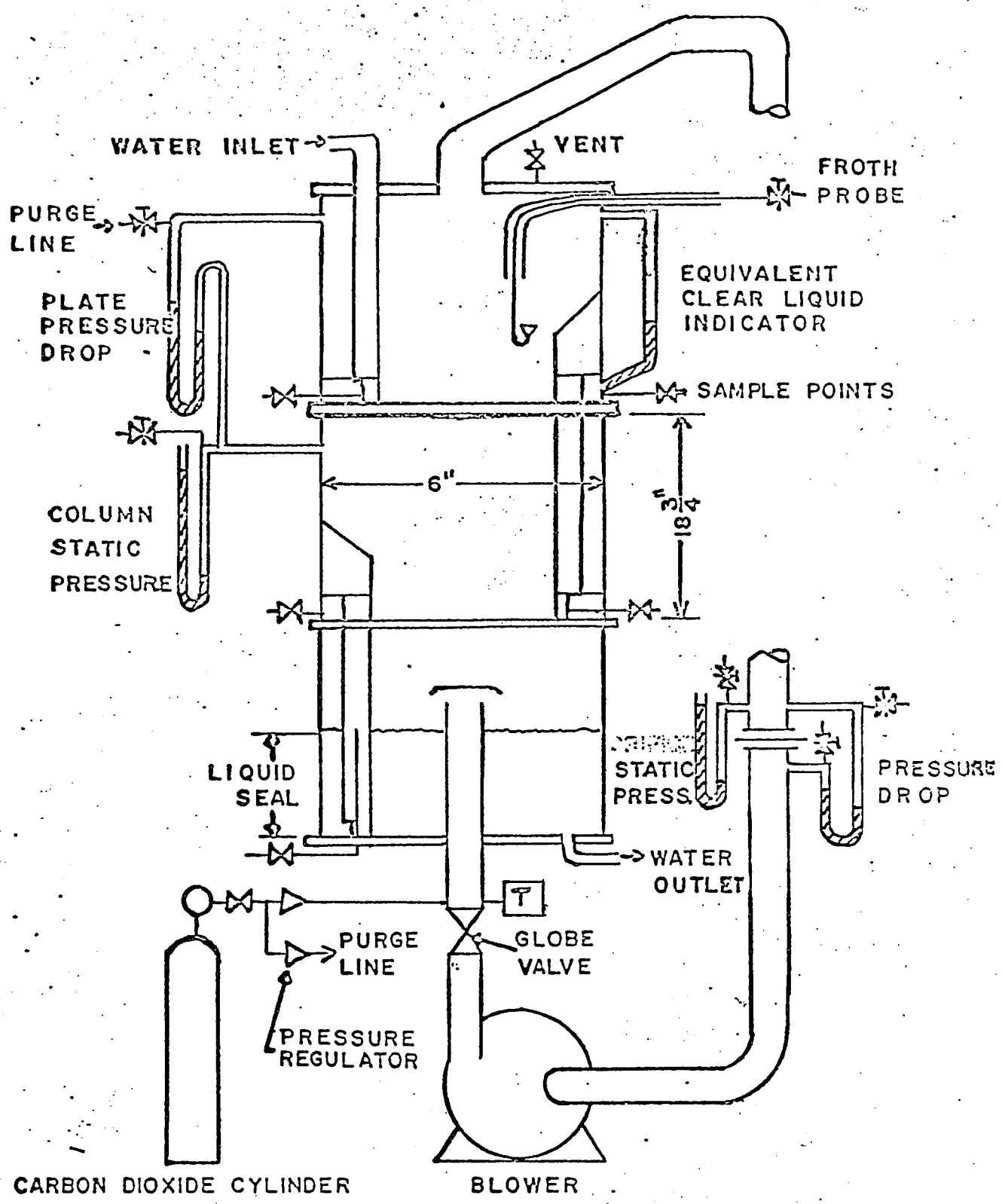

Figure 4. Column Details

length, to develop a uniform velocity profile. The gas was then directed down through an orifice to determine its flow rate. It was then drawn into a centrifugal blower and recycled back into the column. Degassed water at a controlled temperature entered the top of the column. The liquid flow rate was indicated on one of the calibrated rotameters and regulated by adjusting the appropriate globe valve.

Specially designed froth splash baffles were used to prevent froth carry-over and to increase the residence time of the froth on the tray. Each splash baffle was bolted to the downcomer pipe. The baffle consisted of a section of 2-inch copper tube. It was covered at the top by a 1/16-inch thick copper plate. The splash baffle is shown in operation in Figure 36. A liquid baffle, force fitted on the bottom of the downcomer, prevented liquid on the tray from mixing with the liquid within the downcomer. The baffle was made of 1/16-inch thick copper plate and cut as shown in Figure 5. The open sides were covered with 1/16-inch mesh copper screening. The downcomers were lengths of 1-inch copper tubes. The weir height was 1.5 inches. Details of downcomer construction are given in Figure 5.

The liquid samples for the efficiency studies were taken through 1/4-inch stainless steel tubes which were brazed to the ring located above the test tray. The tubes were fitted with 1/4-inch ball valves. Samples for the concentration profiles near the tray floor were taken by way of adjustable 1/8-inch stainless steel tubes. The froth probe, similar to that used in the A.I.Ch.E. study (13), consisted of two concentric

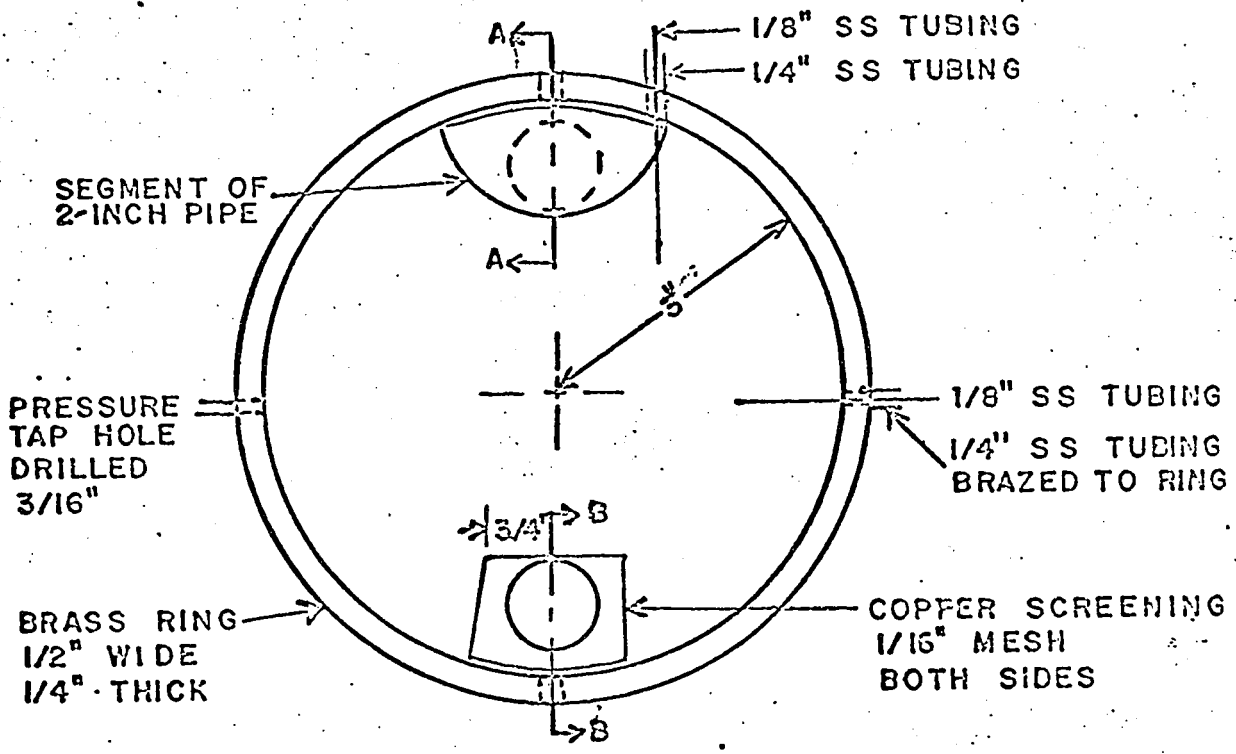

a. TOP VIEW OF TEST TRAY

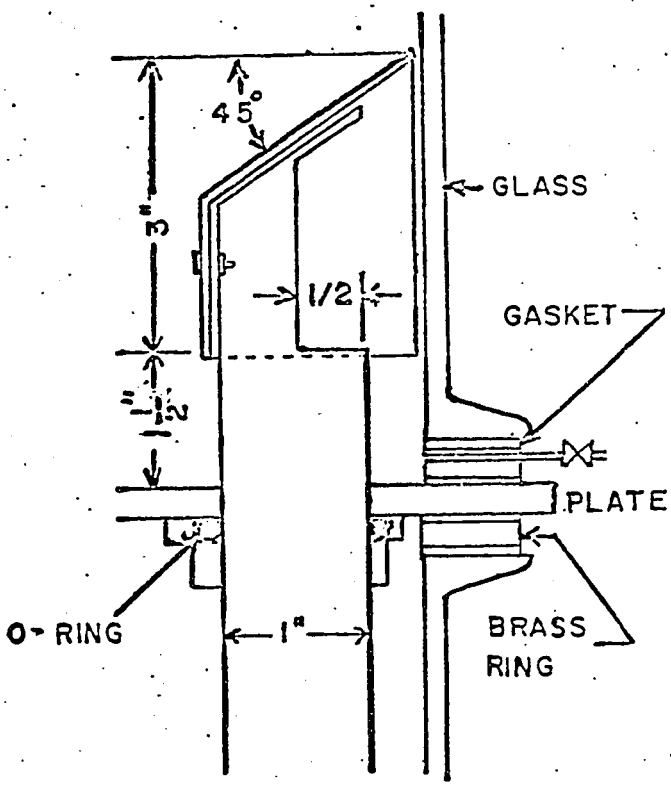

b. SECTION A-A

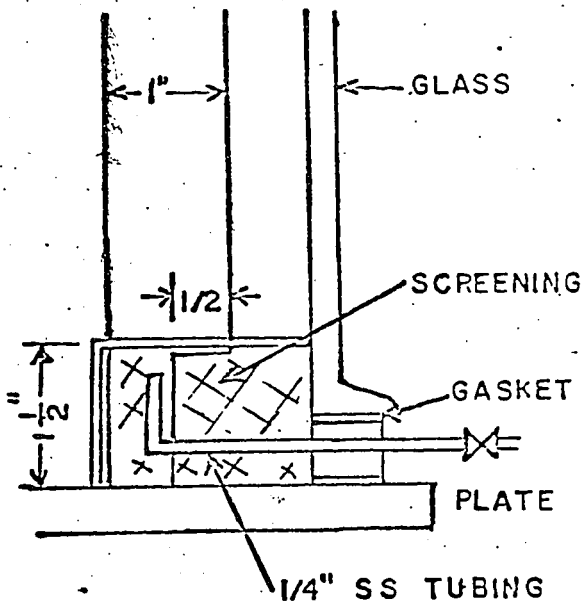

c. SECTION B-B

Figure 5. Downcomer Details

stainless steel tubes of 1/8-inch and 3/16-inch diameters, respectively. The inner tube ended with an inverted bell shape. It slid vertically inside the larger tube. The probe was manually moved parallel to the tray surface. Pressure taps were mounted through the brass ring. In order to correctly measure the wet plate pressure drop gas purge lines were used to keep liquid from entering the manometer lines.

The stripper consisted of one 3-foot long, 6-inch internal diameter QVF glass section with brass plates flanged at both ends. Water from the storage tanks entered the stripper through a 1-inch diameter perforated copper tube closed at one end. Recirculated water was sprayed through a standard shower nozzle. A constant liquid level was maintained in the stripper by an automatic level controller consisting of a mercury-filled manometer used to control the liquid head, and a solenoid valve activated by an electrical contact in the mercury manometer was used to regulate liquid flow from the storage tanks. A regulated flow of steam in an 3/8-inch copper coil was used to heat the liquid in the stripper when required.

Two stainless steel tanks having a capacity of eight and eleven gallons, respectively, were used as storage vessels for fresh water and for water from the bottom of the absorption column. A single pass, countercurrent, shell and tube heat exchanger consisted of a 3-inch diameter copper shell and ten 1/2-inch diameter copper tubes. The heat exchanger's overall length was 5 feet. Water, from the main water supply, was regulated to the heat exchanger by means of two globe valves. All

piping carrying liquid was 1-inch diameter copper tube, except where specified otherwise.

As a result of preliminary trials, it was concluded that the absorption of carbon dioxide by water was rapid and almost complete. Therefore, only two trays were used. Efficiencies and hydraulic data were obtained using the upper test tray. The lower tray was used to cool the gas and to saturate the gas with the liquid. The trays were constructed from brass disks 12-inches in diameter. Six holes were drilled in the tray at a radius of five inches from the centre to facilitate assembly onto the column. A 1-inch diameter hole was drilled in the trays for insertion of a downcomer. The perforations were drilled to $\pm$ 0.002 inches and the plates were machined. Pertinent specifications for the five trays are given in Table 1. Hole configurations are shown in Figure 6. The triangular pitch-hole diameter ratio was constant at 3.0 for all trays. The pitch is defined as the centre-to-centre distance between two adjacent holes. The free area was 5.56 percent for all plates. The bottom tray, having 1/4-inch holes, was unchanged during all the experiments.

TABLE 1

TEST TRAY SPECIFICATIONS

Hole Diameter	Number of Holes	Plate Thickness	Pitch	T/D_h
inches	-	inches	inches	-
TEST PLATES				
0.125	128	0.314	0.375	2.512
0.250	32	0.345	0.750	1.380
0.500	8	0.256	1.500	0.512
1.000	2	0.306	3.000	0.306
BOTTOM PLATE				
0.250	32	0.356	0.750	1.424

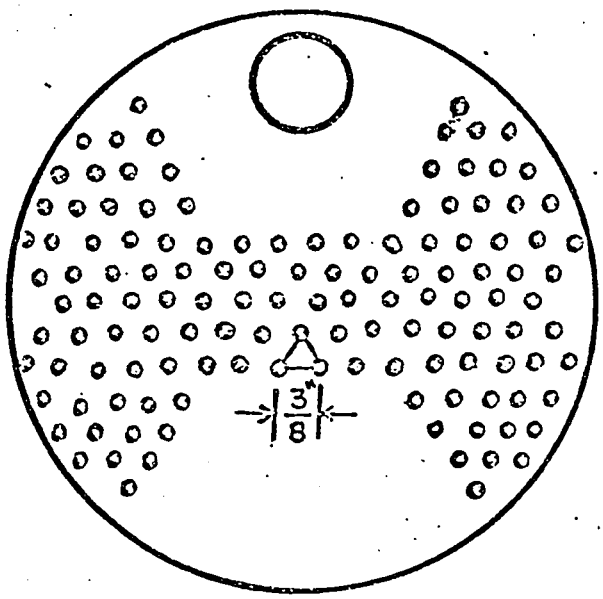

DRILL 128 HOLES $\frac{1}{8}$" DIA.
ON $\frac{3}{8}$" TRIANGULAR PITCH

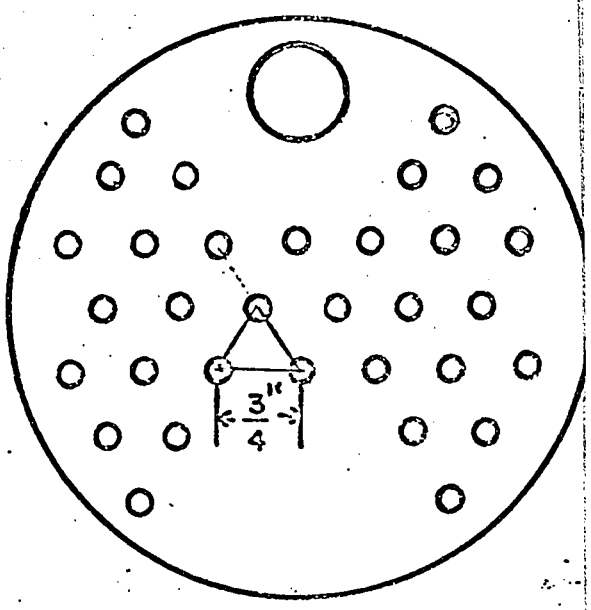

DRILL 32 HOLES $\frac{1}{4}$" DIA.
ON $\frac{3}{4}$" TRIANGULAR PITCH

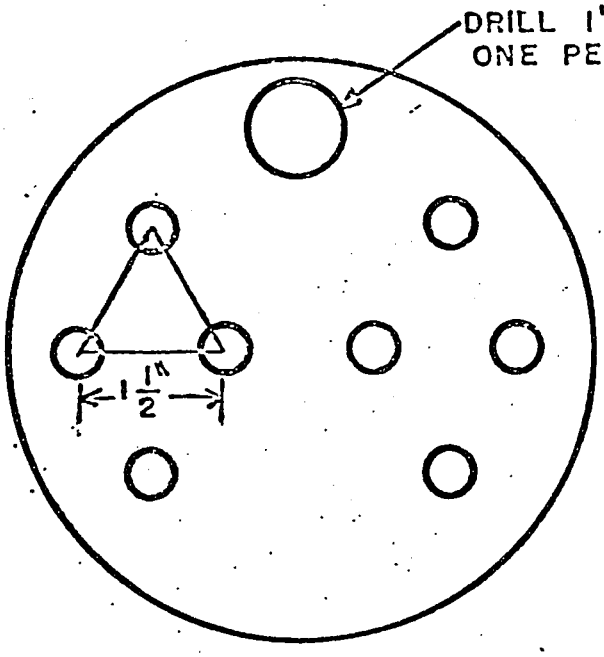

DRILL 8 HOLES $\frac{1}{2}$" DIA.
ON $1\frac{1}{2}$" TRIANGULAR PITCH

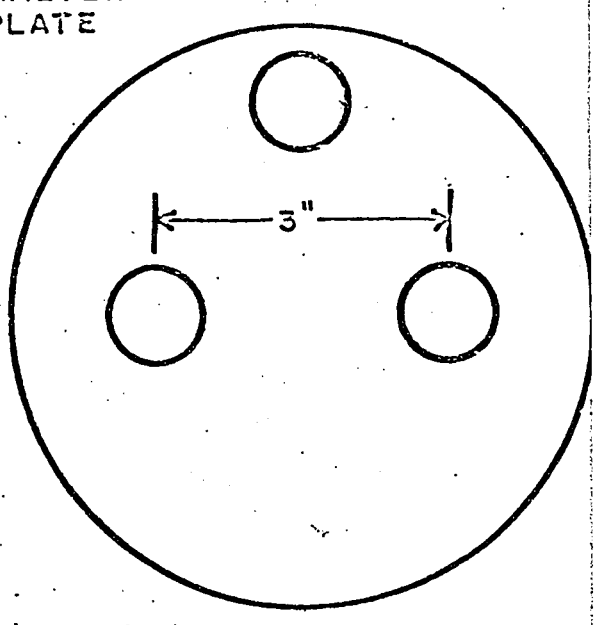

DRILL 2 HOLES 1" DIA.
AT 3" CENTER TO CENTER

Figure 6. Plate Configurations

PROCEDURE

During the operation of the column, a constant liquid rate was maintained while the gas flow rate was decreased in nearly equal increments and samples were taken at each of the gas rates. Preliminary studies indicated that steady-state was quickly established after a change in operating conditions. The column was operated at a temperature of 77.0 $\pm$ 0.2 °F. and a pressure of approximately 40 $\pm$ 2 inches of water above the prevailing atmospheric pressure (about 830 mm. of mercury).

In order to ensure that the gas phase was not contaminated with air, air was initially purged from the column by displacing it with water, which was in turn displaced with carbon dioxide. The procedure was repeated several times. The static pressure inside the column was maintained by continuously adding carbon dioxide to the column from a cylinder through a sensititive pressure regulator. An Orsat gas analyzer showed that the gas phase was 98 to 100 percent carbon dioxide. The flow of gas was measured by a calibrated orifice flowmeter and was regulated by a large gate valve located at the gas blower discharge.

Water was degassed by vacuum and was recycled. The degassed water contained a small amount of carbon dioxide (about 4% of saturation). Fresh water was occasionally added because of sampling losses and evapouration during stripping. The flow of liquid to the absorption column was measured by one of the two calibrated rotameters. Partially saturated liquid was forced out of the column into one of the storage tanks. A U-tube arrangement kept a constant liquid level in the column.

Temperatures of the gas and liquid in the tubing were determined with thermometers. A copper-constantan thermocouple measured the temperature of the gas-liquid mixture on the tray. Water-filled manometers were used to measure the pressure drop of the gas across the orifice plate, the static pressure of the column, and the pressure drop of the gas across the test tray. The dry plate pressure drop data were obtained using sealed downcomers (20,45). The equivalent clear liquid depth was measured in a glass side tube. Froth height was measured with a ruler. Atmospheric pressure was determined using a mercury barometer and was recorded.

Steady-state was rapidly reached but the equipment was operated for an hour before samples were taken. Samples were collected in 25 ml. pipettes connected by rubber tubing to the sample valves. Slow extraction of the sample was necessary to prevent gas from entering the sample lines, otherwise the gas would be absorbed in the sample line and incorrect results would be obtained. Triplicate samples were obtained and duplicate runs were performed in order to determine the reproducibility. A froth probe was used to obtain samples of the froth. Absorption in the tube was prevented by limiting the liquid flow with a fine needle valve and by giving the froth bubbles time to break in the funnel. Samples were titrated to determine the carbon dioxide content.

RESULTS

Experimental results include dry plate pressure drops, wet plate pressure drops, clear liquid depths, and froth heights. The Murphree liquid efficiencies, the dry plate pressure drop coefficient, the weep point, the concentration profiles, the number of liquid phase transfer units, the mass transfer coefficients, and lengths of transfer units were calculated. Numerical values can be found in Appendix A.

A. Murphree Liquid Efficiencies

The variation of Murphree liquid efficiency with the gas flow rate, the liquid flow rate, and the hole diameter can be found in Figures 7 to 17. The Murphree liquid efficiencies decreased with increasing liquid flow rate from 0.2 to 4.0, but only slightly. The behavior at the very low liquid rate of 0.1 gpm. was found to be different from that of the other flow rates in that the efficiencies did not increase rapidly with increasing gas flow rates to a constant value. The effect of the liquid flow rate on the Murphree liquid efficiency was more pronounced with the glycol solution than with the water.

The combined effect of increased liquid viscosity and decreased gas diffusivity was very noticeable. The efficiency for the glycol-carbon dioxide system was much less than the efficiency for the water-carbon dioxide system under similar operating conditions, about 60% compared with about 80%.

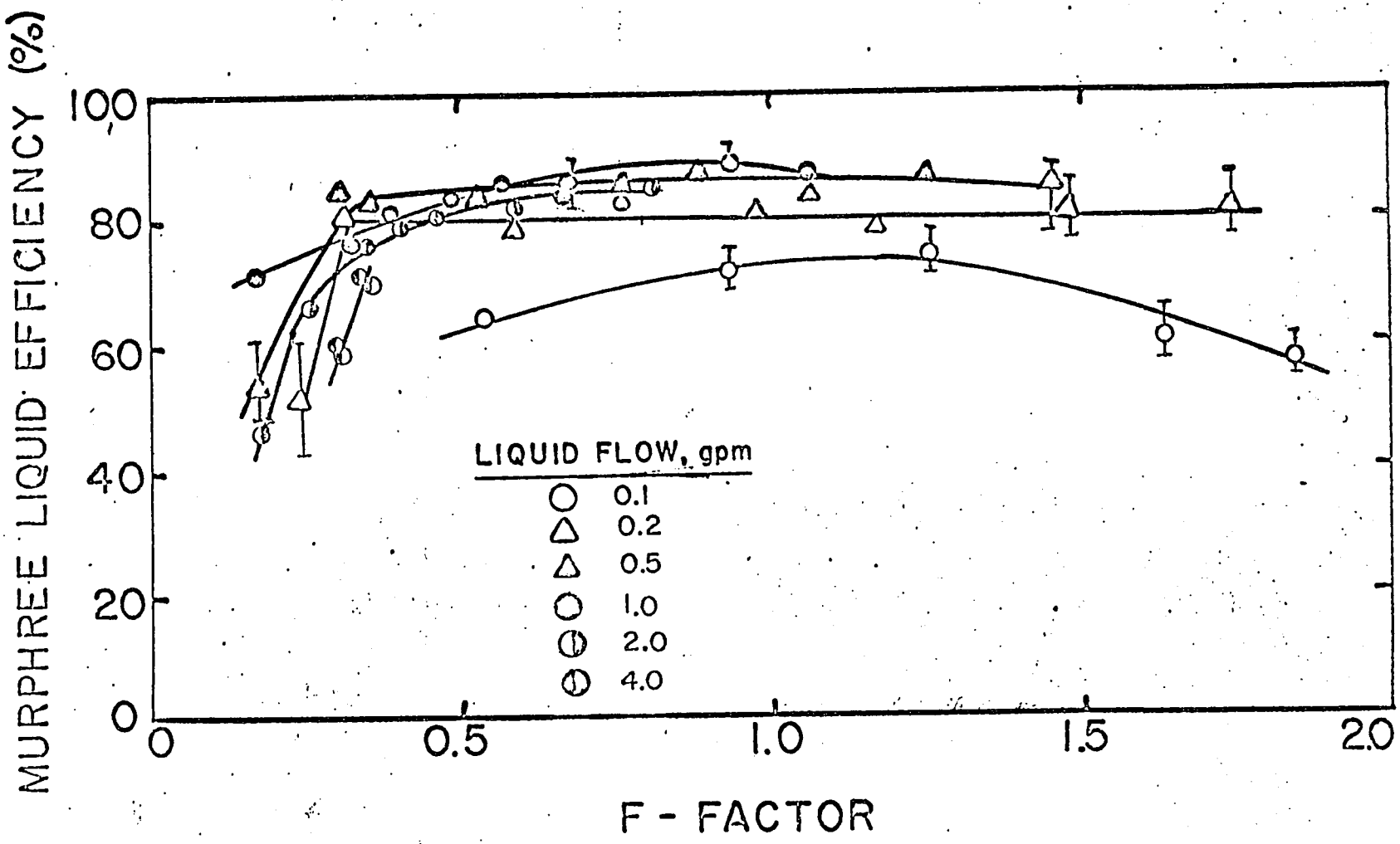

Figure 7. The Variation of Murphree Liquid Efficiency with F-factor for the Water-Carbon Dioxide System using 0.125-inch Diameter Holes

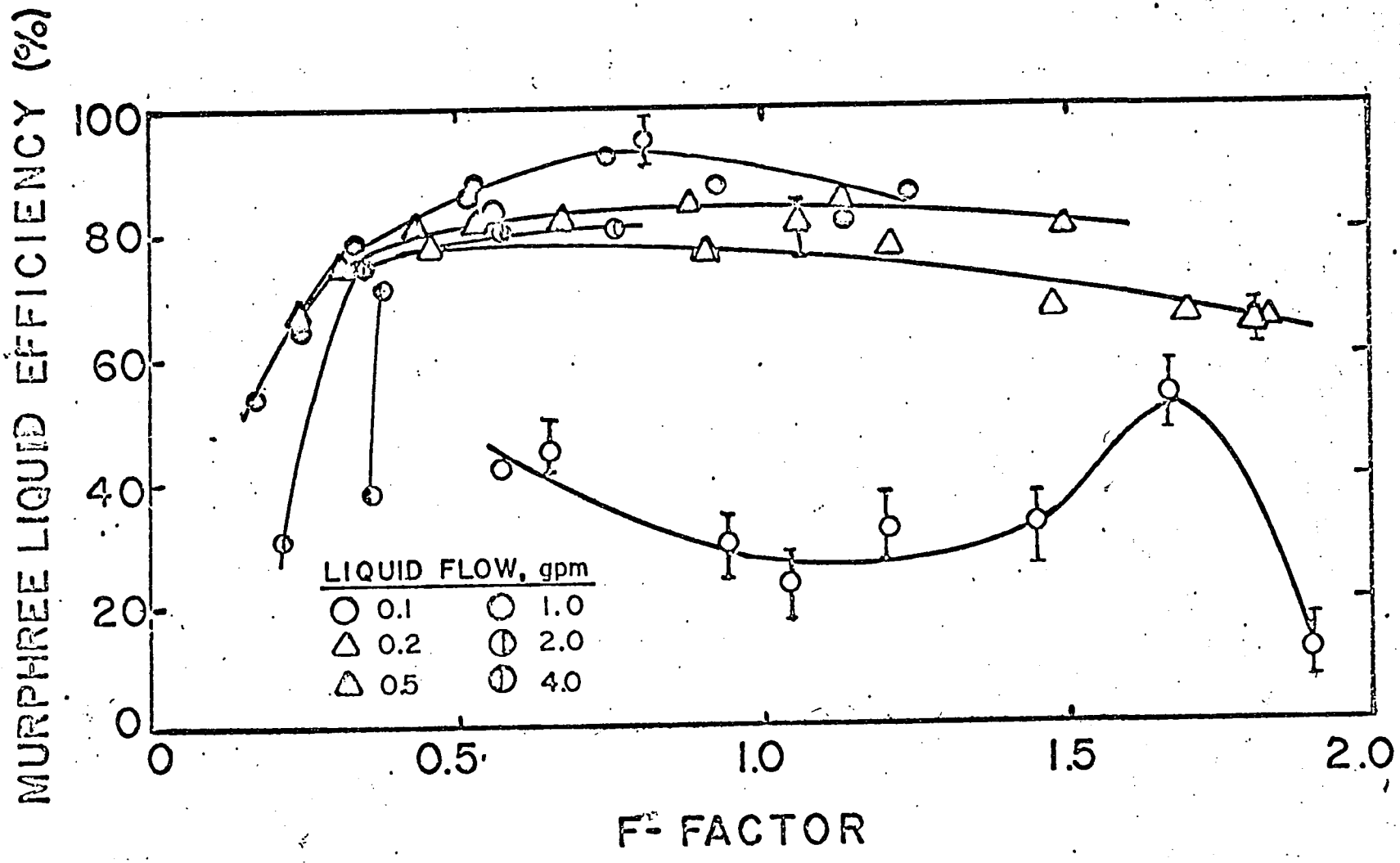

Figure 8. The Variation of Murphree Liquid Efficiency with F-factor for the Water-Carbon Dioxide System using 0.250-inch Diameter Holes

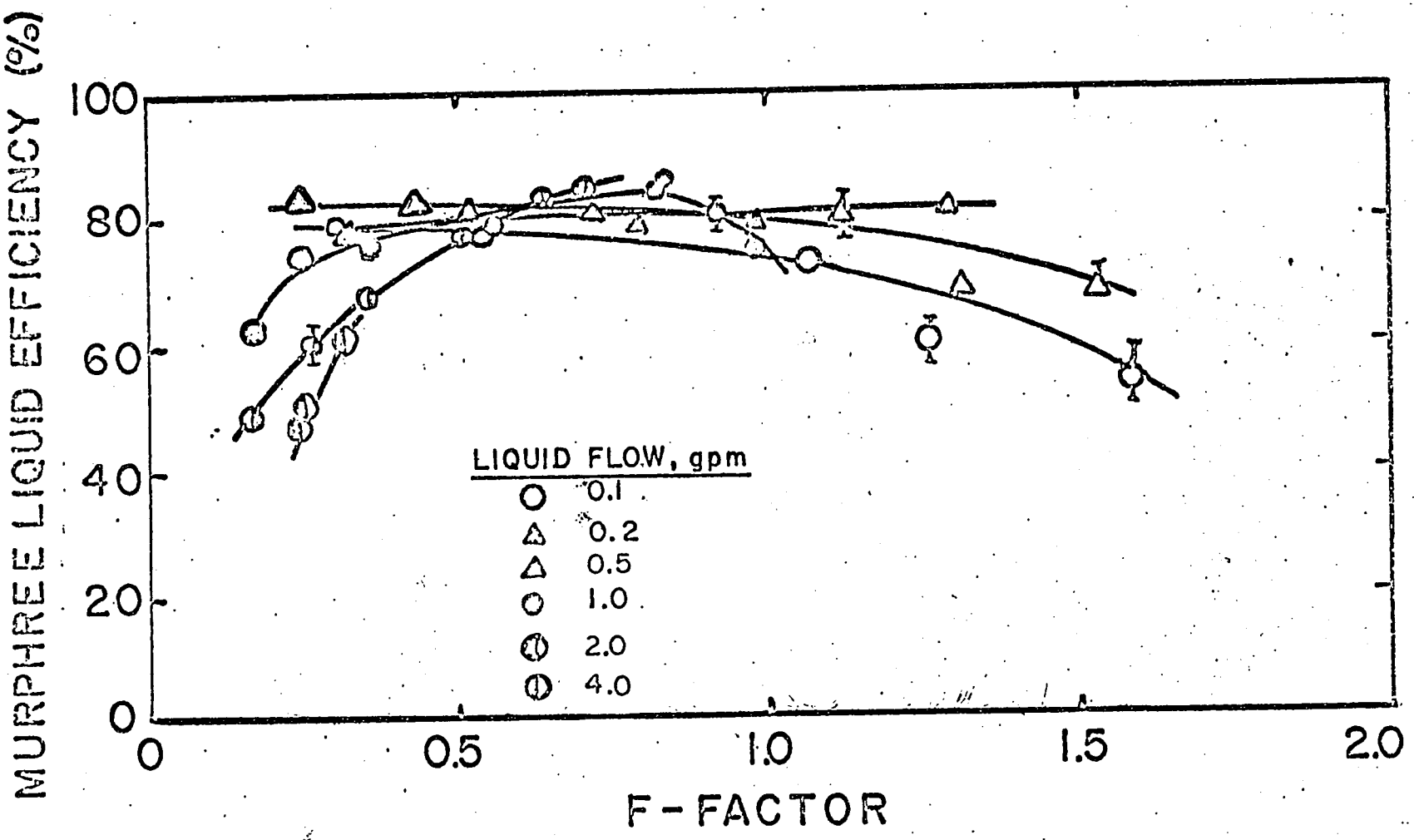

Figure 9. The Variation of Murphree Liquid Efficiency with F-factor for the Water-Carbon Dioxide System using 0.500-inch Diameter Holes

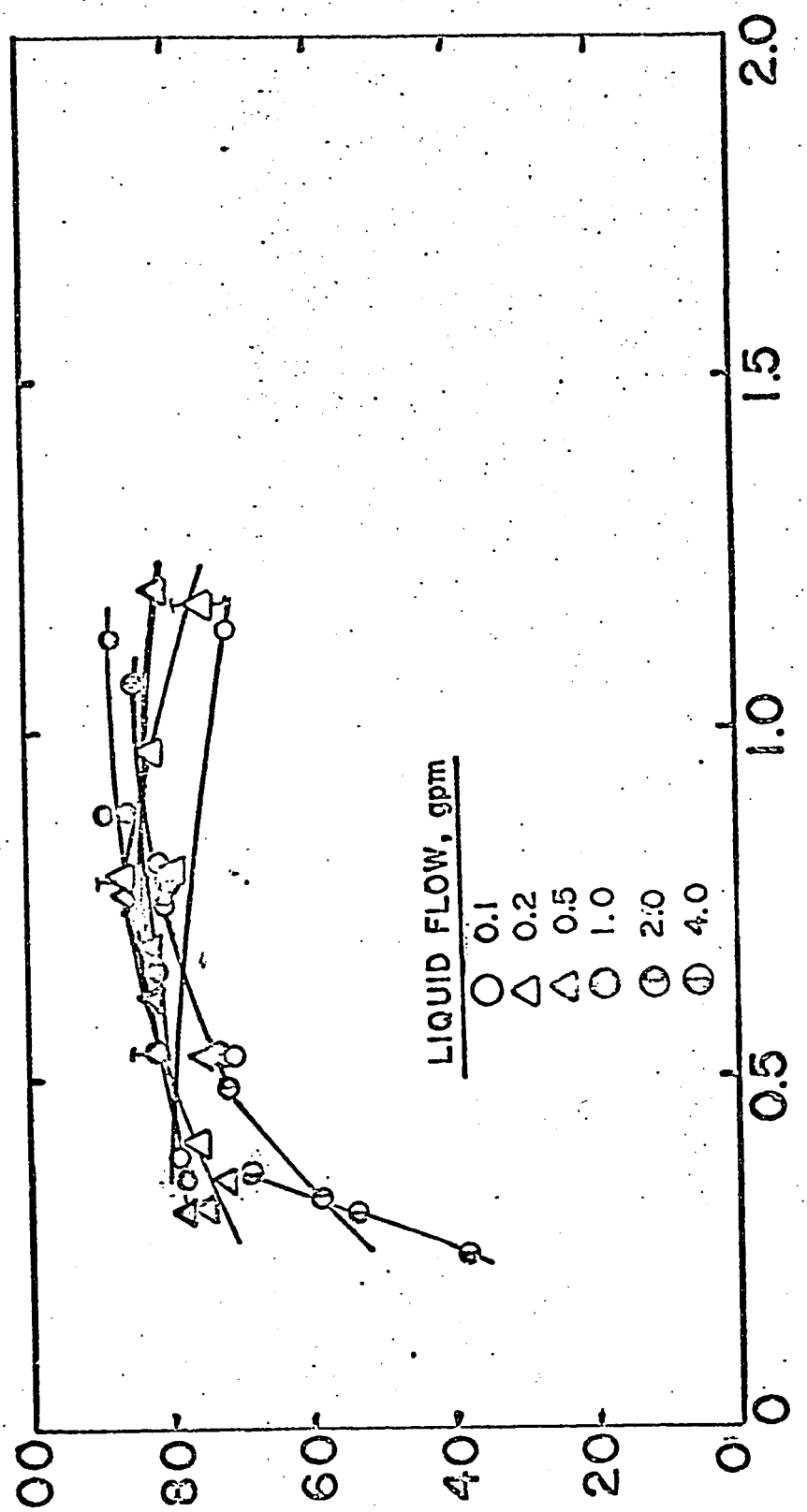

Figure 10. The Variation of Murphree Liquid Efficiency with F-factor for the Water-Carbon Dioxide System using 1.000-inch Diameter Holes

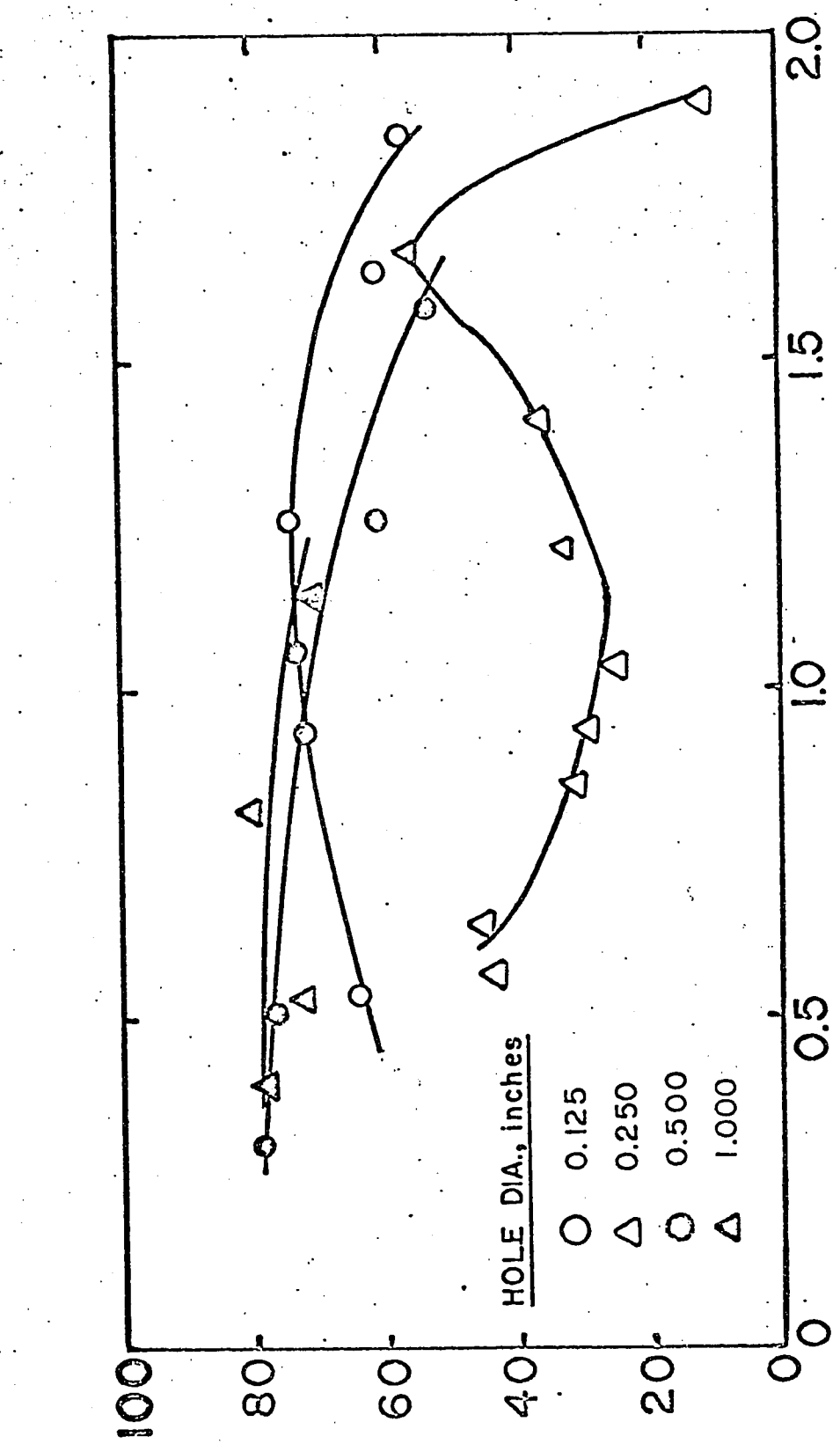

Figure 11. The Variation of Murphree Liquid Efficiency with F-factor for the Water-Carbon Dioxide System using Liquid Rate of 0.1 gpm.

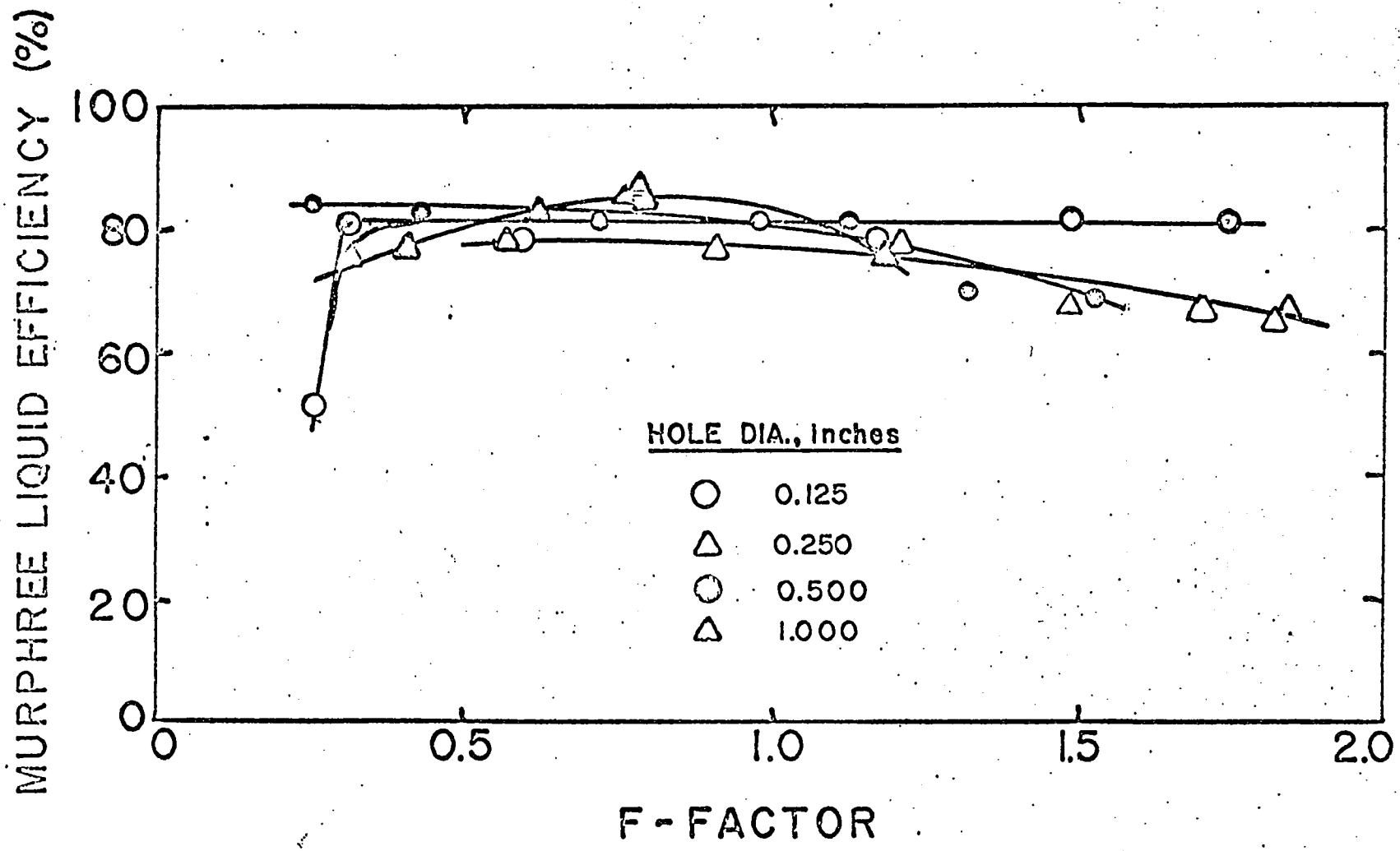

Figure 12. The Variation of Murphree Liquid Efficiency with F-factor for the Water-Carbon Dioxide System using Liquid Rate of 0.2 gpm.

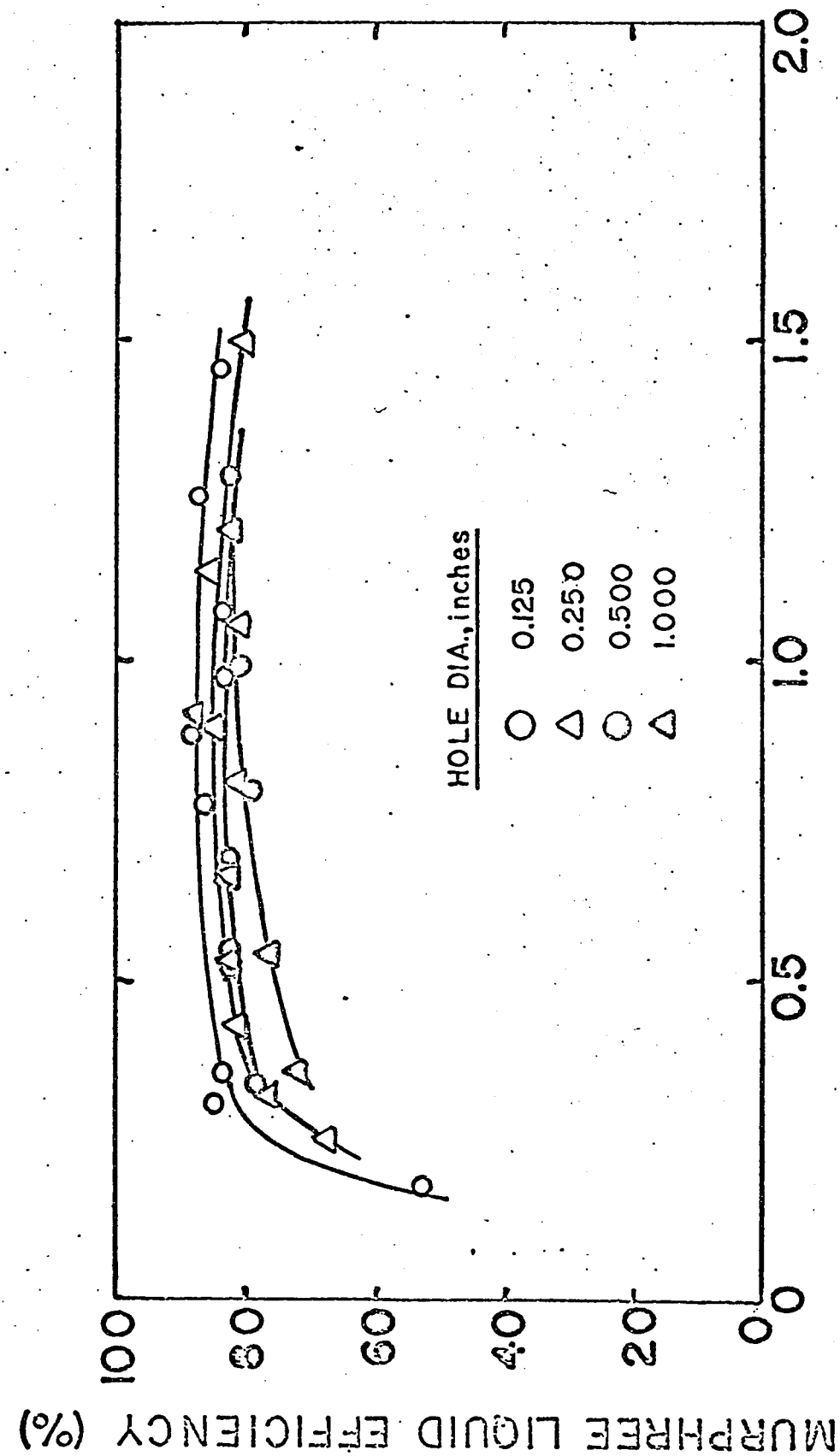

Figure 13. The Variation of Murphree Liquid Efficiency with F-factor for the Water-Carbon Dioxide System using Liquid Rate of 0.5 gpm.

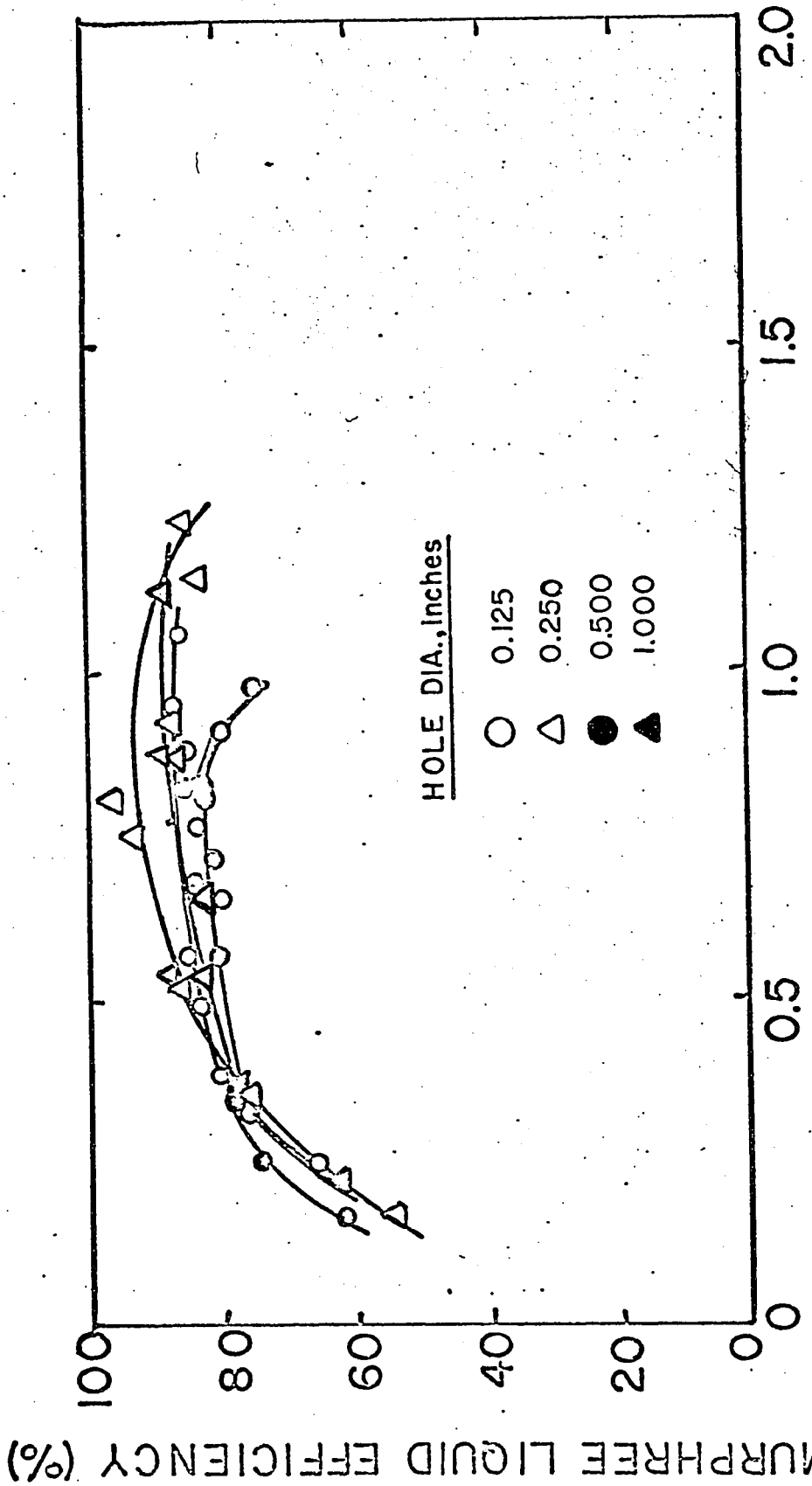

Figure 11. The Variation of Murphree Liquid Efficiency with F-factor for the Water-Carbon Dioxide System using Liquid Rate of 1.0 gpm.

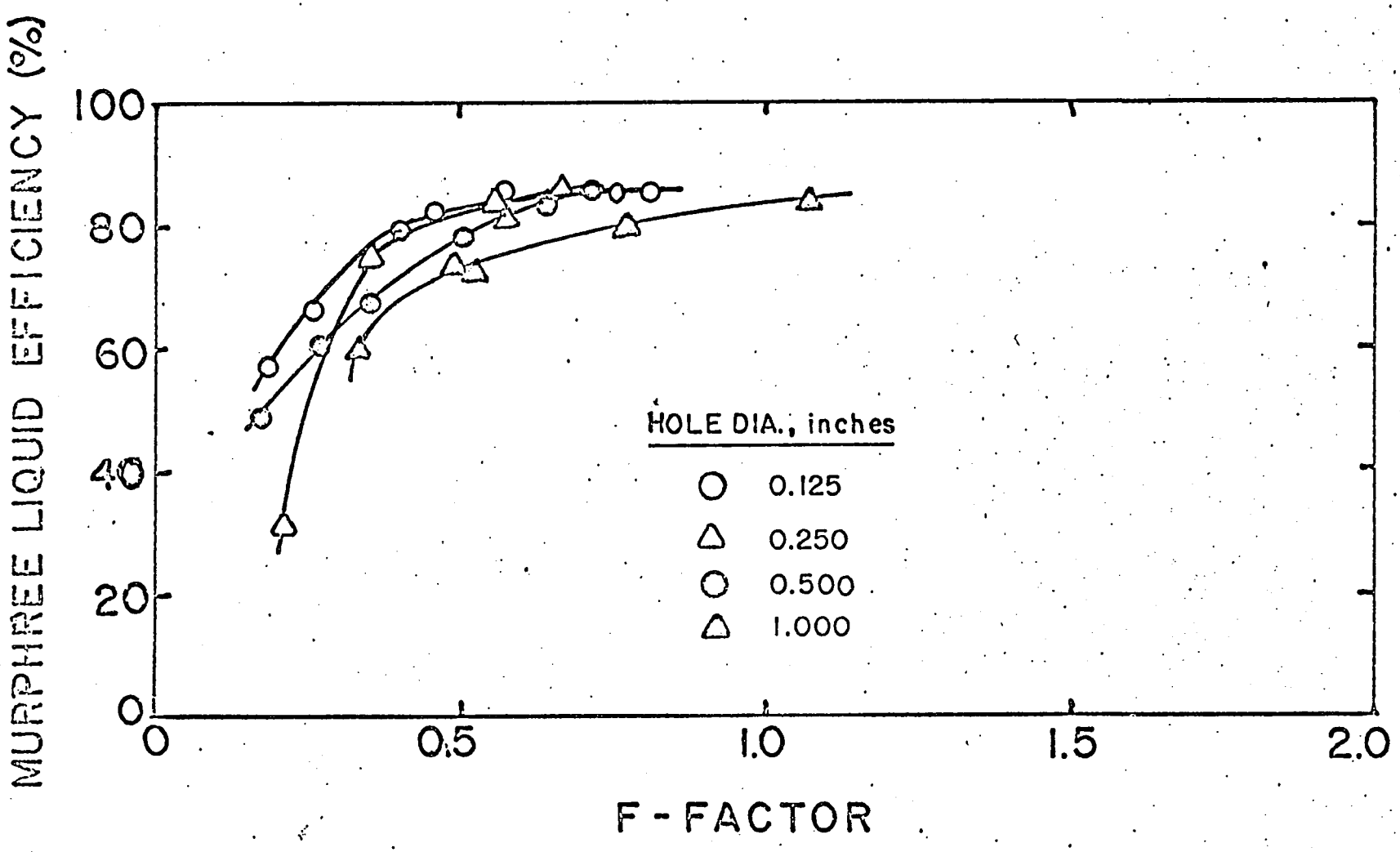

Figure 15. The Variation of Murphree Liquid Efficiency with F-factor for the Water-Carbon Dioxide System using Liquid Rate of 2.0 gpm.

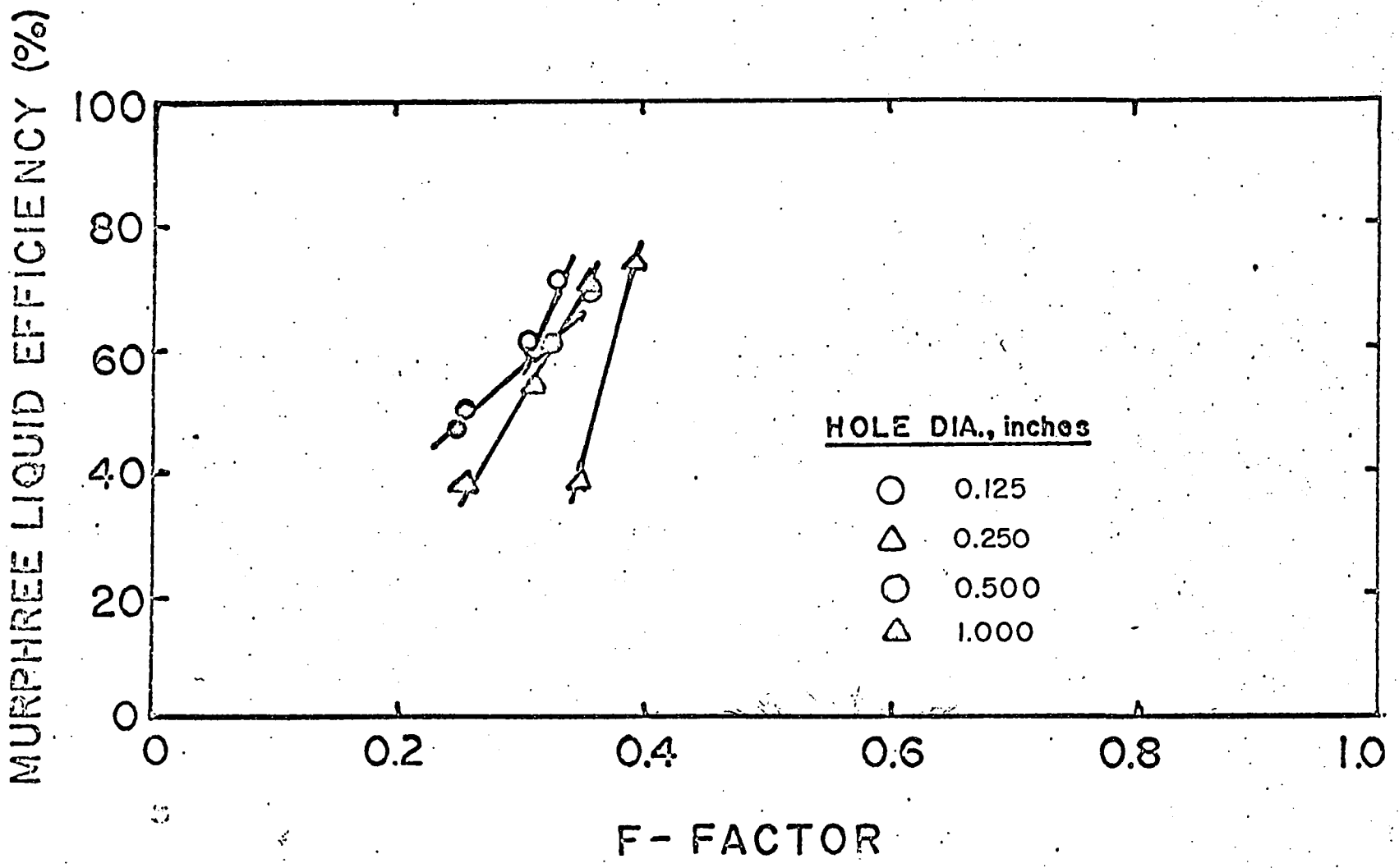

Figure 16. The Variation of Murphree Liquid Efficiency with F-factor for the Water-Carbon Dioxide System using Liquid Rate of 4.0 gpm.

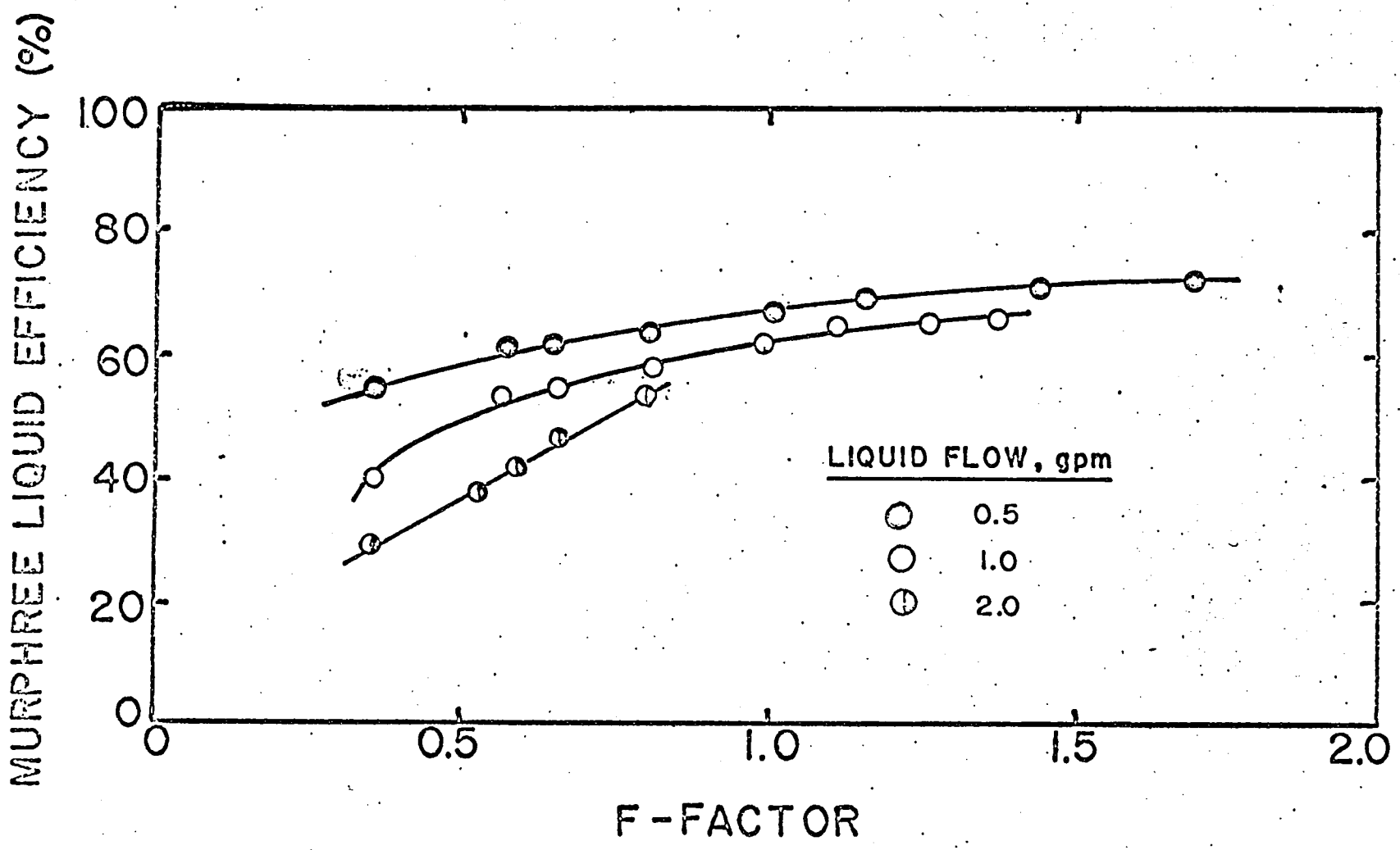

Figure 17. The Variation of Murphree Liquid Efficiency with F-factor for the Glycol-Carbon Dioxide System using 0.250-inch Diameter Holes

B. Dry and Wet Plate Hydraulics

Dry plate pressure drops shown in Figure 18 were calculated from equations 19 and 20. Values of the dry plate pressure drop coefficient, K, calculated using experimental data and equation 20, and also those from the literature (5) are shown in Figure 19. Considering the wide range of the hole diameters used, the agreement was good.

The wet plate pressure drop increased with an increase in the liquid flow rate and gas flow rate. Equation 21 was applicable to all the flow ranges investigated. The residual pressure drop was taken as 0.5 inches of water. Liquid depths on the tray, h_c, were occasionally quite large, especially at high liquid rates, denoting the start of flooding in the column.

A visual determination of the weep point was difficult. Weeping was considered to start when a few holes leaked water continuously. Weeping occurred at random locations through the test tray, not through any specific perforations. The visual weep points were correlated (9,45) and are shown in Figures 25 and 26. The weeping region can be considered to represent the lower operating limit of the column. It was apparent that large holes weeped at a higher gas flow rate than did the smaller holes. An example of weeping from the plate with 1-inch diameter holes can be seen in Figures 38 and 40.

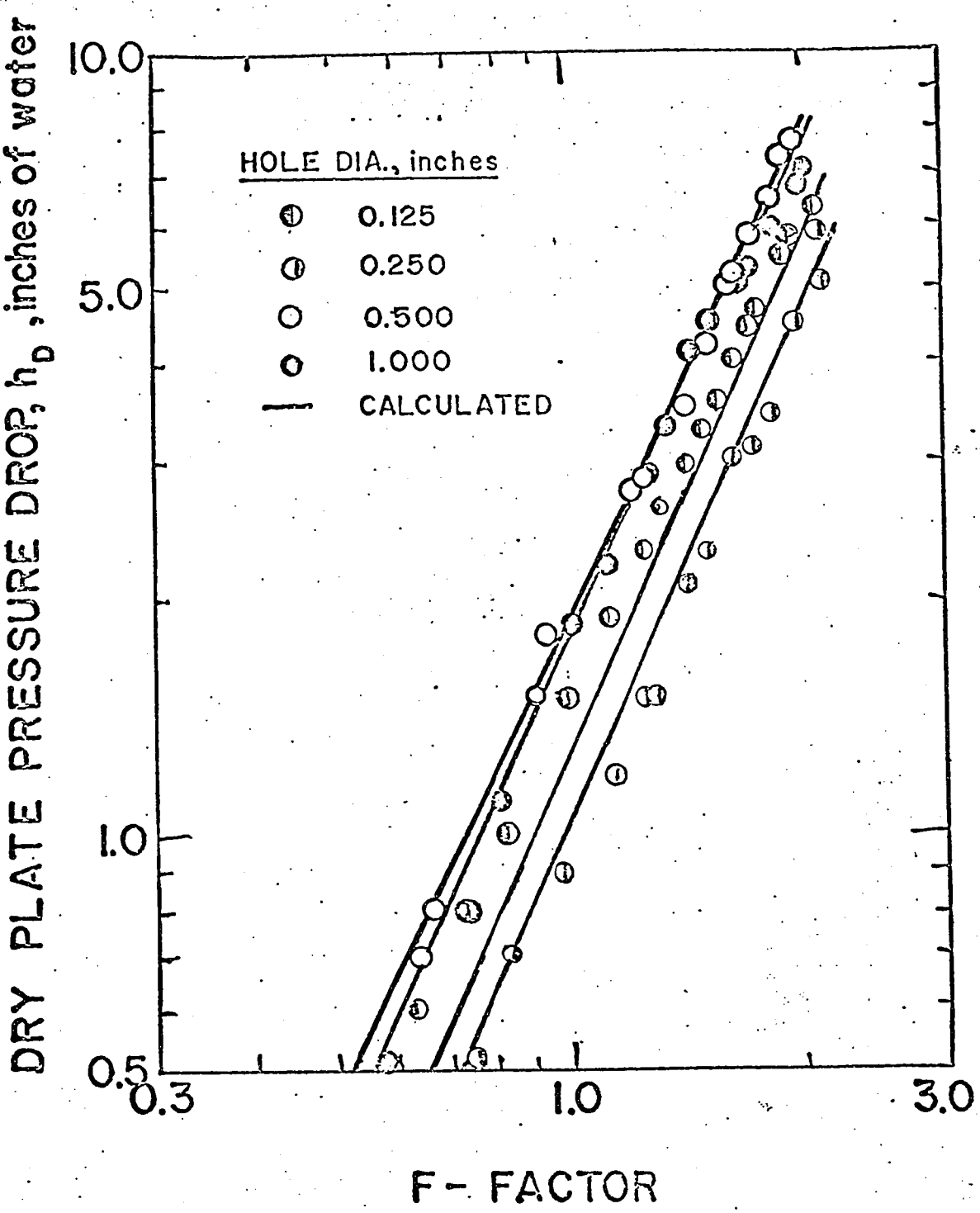

Figure 18. Dry Plate Pressure Drop and corresponding F-factor

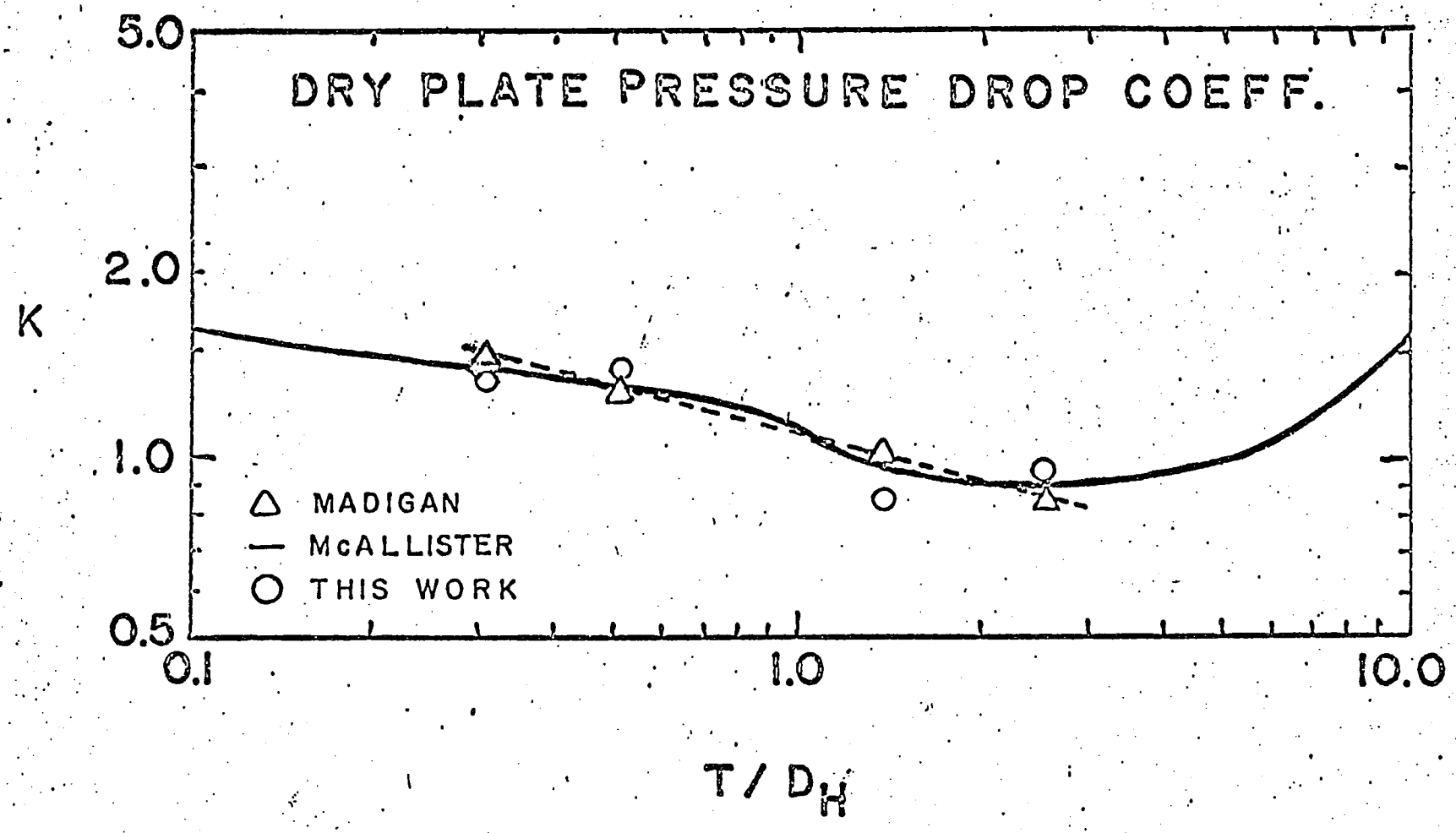

Figure 19. The Dry Plate Pressure Drop Coefficient as a Function of Plate Thickness – Hole Diameter Ratio

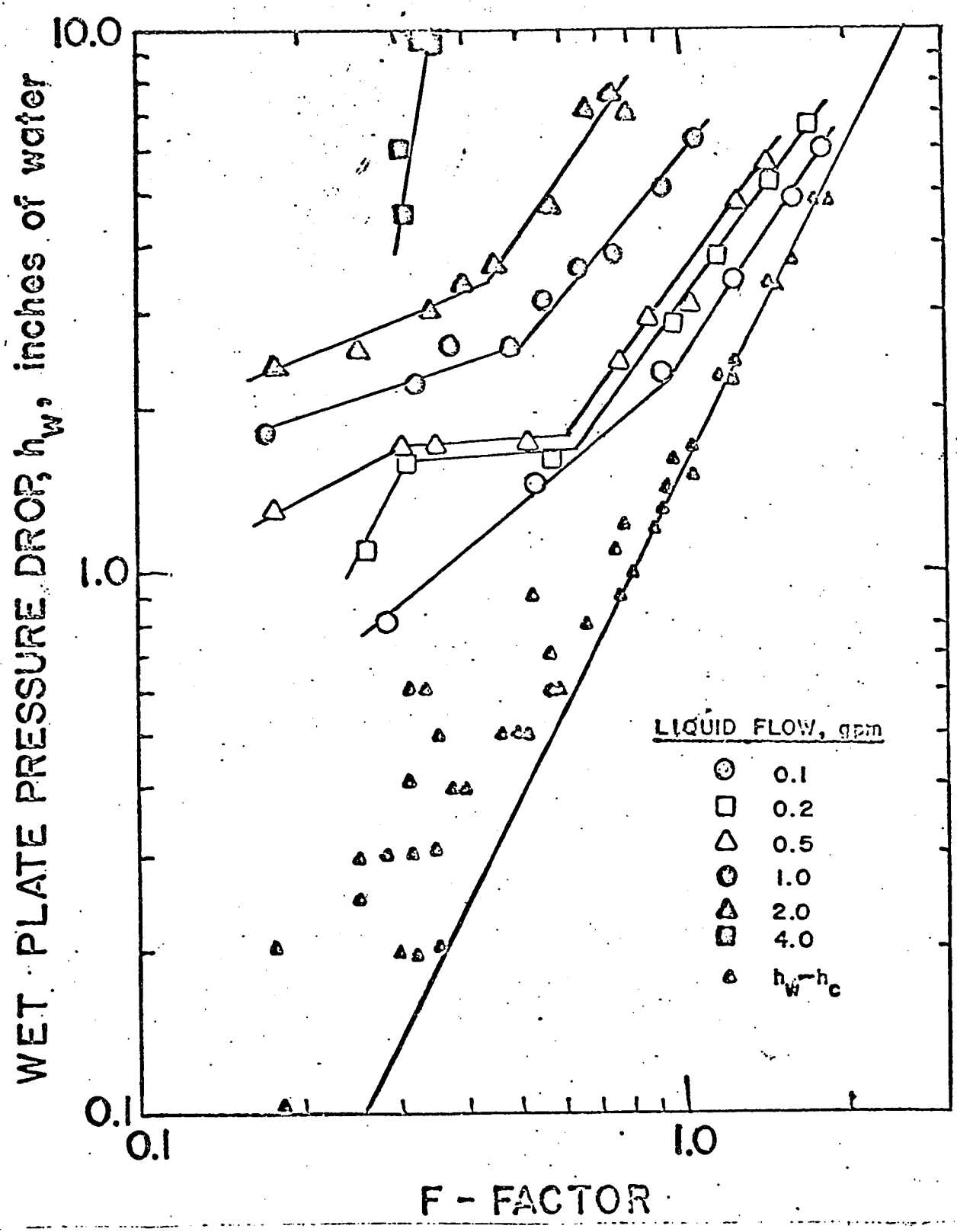

Figure 20. The Variation of Pressure Drop across an operating tray with F-factor for the Water-Carbon Dioxide System using a Hole Diameter of 0.125 inches

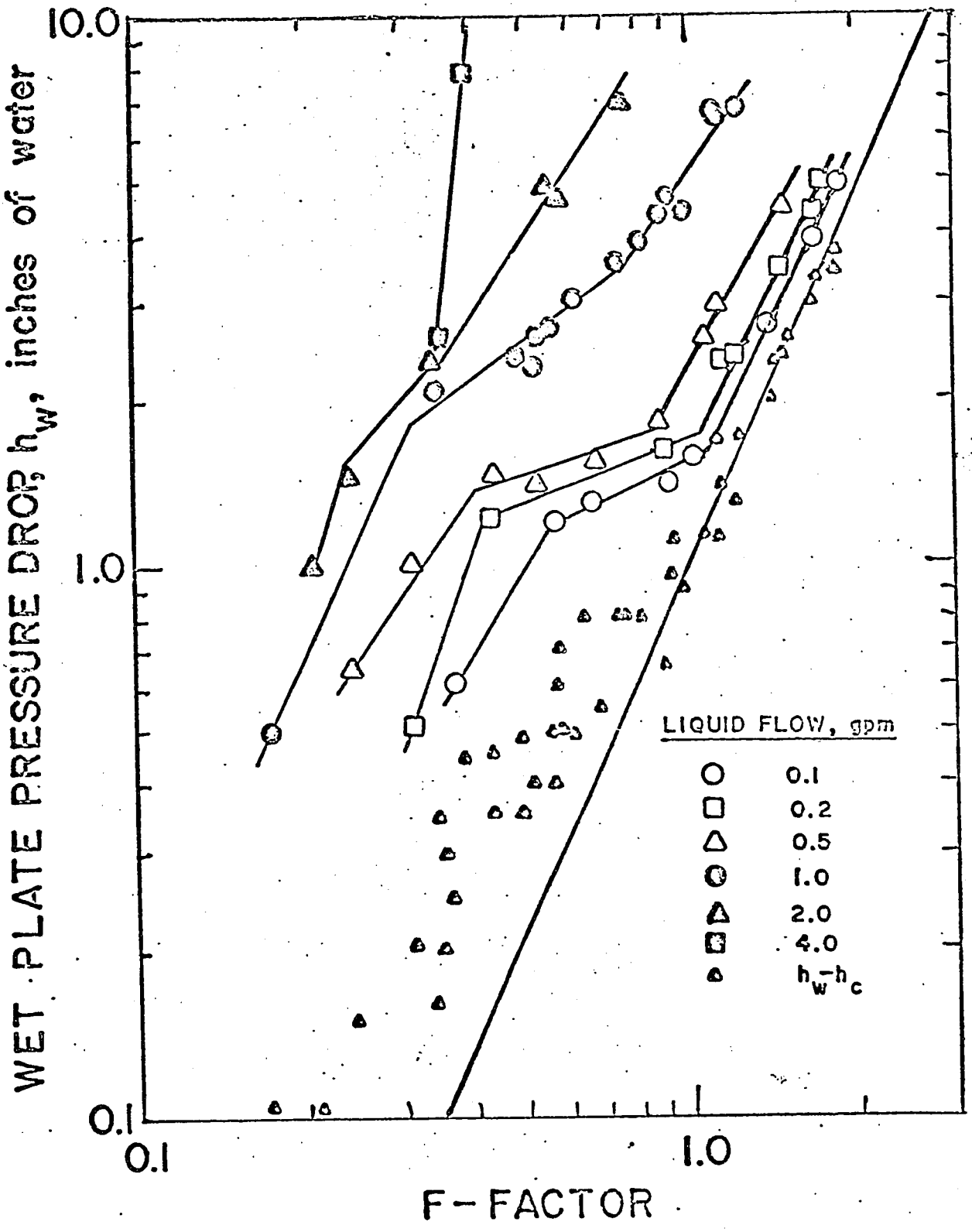

Figure 21. The Variation of Pressure Drop across an operating tray with F-factor for the Water-Carbon Dioxide System using a Hole Diameter of 0.250 inches

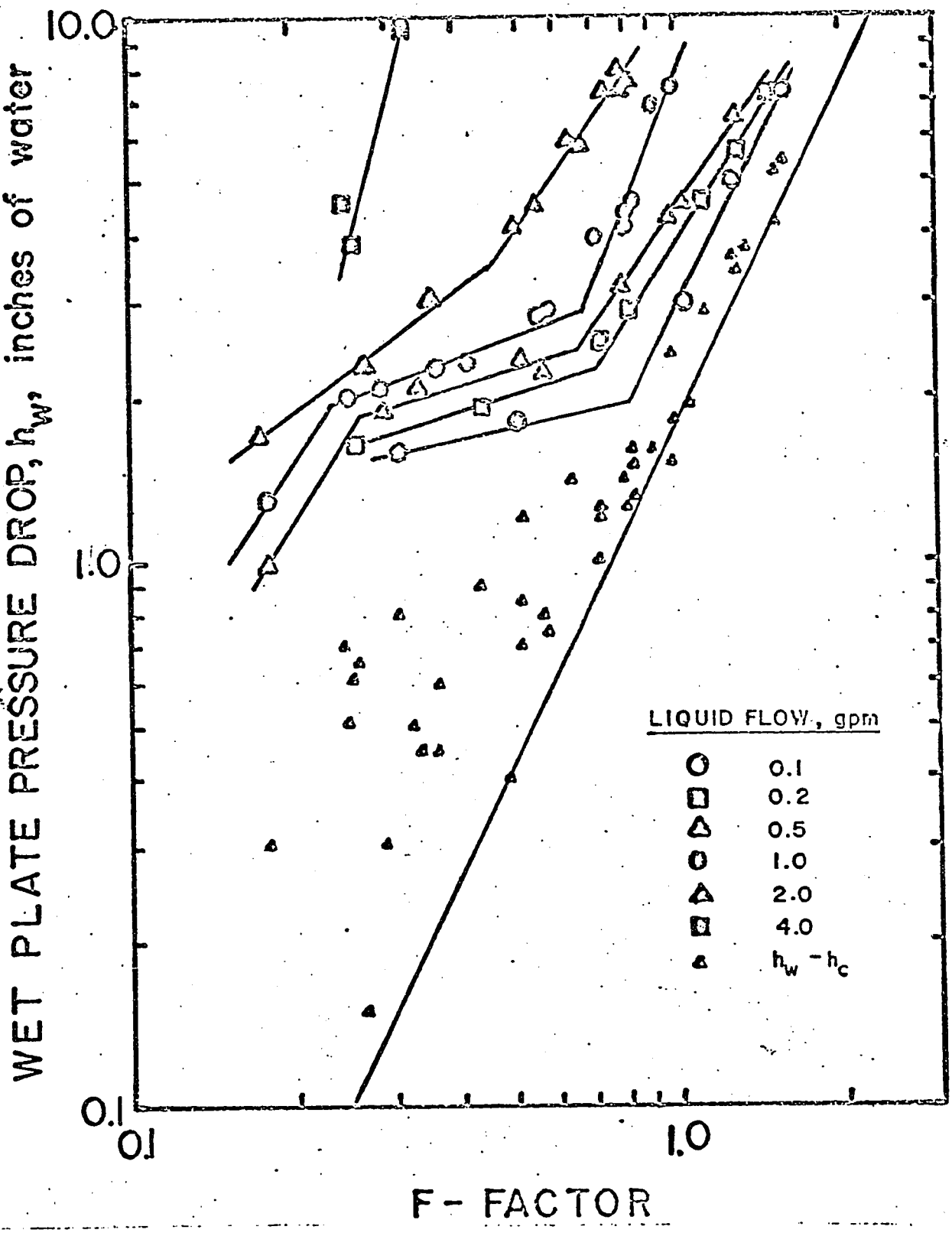

Figure 22. The Variation of Pressure Drop across an operating tray with F-factor for the Water-Carbon Dioxide System using a Hole Diameter of 0.500 inches

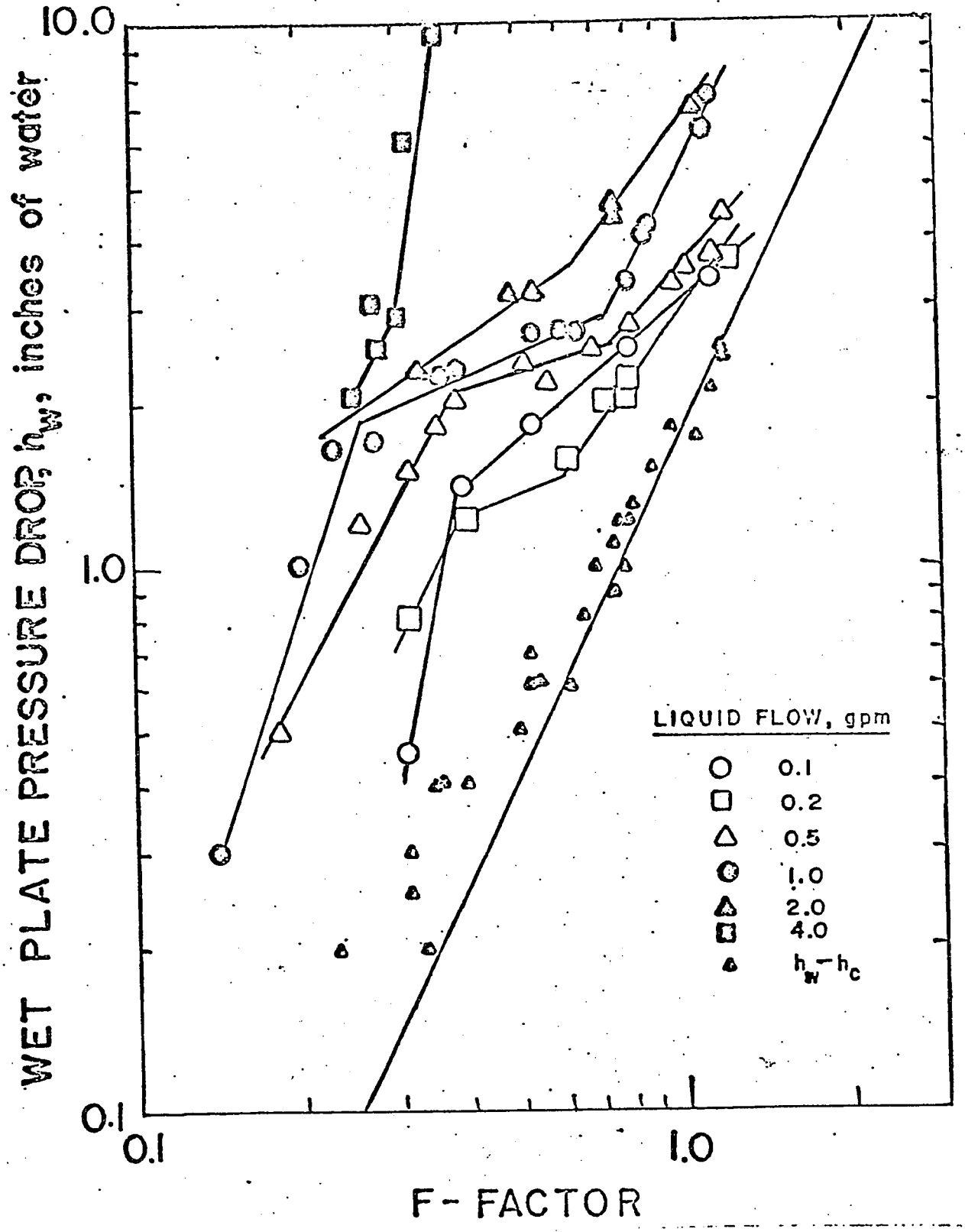

Figure 23. The Variation of Pressure Drop across an operating tray with F-factor for the Water-Carbon Dioxide System using a Hole Diameter of 1.000 inches

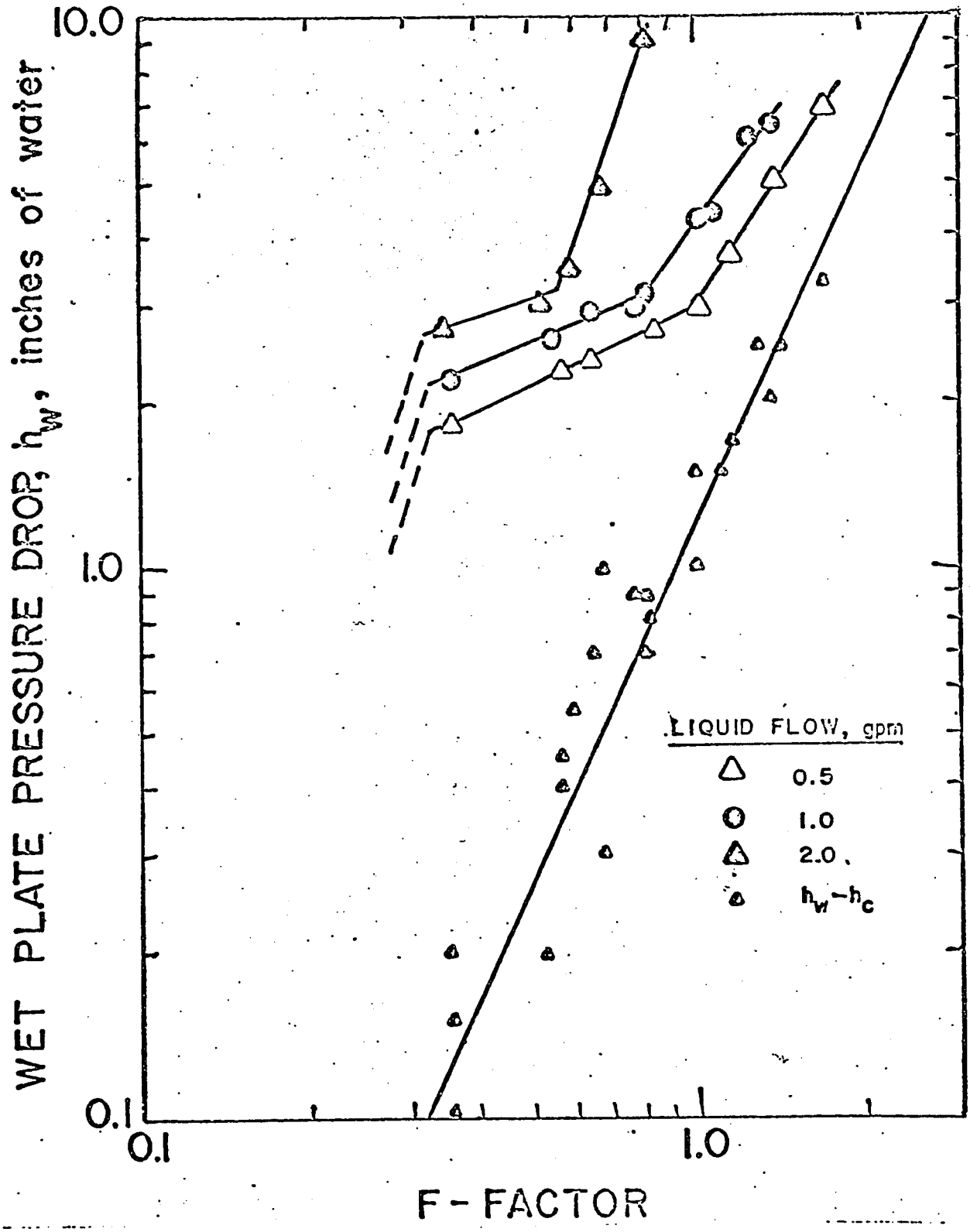

Figure 24. The Variation of Pressure Drop across an operating tray with F-factor for the Glycol-Carbon Dioxide System using a Hole Diameter of 0.250 inches

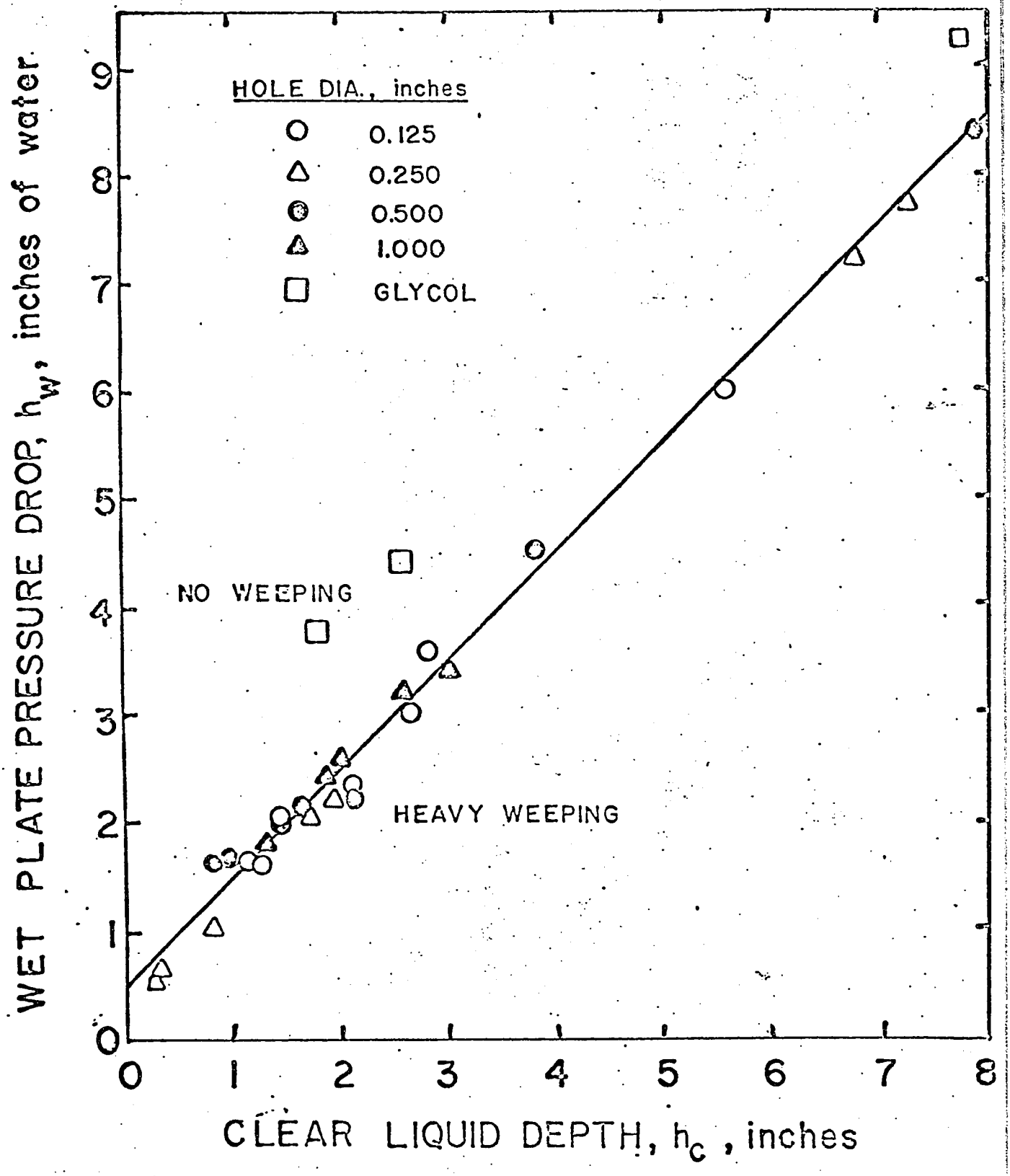

Figure 25. Weep Point Correlation

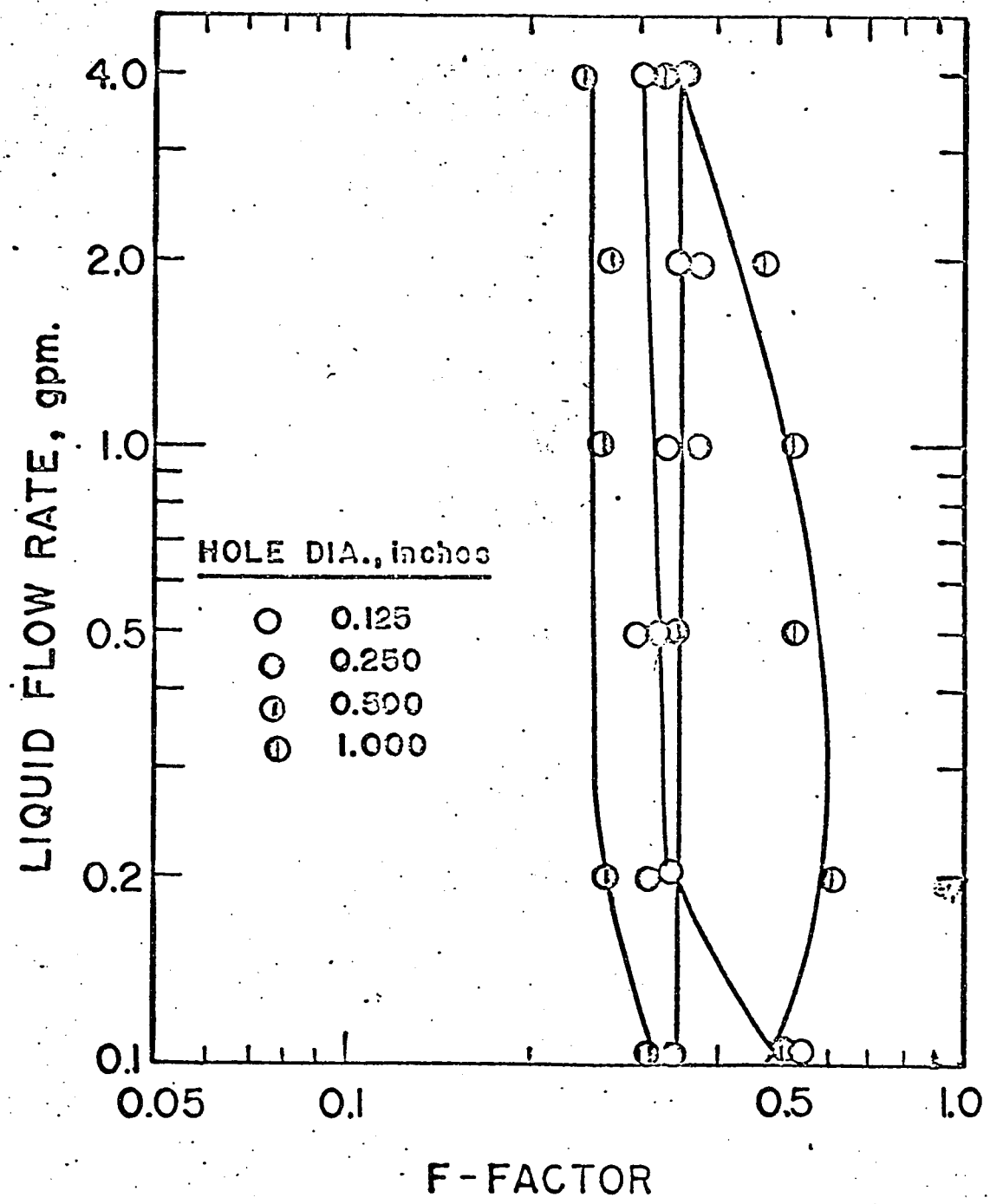

Figure 26. Weep Point Correlation

C. Concentration Profiles

The largest concentration gradient occurred in the region of the froth which lay below the weir height. The froth at an elevation above the weir had an almost constant composition. Figures 27 to 31 are the vertical concentration profiles at various positions above the tray. In the figures, h is the vertical distance from the tray floor and z is the horizontal distance from the inlet downcomer. The concentrations shown were subject to a considerable error, chiefly because of the difficulty in obtaining liquid phase samples from the two-phase liquid and gas mixture. For the water-carbon dioxide system there was a layer of liquid near the tray floor which had a very low concentration of carbon dioxide. This layer also seemed to extend around the periphery of the plate. The concentration profiles were apparently almost independent of the gas and liquid flow rates. The layer of liquid of low carbon dioxide concentration was not as prevalent in the glycol-carbon dioxide system. Figure 32 indicates typical concentration profiles calculated from equation 36 in comparison with experimental ones. It is noted that the calculated profiles only roughly approximate the experimental data.

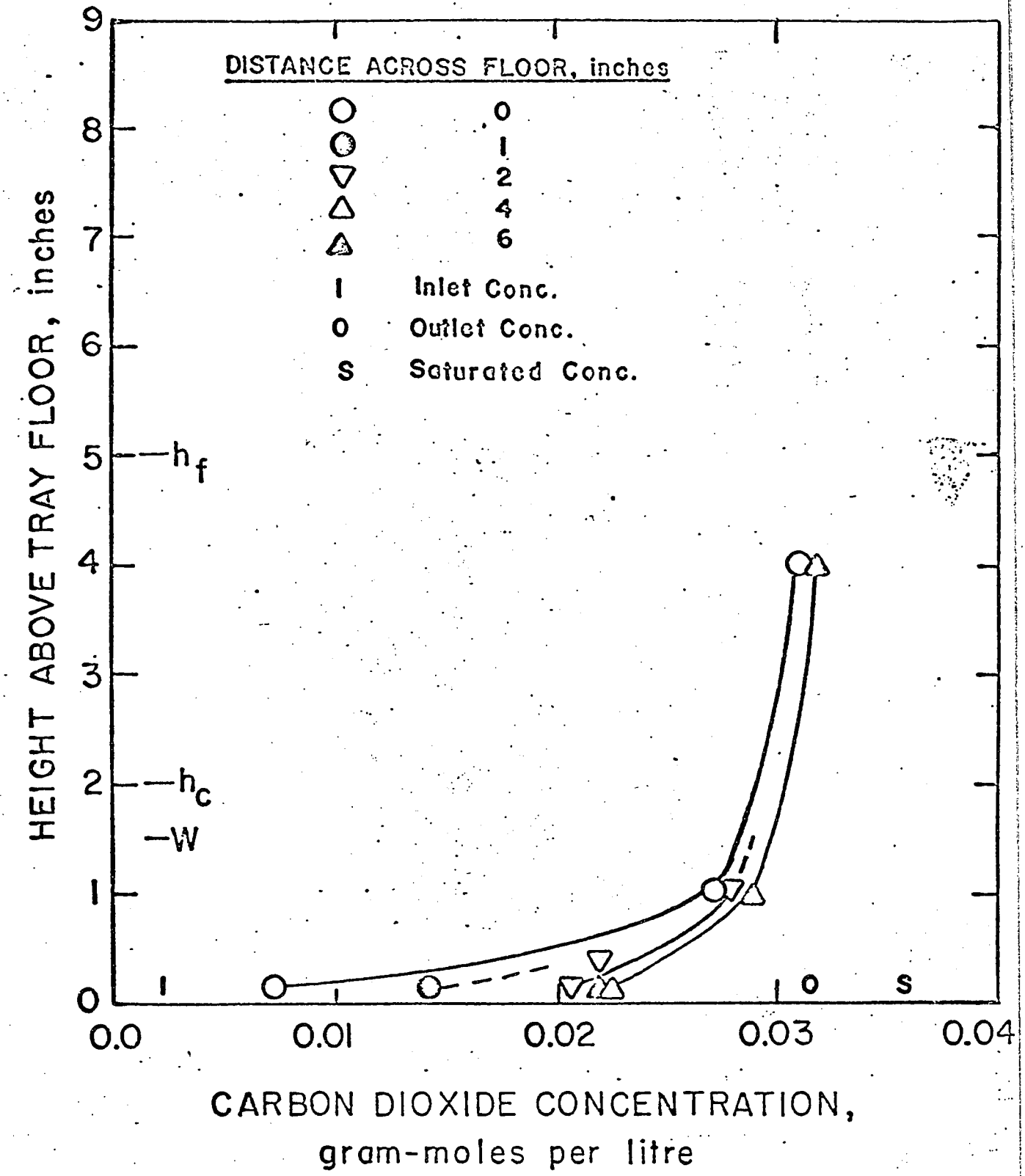

Figure 27. Concentration Profile for Water and Carbon Dioxide
L = 1.0 gpm.; Q = 0.295 cu. ft./sec.

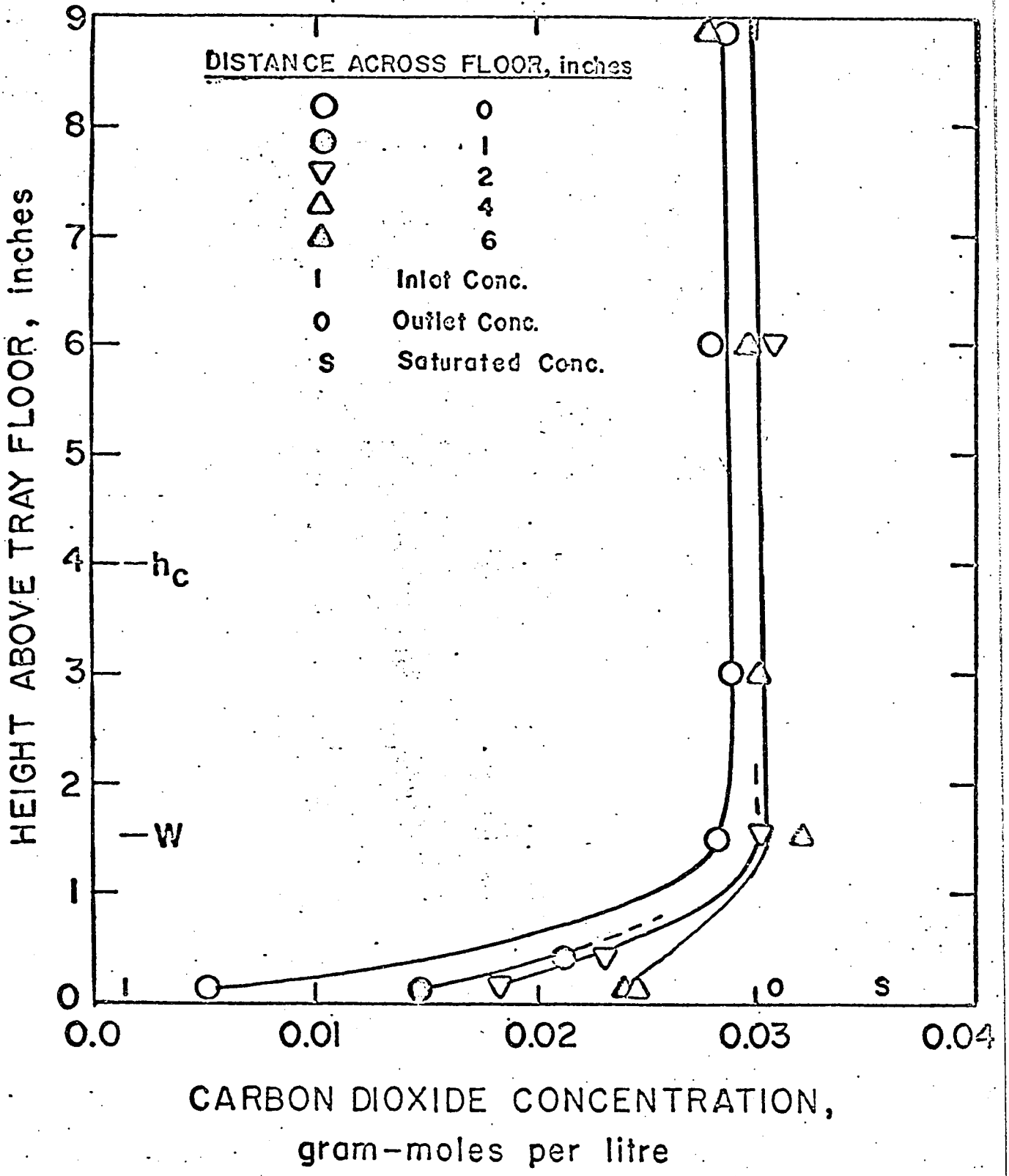

Figure 28. Concentration Profile for Water and Carbon Dioxide
L = 1.0 gpm.; Q = 0.51 cu. ft./sec.

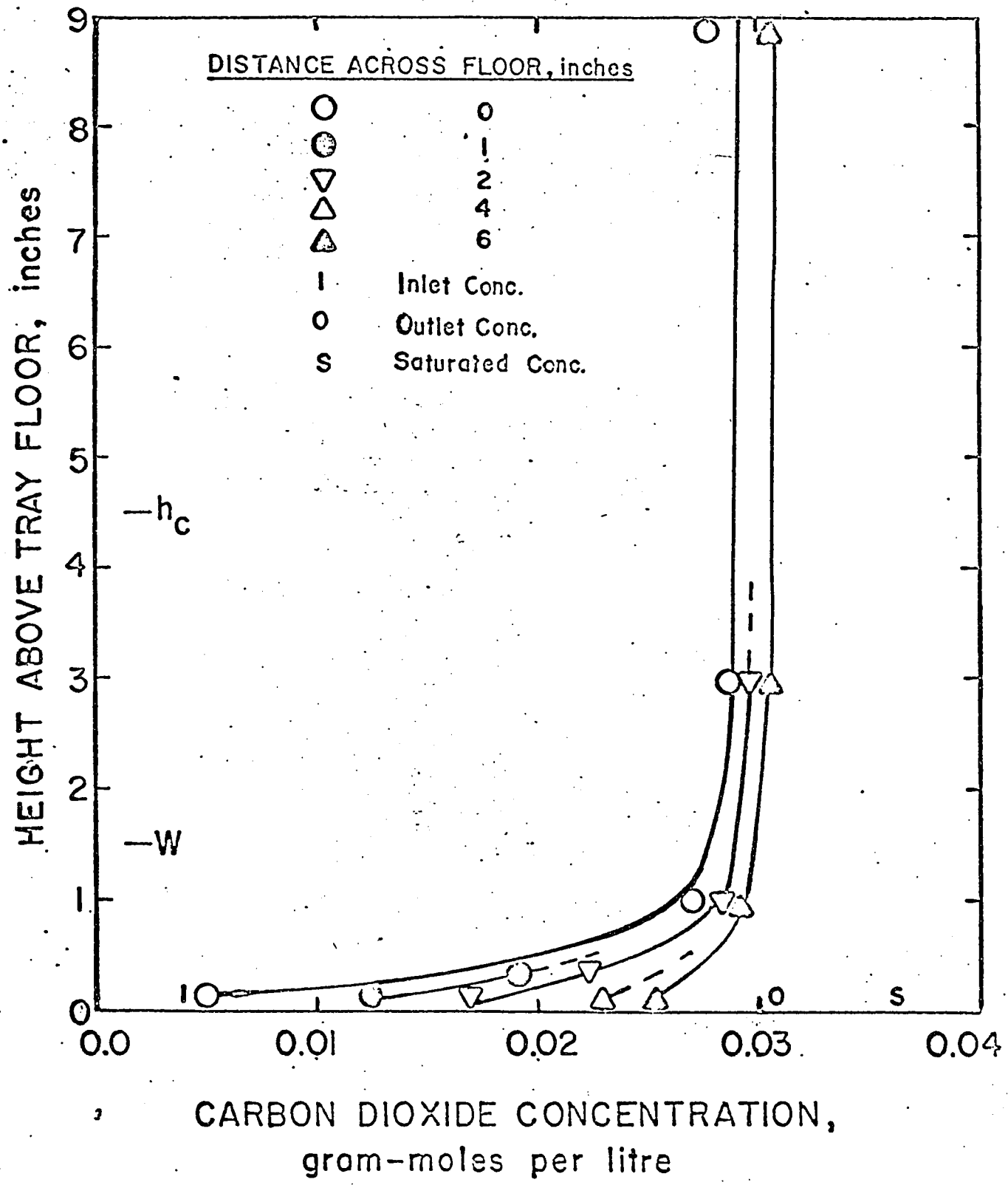

Figure 29. Concentration Profile for Water and Carbon Dioxide

L = 2.0 gpm.; Q = 0.315 cu. ft./sec.

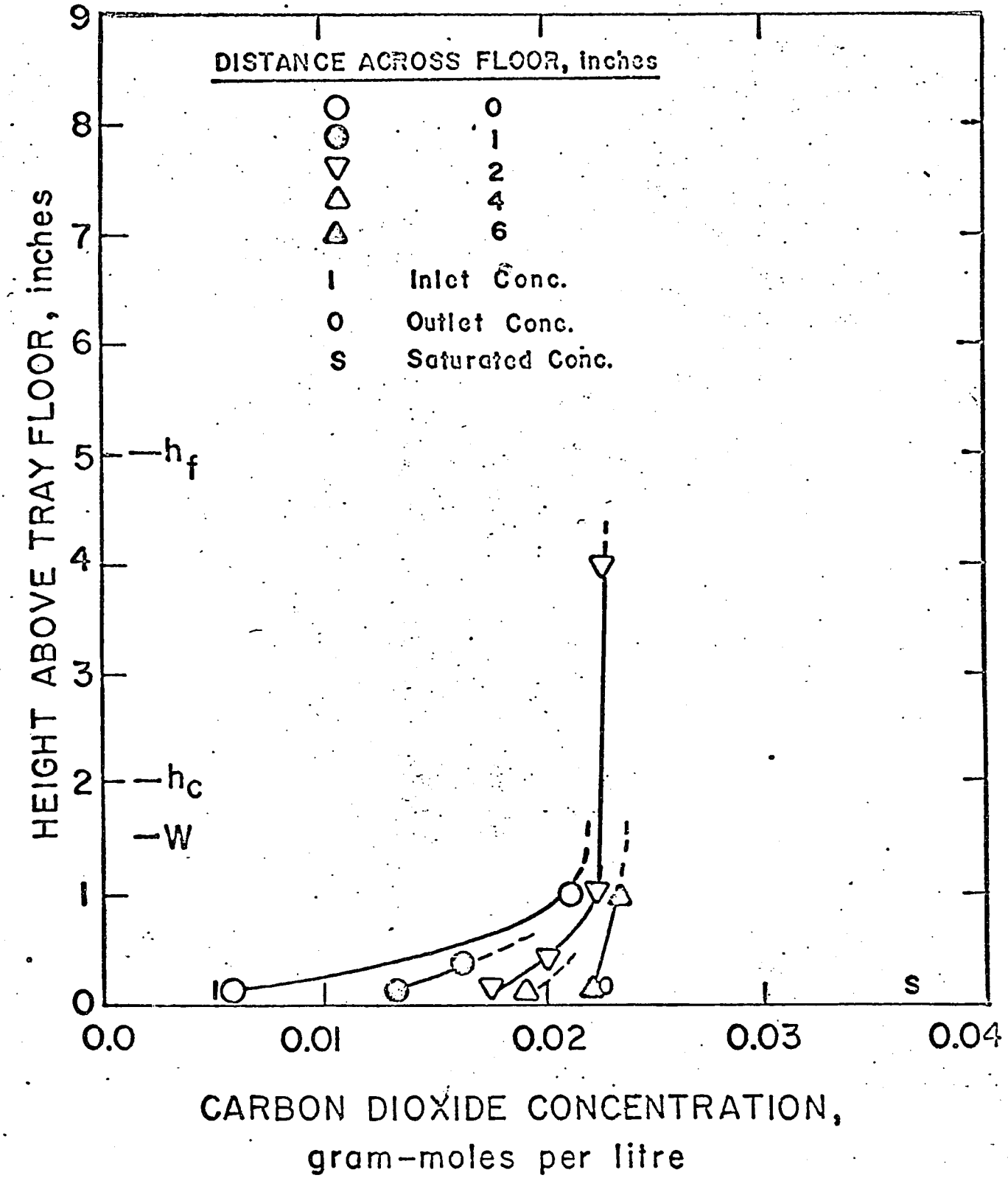

Figure 30. Concentration Profile for Water and Carbon Dioxide
L = 4.0 gpm.; Q = 0.246 cu. ft./sec.

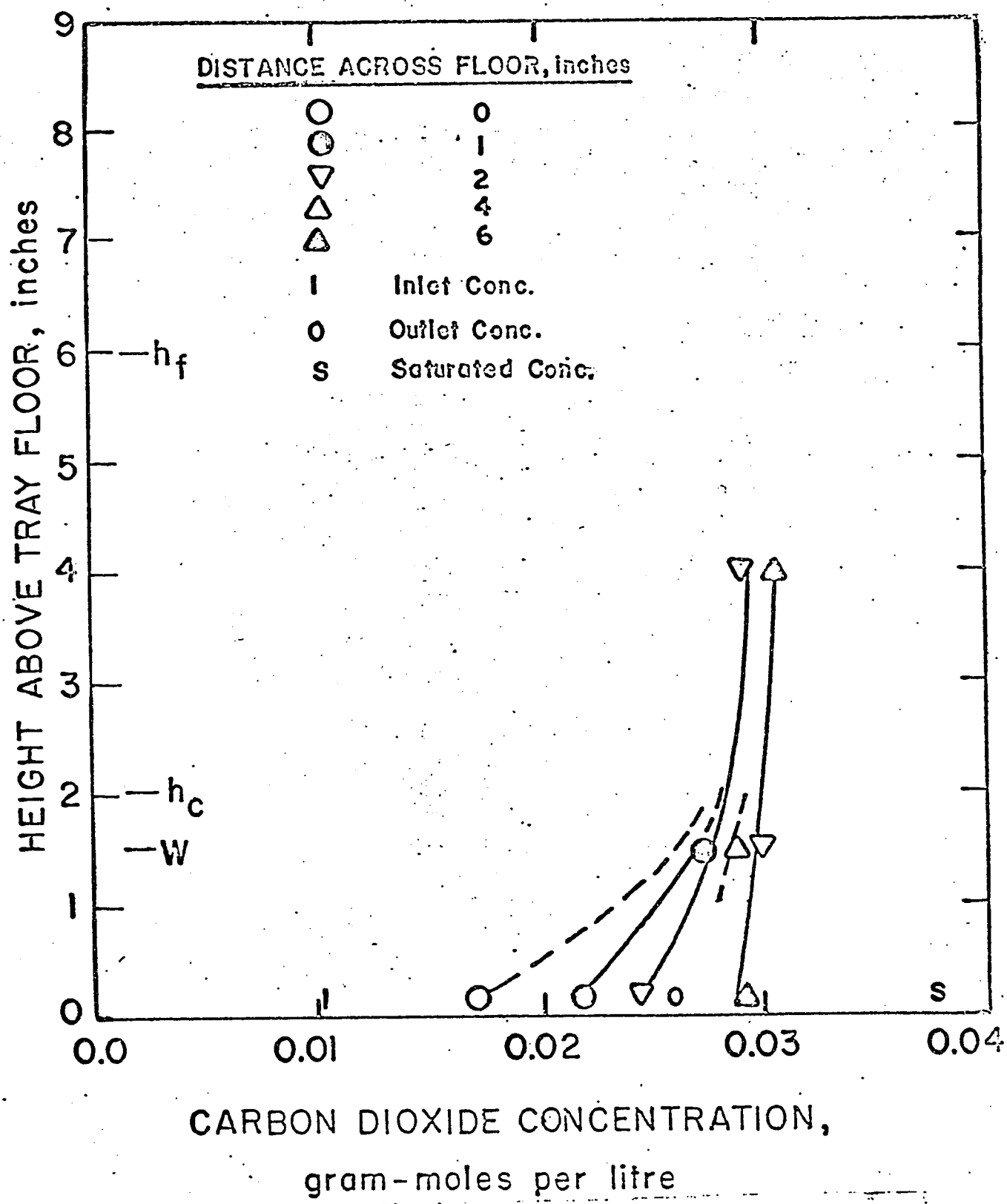

Figure 31. Concentration Profile for Glycol and Carbon Dioxide

L = 1.0 gpm.; Q = 0.44 cu. ft./sec.

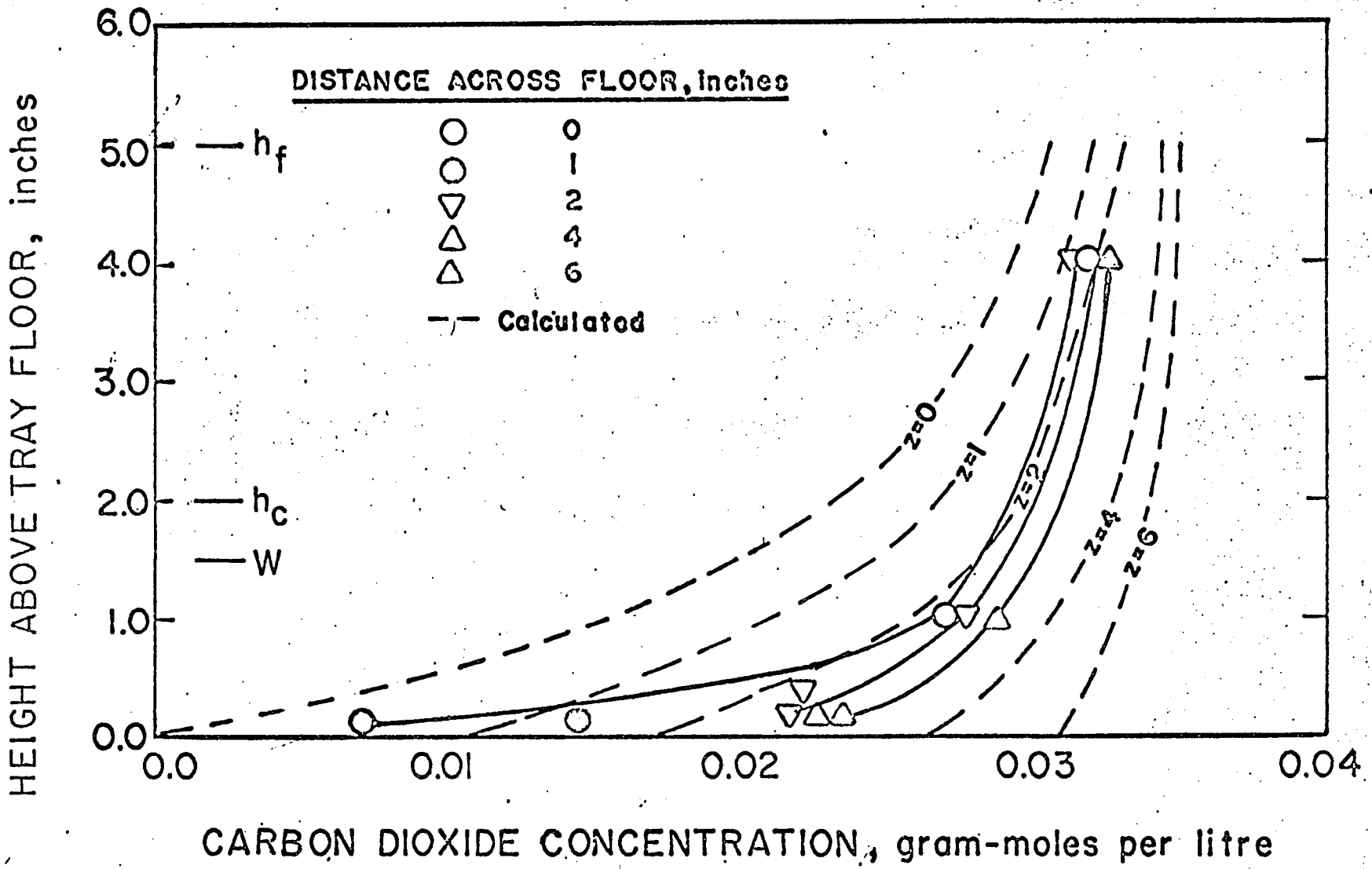

Figure 32. Calculated Concentration Profile for the Water-Carbon Dioxide System,

Liquid flow rate: 1.0 gpm.

Gas flow rate: 0.295 cu. ft./sec.

D. Mass Transfer

The experimentally measured concentration profiles were graphically integrated to give the number of transfer units which are shown in Figure 33. Excluding the glycol-carbon dioxide system, the values obtained for the number of transfer units favoured the plug flow model. As a result, the number of transfer units were calculated using equation 9. For the glycol, the number of transfer units were calculated from

$$N_{tL} = 1.9 \ln \left[1.0 + \frac{E_{ML}}{1.9(1.0-E_{ML})} \right] \qquad (37)$$

This is an emperical equation which was used to relate the Murphree liquid efficiency to the number of transfer units when the liquid was partially mixed (13). The numerical constant, 1.9, was calculated from experimental data. Some typical values of a length of a transfer unit, calculated from equation 12, are shown in Figure 34.

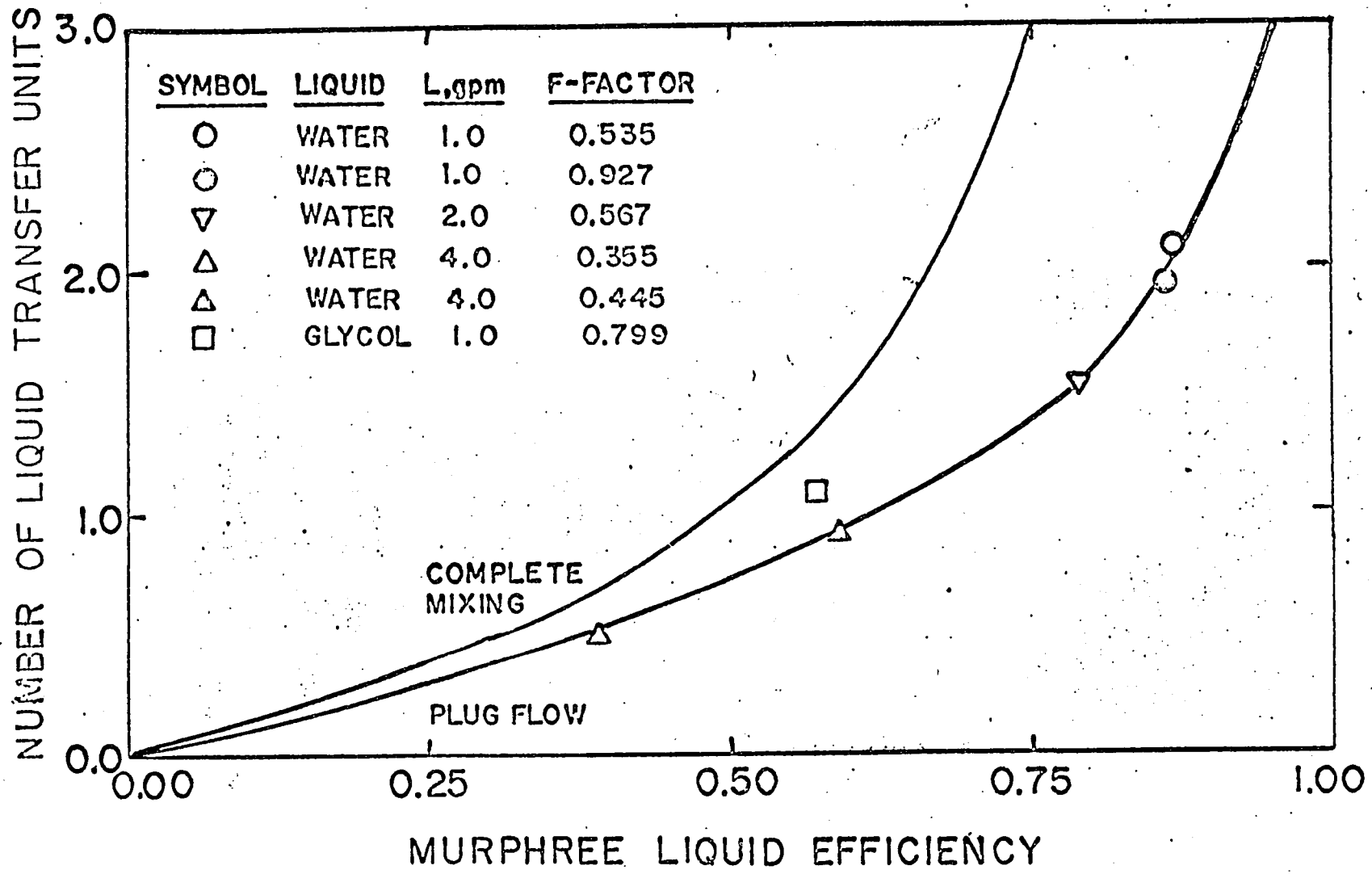

Figure 33. Number of Mass Transfer Units versus Murphree Liquid Efficiency

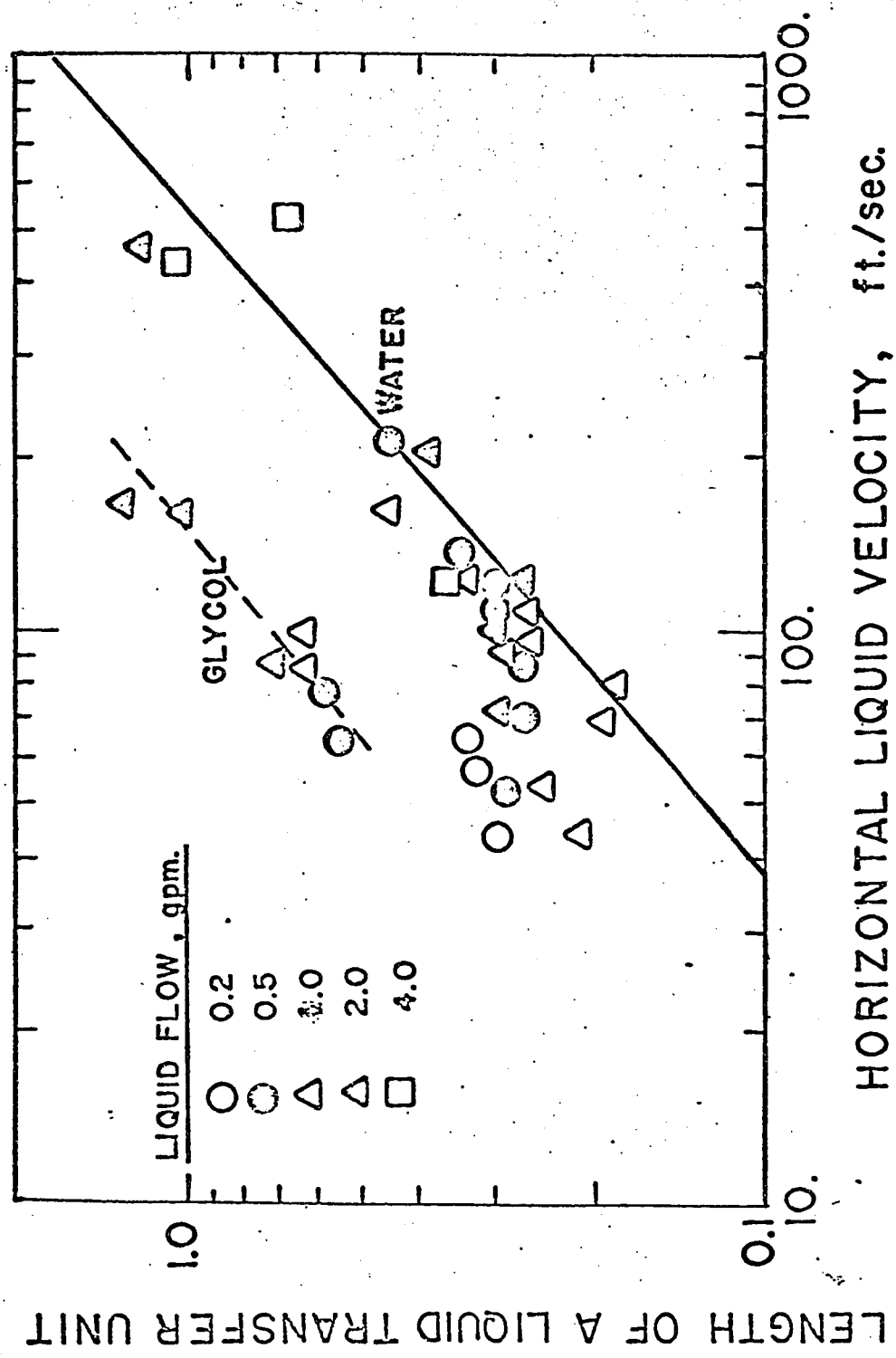

Figure 34. Length of a Transfer Unit versus Horizontal Liquid Velocity Correlation

E. Visual Results

The photographs show the difference in performance between large and small holes. The top and bottom plates had holes of 1-inch and 1/4-inch diameter, respectively. Two types of froth were observed, one which formed at only low gas flow rates and consisted of large coarse varying-sized bubbles as shown in Figures 37 and 38, and the other which occurred at intermediate and high gas flow rates and consisted of small bubbles nearly uniform in size as shown in Figures 39 and 40. The division line between the two types of froth was indistinct although the first type usually began to appear as the gas flow rate was reduced below the weeping point.

At extremely low gas flow rates when considerable weeping started, the liquid layer had the appearance of a pool of liquid through which bubbles were rising. Usually the trays were covered with a froth. Above the froth droplets of liquid were sprayed up by the gas into a clear zone as shown in Figures 38 and 39. The demarcation line between the froth and the clear zone above it was quite distinct.

With large hole sizes and low liquid flow rates, the liquid was sprayed from the tray floor. The liquid oscillated from one side of the tray to the other, and the froth lacked the fine bubble structure obtained with smaller holes. However, the efficiency was still quite high. The physical appearance of glycol above the tray was different from that of water. The glycol froth lacked the fine bubble structure. The effect of increasing liquid flow rate at a constant gas rate can be seen

in Figures 37, 38, and 39. At a constant liquid flow rate, the effect of increasing gas flow rate can be seen by the series of Figures 40, 41, 42, and 39.

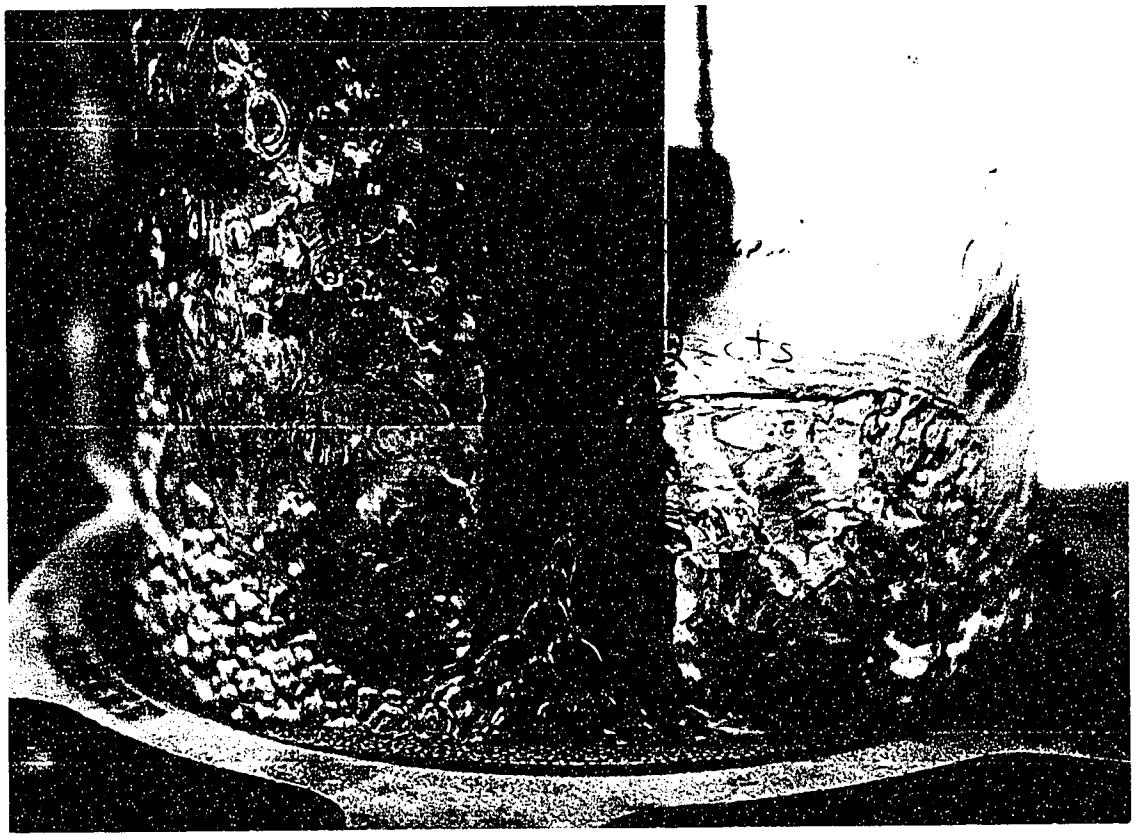

Figure 35

Bubbling action on plate with 1-inch diameter holes.

Gas flow rate: 0.2 cu. ft./sec.

Liquid flow rate: 1.0 gpm.

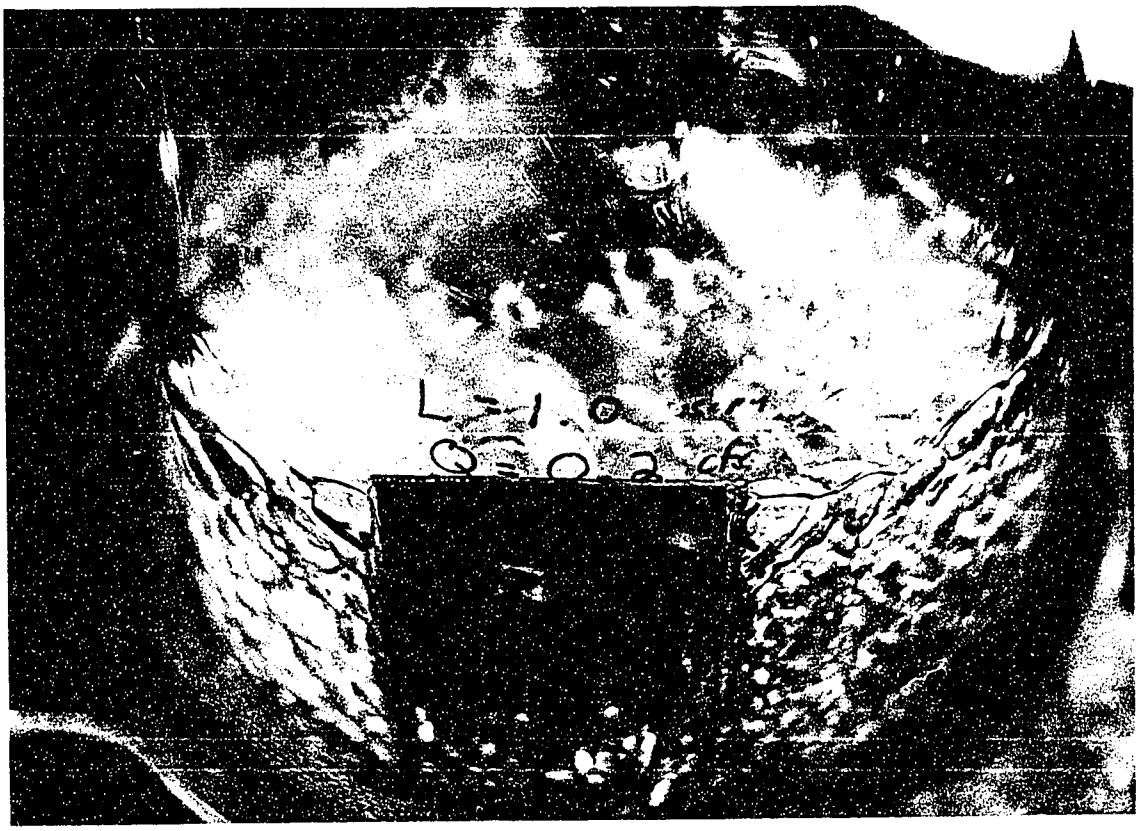

Figure 36

Bubbling action on plate with 1/4-inch diameter holes.

Gas flow rate: 0.2 cu. ft./sec.

Liquid flow rate: 1.0 gpm.

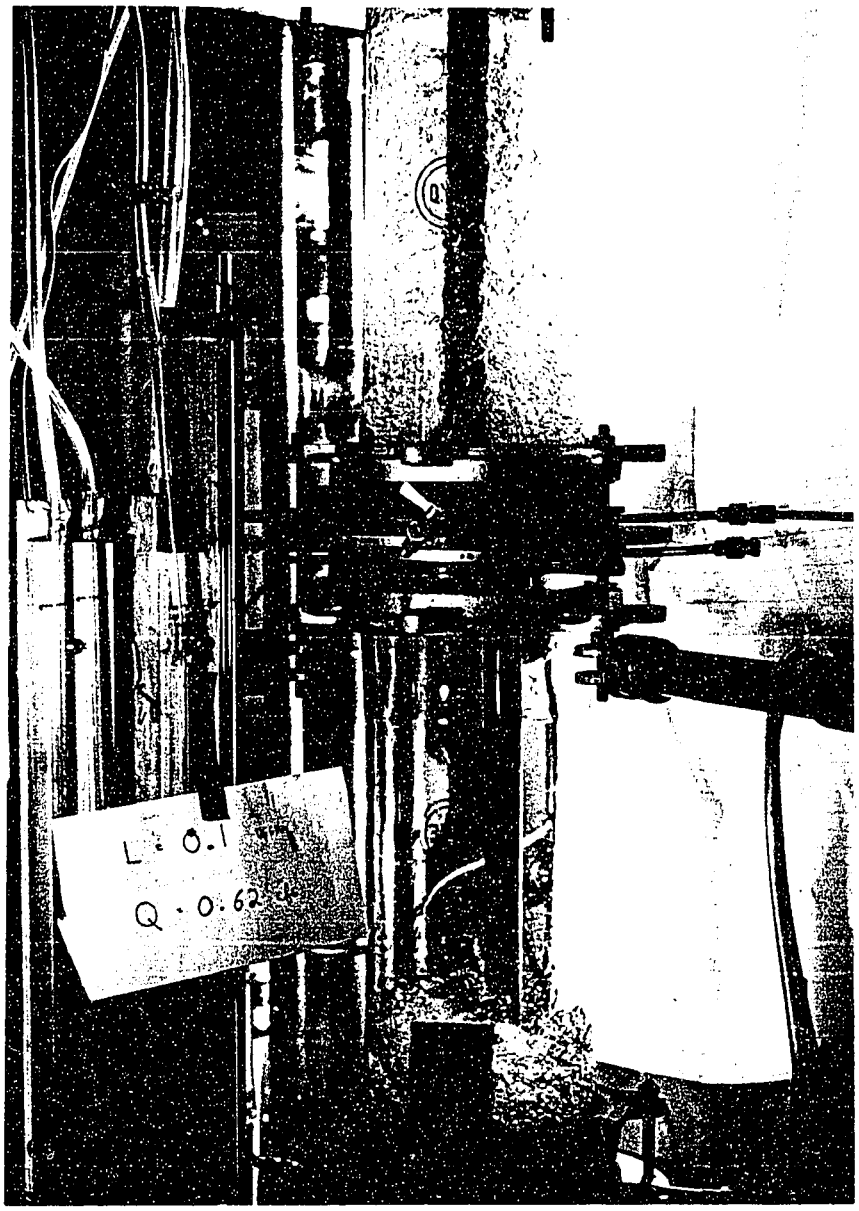

Figure 37

Comparison of froth formed using large and small diameter holes.

Gas flow rate: 0.62 cu. ft./sec.

Liquid flow fate: 0.1 gpm.

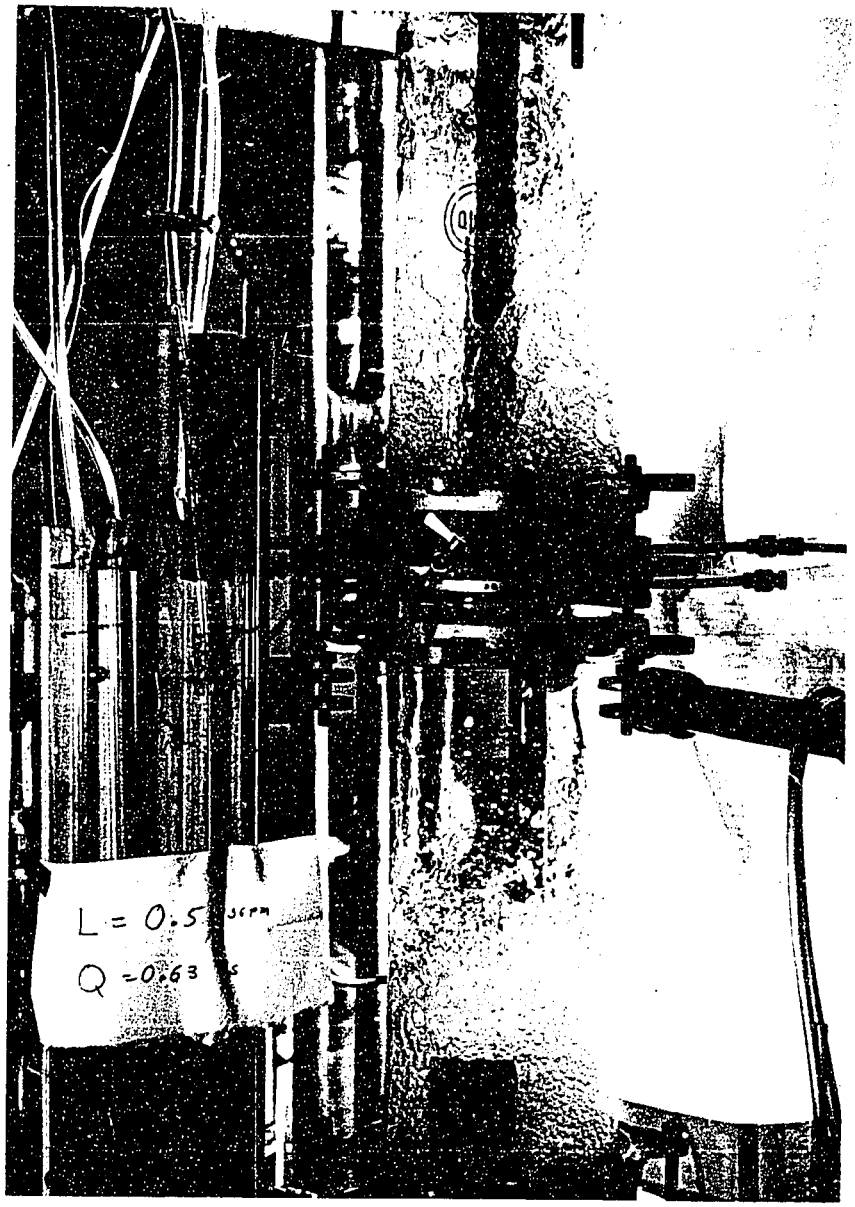

Figure 38

Comparison of froth formed using large and small diameter holes.

Gas flow rate: 0.63 cu. ft./sec.

Liquid flow rate: 0.5 gpm.

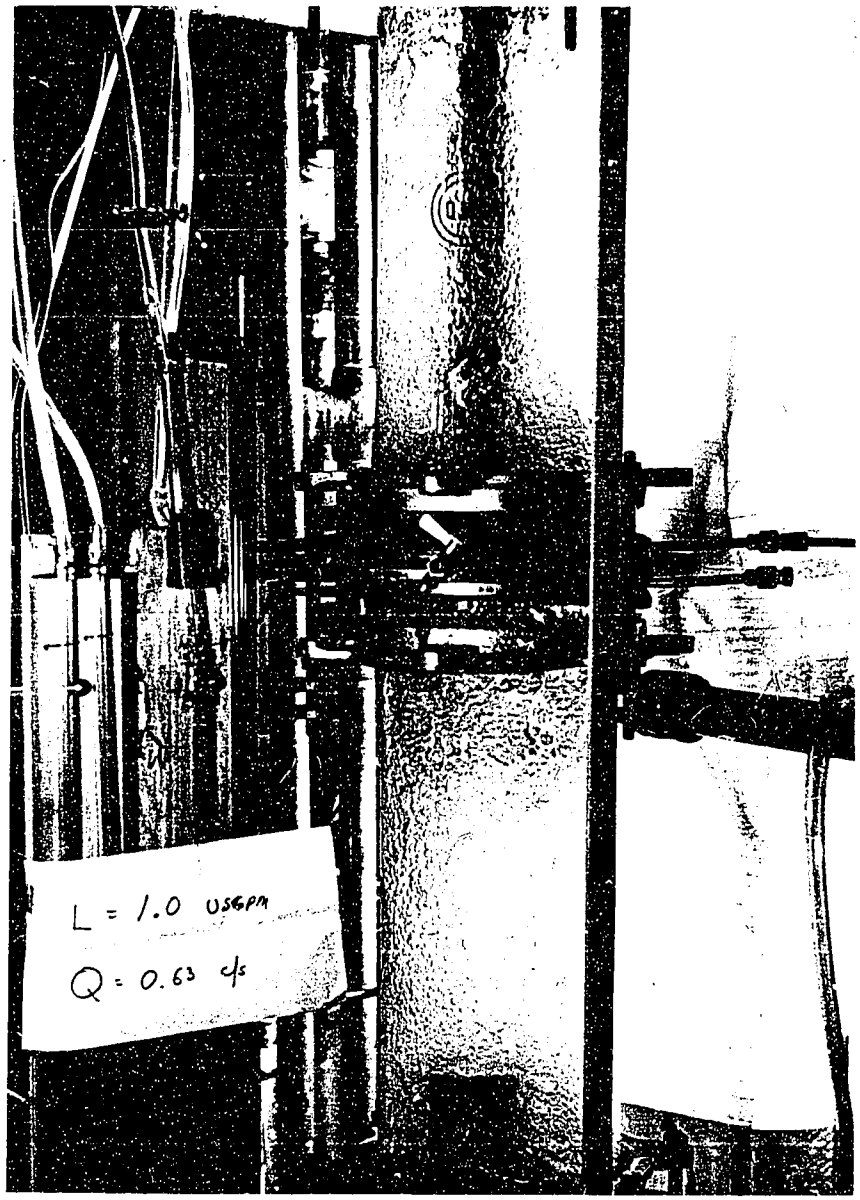

Figure 39

Comparison of froth formed using large and small diameter holes.

Gas flow rate: 0.63 cu. ft./sec.

Liquid flow rate: 1.0 gpm.

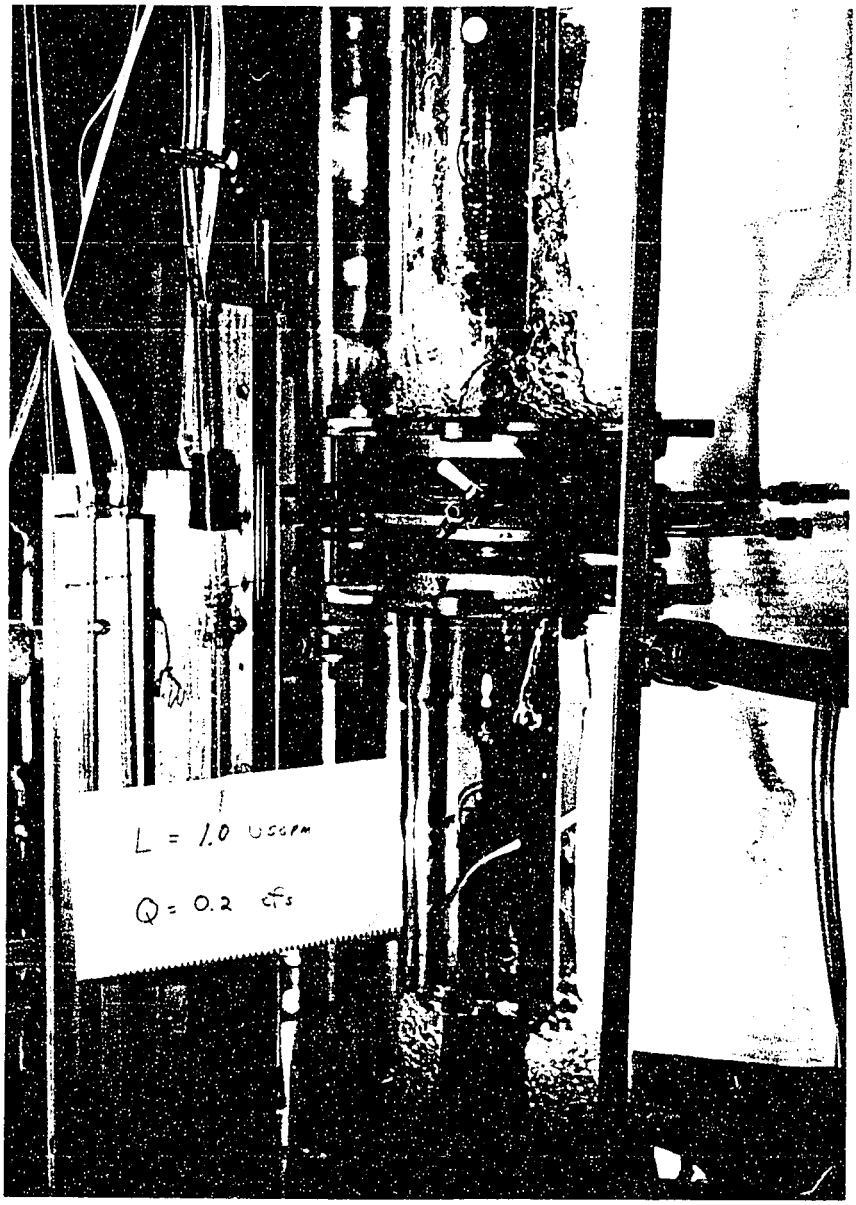

Figure 40

Comparison of froth formed using large and small diameter holes.

Gas flow rate: 0.2 cu. ft./sec.

Liquid flow rate: 1.0 gpm.

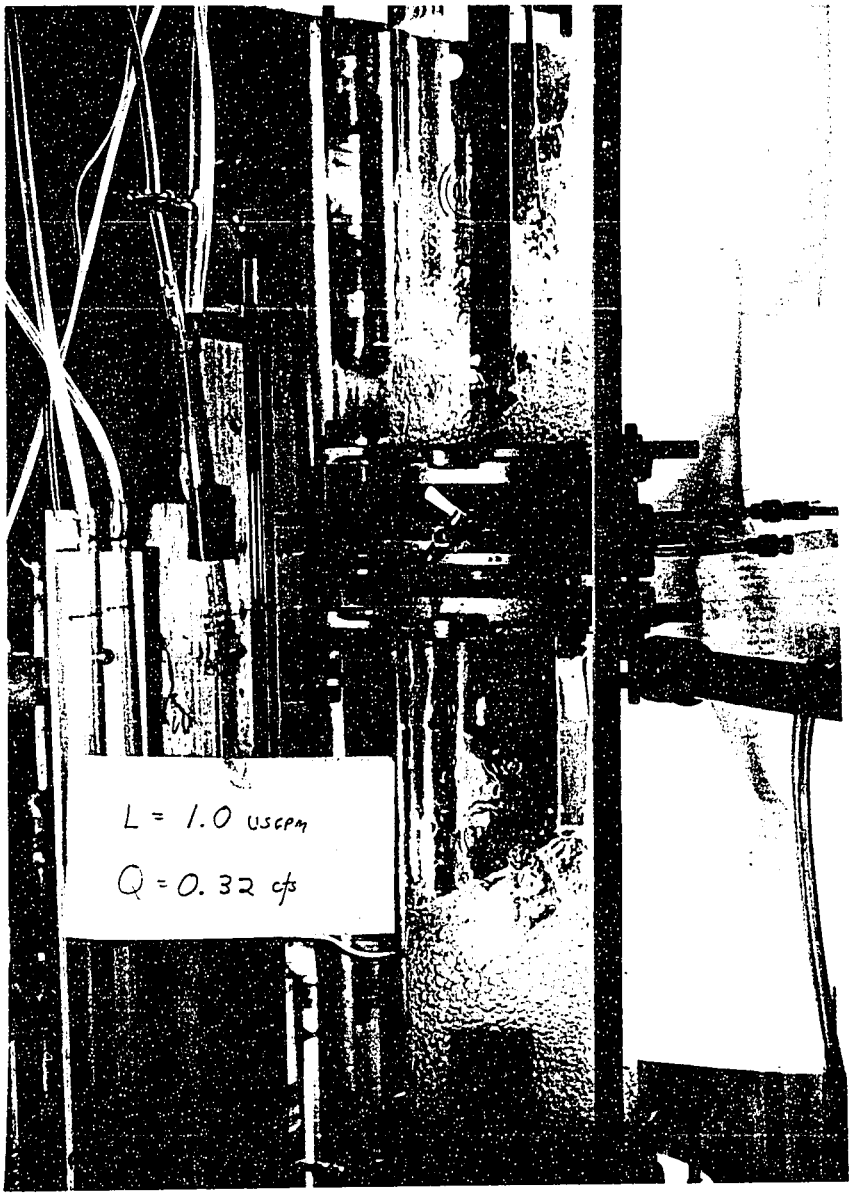

Figure 41

Comparison of froth formed using large and small diameter holes.

Gas flow rate: 0.32 cu. ft./sec.

Liquid flow rate: 1.0 gpm.

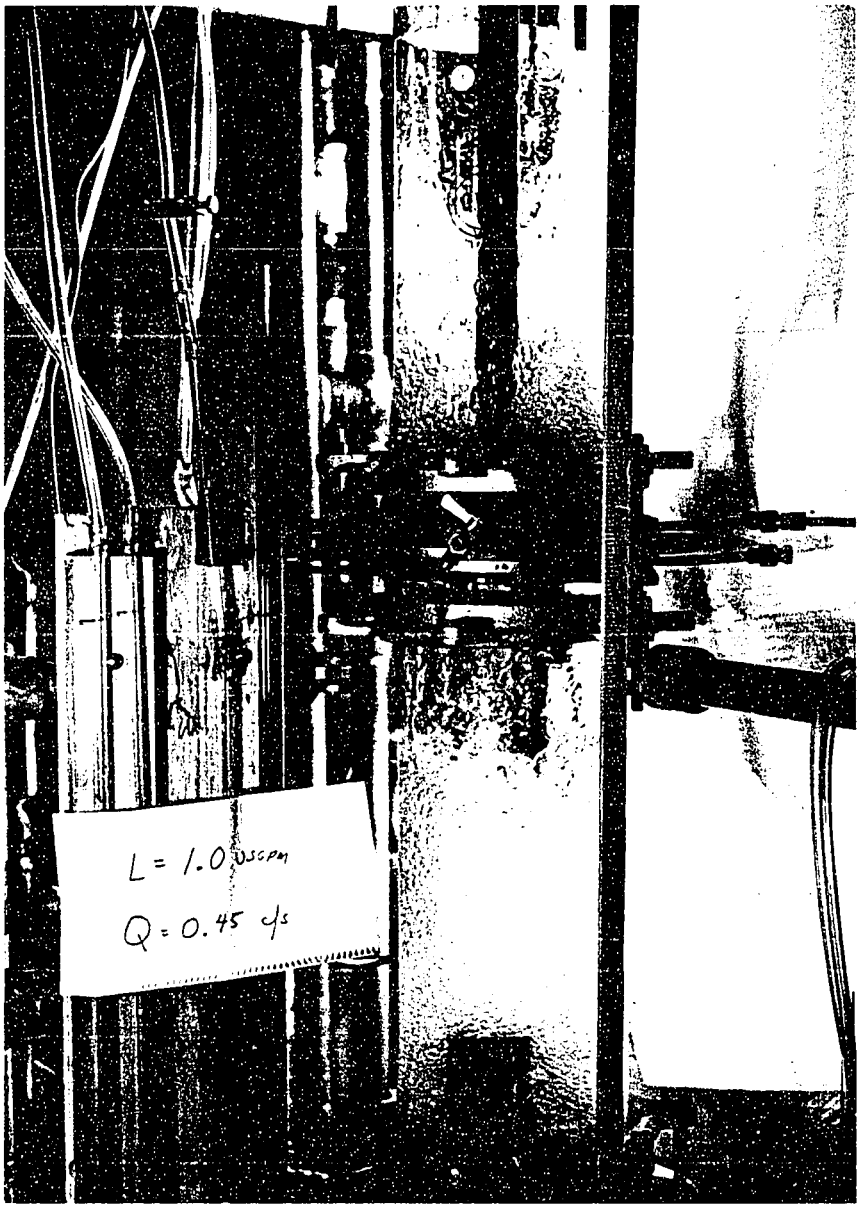

Figure 42

Comparison of froth formed using large and small diameter holes.

Gas flow rate: 0.45 cu. ft./sec.

Liquid flow rate: 1.0 gpm.

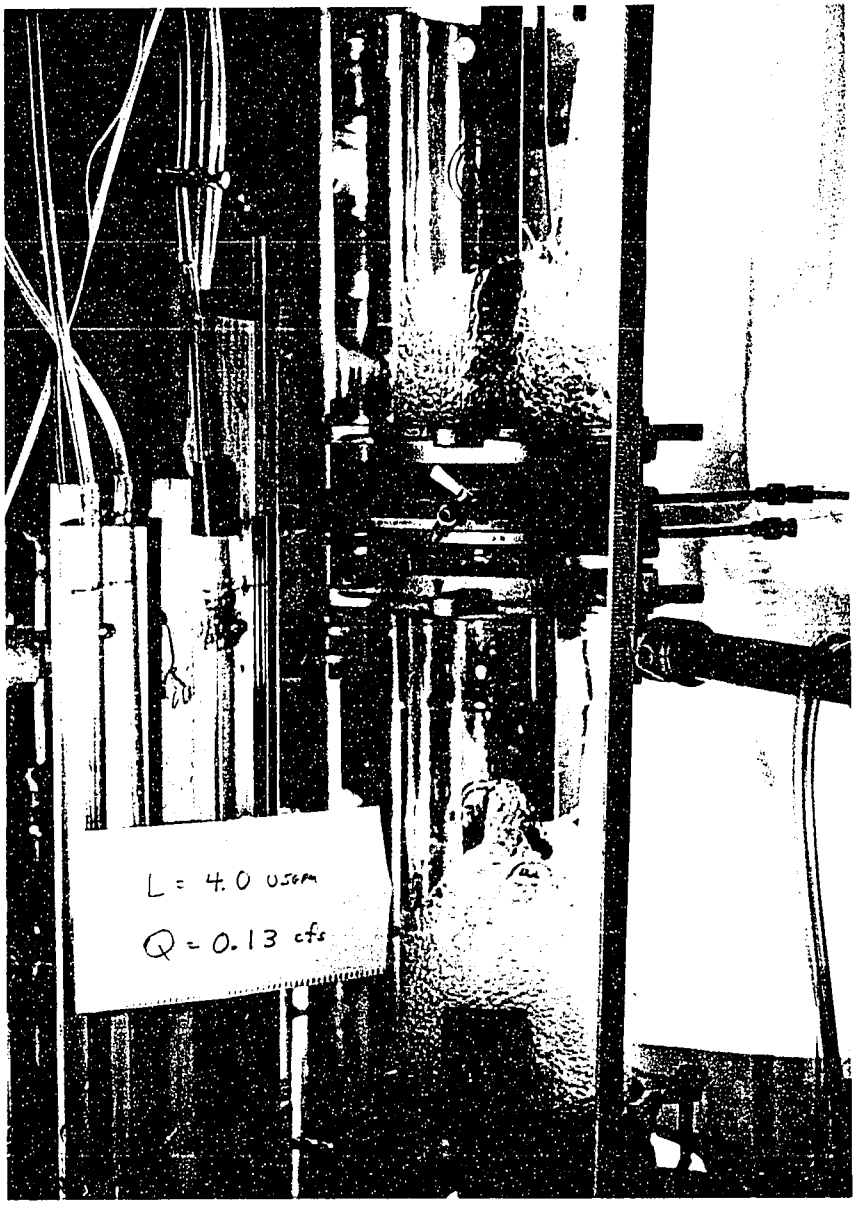

Figure 43

Comparison of froth formed using large and small diameter holes.

Gas flow rate: 0.13 cu. ft./sec.

Liquid flow rate: 4.0 gpm.

DISCUSSION

A. Murphree Liquid Efficiency

Generally the efficiency was found to be almost independent of the gas flow rate except in the weeping region. For the higher liquid flow rates (0.5 to 2.0 gpm.) the efficiency seemed to reach a maximum value and then decline with increasing gas flow rate. This effect was the result of flooding and some entrainment from the tray below. Minor weeping had almost no adverse effect on the efficiency. Even although weeping occurred the mixing was still considerable because of downcomer design and the large liquid holdup. When weeping was severe the efficiency dropped drastically. For F-factors less than 0.3, heavy weeping resulted in liquid by-passing the tray and the efficiency was reduced. The effect of the lowest liquid rate (0.1 gpm.) on efficiency was a result of an inability to obtain an accurate sample of the inlet liquid. Similar behavior has been observed elsewhere (51).

It was apparent that the hole diameter had almost no effect on the Murphree liquid efficiency. The data for the liquid flow rates greater than 0.1 gpm. with all hole sizes were plotted in Figure 44. It is apparent that for an eight fold range of hole diameters, a twenty fold range of liquid flow rates, and a ten fold range of gas flow rates, the efficiency was consistently high. A least squares linear regression of the data for the water-carbon dioxide system produced the following equation

$$E_{ML} = 0.772 - 0.012F - 0.020L + 0.010D_h \qquad (38)$$

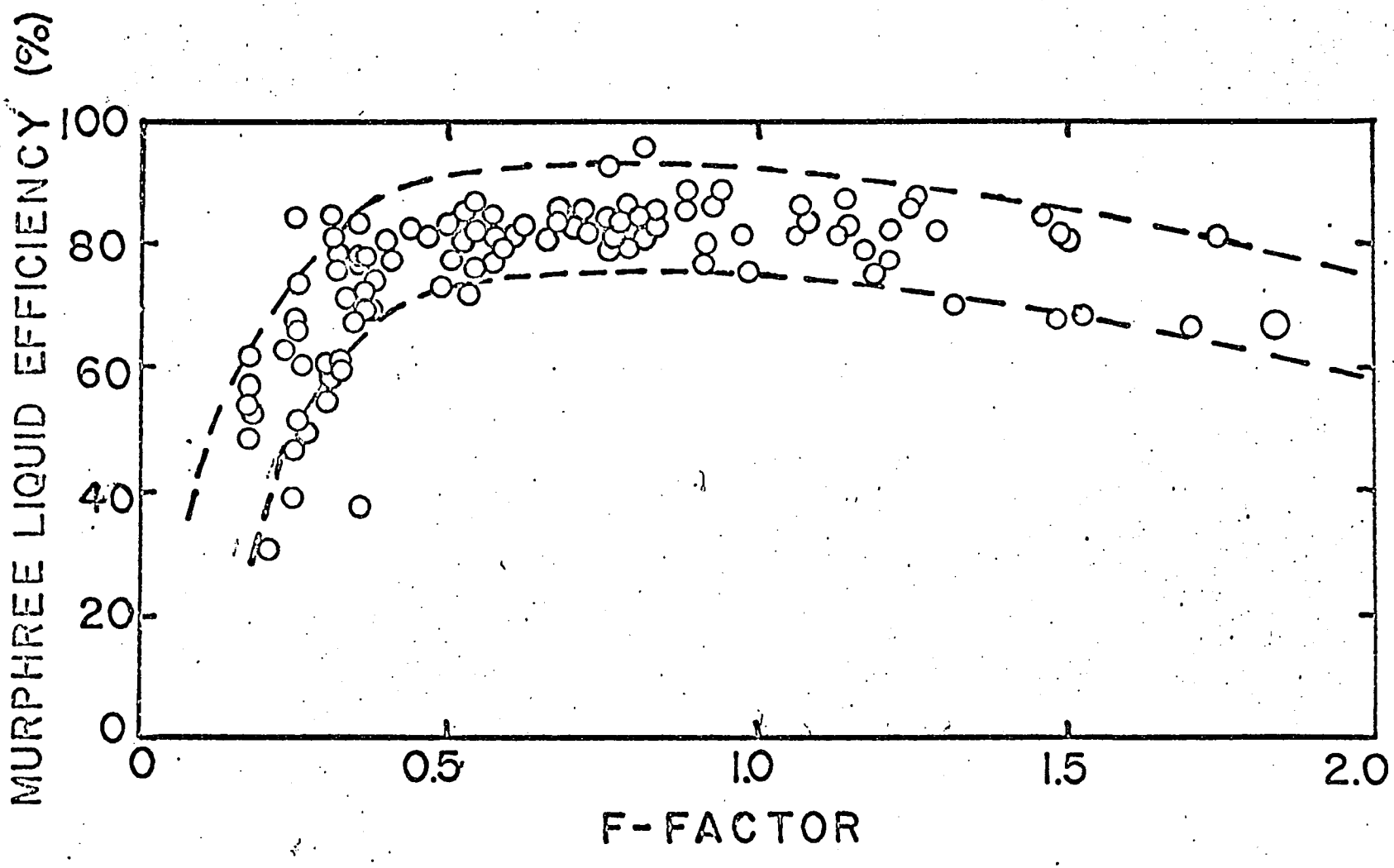

Figure 44. Generalized Murphree Liquid Efficiency versus F-factor for the Water-Carbon Dioxide System

Both correlations readily show the small dependence of the efficiency upon the gas flow rate, the liquid flow rate, and the hole diameter. Both Figure 44 and equation 38 are correlated to within ±10%. It seemed that the 1-inch diameter holes produced a smaller operating range than the smaller hole sizes. This was correct for low liquid flow rates but for liquid flow rates of 0.5 gpm. and higher the operating regions for all hole diameters were similar. The limiting operational factor appeared to be the liquid handling capacity of the downcomer. Literature correlations (52,53) were used to estimate the efficiency of the water-carbon dioxide system at approximately 70%.

It has been found experimentally that the interfacial area increased with increasing gas flow rate until it reached a maximum value. With further increases in gas flow rate the interfacial area was reduced because of non-uniformity of bubble sizes and jetting which caused the formation of larger elongated bubbles (54). The interfacial area has been found to vary inversely with hole diameter for small holes up to 1/4-inch in diameter. There is some evidence that large diameter bubbles are unstable in low viscosity fluids (49,55) and break up into small bubbles. It was observed that bubble sizes were almost independent of hole sizes as shown in Figures 38, 39, 41, 42, and 43. The 1-inch diameter holes still formed small bubbles about the size of those formed by the 1/4-inch diameter holes. Hence interfacial area is independent of large hole diameter. It was concluded that $k_L a$ is independent of hole diameter, that is that for smaller holes k_L is probably less than the value for larger

holes, at comparable gas and liquid flow rates.

The efficiency for the glycol-carbon dioxide system was less than the efficiency of the water-carbon dioxide system with similar operating conditions. The diffusivity of carbon dioxide in the glycol solution was 0.39×10^{-5} sq. cm./sec., while the diffusivity of carbon dioxide in water was 1.94×10^{-5} sq. cm./sec. (50). The viscosity of the glycol solution was 15.8 centipoises while the viscosity of the water was 1.0 centipoises (50). Both effects might be expected to cause a reduction in tray efficiency. The efficiency of the glycol-carbon dioxide system depended heavily on the gas and liquid flow rates as shown in Figure 17. A linear regression of the data produced

$$E_{ML} = 1.05 - 0.18F - 0.20L \qquad (39)$$

As the liquid flow rate was increased, the contacting time between the liquid and the gas was reduced so that less gas was absorbed and the efficiency was decreased.

Although entrainment was not studied, general correlations (4,46) were used to determine that entrainment was negligible and no correction was necessary to account for the effect of it on the efficiency.

B. Dry and Wet Plate Hydraulics

Because of friction losses in the perforations, large diameter holes can have higher pressure drops than small diameter holes. This phenomenon has been observed by others (5,12). The correlation presented in Figure 18 was useful in predicting dry plate pressure drops.

Wet plate pressure drop data were difficult to interpret.

Equation 21 was valid in correlating the wet plate pressure drop, h_w, but correlations for the equivalent clear liquid depth were not sufficiently accurate. The data were correlated (to ±25%) with linear regression equations similar to equation 23. For the water-carbon dioxide system:

$$h_w = -0.56 + 3.72F + 1.56L - 0.36D_h \quad (40)$$

$$h_c = -0.06 + 1.43F + 1.51L - 0.54D_h \quad (41)$$

$$h_f = -1.00 + 8.19F + 3.55L - 2.07D_h \quad (42)$$

For the glycol-carbon dioxide system:

$$h_w = 1.81 + 1.50F + 0.93L \quad (43)$$

$$h_c = 2.65 - 1.00F + 1.16L \quad (44)$$

$$h_f = 7.25 + 1.11F + 1.37L \quad (45)$$

The effect of hole size was small for h_w, h_c, and h_f. The residual pressure drop (equations 21 and 22) was very small and could be assumed to be 0.5 inches of water with no loss in accuracy. The observed results that h_R could be positive or negative were a result of measurement error.

The lower operating limit of the column was determined by weeping. Correlations for the start of weeping were given in Figures 25 and 26. Large holes began to weep at a higher gas flow rate than small holes because the liquid surface tension was not sufficient to keep liquid from falling through the holes at low gas flow rate. The glycol began to weep at a higher gas flow rate than the water. However, this was expected because the surface tension of glycol is 56.3 dynes/cm. while the surface tension of water is 72.4 dynes/cm. (24). Because

of the importance of determining the minimum gas flow rate to prevent weeping, Figure 26 was a more useful correlation than Figure 25.

The upper operating limit of the column was determined by flooding. Correlations (39) were used to predict that the flooding of the downcomer was the limiting condition rather than the flooding of the column. However, large liquid depths (up to 10 inches of water) on the trays seemed to offer no operating problems.

C. Concentration Profiles

The liquid layer of low carbon dioxide concentration has been observed by others (13,18,37). Eden (37) noted that for high liquid flow rates the gas tended to channel through the liquid at some distance before agitating it while near the walls and tray floor the liquid remained essentially unmixed. For the glycol solution, the concentration of carbon dioxide was a function of both h and z everywhere on the tray. The layer of liquid of low carbon dioxide concentration was not as prevalent in the glycol as it was in the water.

It was a basic assumption in the derivation of the profile equation (equation 36) that the liquid flow rate was constant everywhere in the froth above the tray. It appears possible that the liquid velocity profile in the vertical direction is not uniform. In fact the appearance of the concentration profiles suggests that a region of higher velocity exists near the surface of the tray, so that the bulk of the liquid flows adjacent to the tray floor and then up to the overflow weir. Such a flow

pattern would explain the observed concentration profiles. No verification was possible because local velocities were not measured.

D. Mass Transfer

The concept of plug flow was used often for large trays, but even these small trays seemed to approximate the plug flow model. For the glycol-carbon dioxide system, the number of mass transfer units was higher than the number predicted using the simple plug flow model. It was concluded that the mixing of the glycol solution was better than the mixing of the water. The length of a transfer unit was correlated and was in agreement with the literature results except for the low liquid flow rates. The results were almost independent of the gas flow rates. According to Sherwood and Pigford (1), the length of a transfer unit increased with viscosity, and hence the number of transfer units decreased. The number of transfer units for the high viscosity glycol was about half the number of transfer units for water under similar liquid and gas flow conditions. Moreover, the length of a transfer unit for the higher viscosity glycol was greater than the length of a transfer for water as shown in Figure 34.

E. Visual Results

Even though the mixing action with large holes appeared different than the mixing action with small holes, the efficiencies did not show any effect. The fine bubble structure and large interfacial area may not be essential for mass transfer in a liquid phase controlled system. The trilayer

effect has been observed elsewhere (18,48). Although the bottom liquid layer was not seen all the time because of the froth, the concentration profiles tended to strengthen the theory that a layer of liquid near the tray floor was probably always present to some extent.

CONCLUSIONS

1. Performance of sieve trays with large diameter holes could be expected to be comparable to those hole sizes more frequently used in liquid phase controlled absorption processes. When fouling is expected to be significant, sieve holes of large diameter could be used with almost no decrease in efficiency.
2. The combined effect of a large increase in solvent viscosity and a decrease in solute diffusivity in the solvent did not alter the efficiency of the gas-liquid contacting to any large extent.
3. Unless there is experimental data to prove otherwise, it is probably advantageous to assume the plug flow mixing model and to use the length of a transfer unit concept for liquid phase controlled gas-liquid contacting systems.
4. For the theoretical concentration profile, it was concluded that the velocity profile of the liquid was essential to the model used. With local liquid velocity distributions and the concentration profiles known, an accurate description of the mass transfer mechanism on sieve trays could be determined.

REFERENCES

1. Sherwood, T. K., and Pigford, R. L., "Absorption and Extraction", 1952 (McGraw Hill Book Company Ltd., New York).
2. Ellis, S. R. M., and Moyade, H. K., Brit. Chem. Eng., 4, 342 (1959).
3. Foss, A. S., and Gerster, J. A., Chem. Eng. Prog., 52, 28 (1956).
4. Huang, C. J., and Hodson, J. R., Pet. Ref., 37, 103 (1958).
5. McAllister, R. A., McGinnis, P. H., and Plank, C. A., Chem. Eng. Sci., 9, 25 (1958).
6. Harris, I. J., and Roper, G. H., Can. J. Chem. Eng., 40, 245 (1962).
7. Rennie, J., and Evans, F., Brit. Chem. Eng., 7, 498 (1962).
8. Jones, J., and Pyle, C., Chem. Eng. Prog., 51, 424 (1955).
9. Lee, D. C., Chem. Eng., 61, 179 (1954).
10. Prince, R. H., International Symposium on Distillation, 177 (1960).
11. Arnold, D., Chem. Eng. Prog., 45, 663 (1952).
12. Hunt, C., Hanson, D. N., and Wilke, C. R., AIChE Journal, 1, 441 (1955).
13. American Institute of Chemical Engineers Final Report, University of Michigan, 1960.
14. Smith, B. D., "Design of Equilibrium Stage Processes", 1963 (McGraw Hill Book Company Ltd., New York).
15. Molahanov, Y. K., International Chem. Eng., 3, 157 (1963).
16. Ellis, S. R. M., and Biddulph, M. W., Trans. Chem. Engrs., 45, T223 (1967).

17. Harris, I. J., Brit. Chem. Eng., 10, 377 (1965).

18. Hay, J. M., and Johnson, A. I., AIChE Journal, 6, 373 (1960).

19. Hellums, J. D., Braulik, C. J., Lyda, C. D., and Van Winkle, M. V., AIChE Journal, 4, 465 (1958).

20. Detman, R. F., Pet. Ref., 42, 147 (1963).

21. Fryback, M. G., and Hufnagel, J. A., Ind. Eng. Chem., 52, 654 (1960).

22. Patton, B. A., and Pritchand, B. L., Pet. Ref., 39, 95 (1960).

23. Lange, N. A.,"Handbook of Chemistry", 1956 (McGraw Hill Book Company Ltd., New York).

24. Perry, J. H., "Chemical Engineer's Handbook", 1963 (McGraw Hill Book Company Ltd., New York).

25. Finch, R., and Van Winkle, M., Ind. Eng. Chem. (Process Design and Developement), 3, 106 (1964).

26. Umholtz, C., and Van Winkle, M., Ind. Eng. Chem., 44, 232 (1957).

27. Gerster, J. A., Chem. Eng. Prog., 47, 522 and 621 (1951).

28. Koch, R., International Chem. Eng., 4, 655 (1964).

29. Calderbank, P. H., Evans, F., and Rennie, J., International Symposium on Distillation, 51 and 59 (1960).

30. Walter, J. F., and Sherwood, T. K., Ind. Eng. Chem., 33, 493 (1941).

31. West, F., Gilgert, W. P., and Shimiza, T., Ind. Eng. Chem., 44, 2470 (1952).

32. Gerster, J. A., Chem. Eng. Prog., 59, 35 (1963).

33. Danilychev, I. A., Planovskii, A. N., and Chekhov, O. S., International Chem. Eng., 6, 272 (1966).

34. Ellis, S. R. M., and Rose, L. M., Can. J. Chem. Eng., 41, 146 (1963).

35. Harris, I. J., and Roper, G. H., Can. J. Chem. Eng., 41, 159 (1963).

36. Johnson, A. I., and Bowman, C. W., Can. J. Chem. Eng., 36, 253 (1958).

37. Eden, C. D., and Pigford, R. L., Chem. Eng. Sci., 20. 803 (1965).

38. Sterbacek, Z., Brit. Chem. Eng., 10, 772 (1965).

39. Treybal, R. E., "Mass Transfer Operations", 1967 (McGraw Hill Book Company Ltd., New York).

40. Harada, M., Adachi, M., Egucki, W., and Nagata, S., International Chem. Eng., 4, 165 (1964).

41. Madigan, A. L., University of New York M.Sc. Thesis, 1965.

42. Umholtz, C., Pet. Ref., 34, 114 (1955).

43. Garner, F., Trans. Chem. Engrs., 35, 61 (1957).

44. Gilbert, T. J., Chem. Eng. Sci., 10, 243 (1959).

45. Mayfield, F. D., Church, W. L., Green, A. C., Lee, D. C., and Rasmussen, R. W., Ind. Eng. Chem., 44, 2238 (1952).

46. Sastri, S. R. S., Brit. Chem. Eng., 11, 62 (1966).

47. Oliver, E. D., and Walson, C. C., AIChE Journal, 2, 18 (1956).

48. Johnson, A. I., and Marangozis, J., Can. J. Chem. Eng., 36, 161 (1958).

49. Calderbank, P. H., Trans. Chem. Engrs., 34, 79 (1956).

50. Malik, V. K., personal communication.

51. Rampacek, C. M., and Van Winkle, M., Ind. Eng. Chem. (Process Design and Developement), 7, 313 (1960).

52. Chidambarum, S., Brit. Chem. Eng., 11, 288 (1966).

53. Chidambarum, S., Brit. Chem. Eng., 11, 508 (1966).

54. Garner, F. H., and Porter, K. E., International Symposium on Distillation, 43 (1960).

55. Sideman, S., Hortascu, O., and Fulton, J., Ind. Eng. Chem., 58, 32 (1966).

56. Stearns, R. F., "Flow Measurement with Orifice Meters", 1951 (Van Nostrand, New York).

APPENDIX A

1. Experimental Efficiency and Hydraulic Data.
2. Dry Plate Pressure Drop Data.
3. Concentration Profile Data.
4. Calculated Results for N_{tL}, $k_L a$, and h_L.

1. Experimental Efficiency and Hydraulic Data

Tables 2 to 6 contain the experimental efficiency and hydraulic data which were obtained during the test runs. Because of the way the data is presented it is necessary to note that where the Murphree liquid efficiency is listed as zero, it is to be interpreted as no data taken. Also the column titles conform to the following nomenclature.

POINT	data run	
Q	gas flow rate	cu. ft./sec.
F	F-factor	$ft./sec.(lb./cu.\ ft.)^{\frac{1}{2}}$
EFF1	Murphree liquid efficiency (sample 1)	
EFF2	Murphree liquid efficiency (sample 2)	
EFF3	Murphree liquid efficiency (sample 3)	
AEFF	average Murphree liquid efficiency	
PPD	wet plate pressure drop, h_w	inches of water
ZC	clear liquid depth, h_c	inches of water
ZF	froth height, h_f	inches of water
DENCO2	carbon dioxide density, ρ_G	lb./cu. ft.

The values for the clear liquid depth and the froth height for the glycol solution have been converted to their equivalents in inches of water.

TABLE 2

EXPERIMENTAL RESULTS FOR WATER-CARBON DIOXIDE USING 0.125 INCH DIAMETER HOLES

POINT	Q	F	EFF1	EFF2	EFF3	AEFF	PPD	ZC	ZF	DENCO2
LIQUID RATE IS 0.1 U.S.G.P.M.										
1	0.160	0.287	0.0	0.0	0.0	0.0	0.80	0.50	1.0	0.1239
2	0.303	0.543	62.7	63.7	66.8	64.4	1.50	0.60	3.0	0.1236
3	0.520	0.937	70.4	69.3	75.8	71.8	2.30	1.00	3.0	0.1252
4	0.700	1.259	72.4	72.3	78.2	74.3	3.40	1.00	5.0	0.1248
5	0.910	1.639	60.1	56.4	65.1	60.5	4.90	1.20	7.0	0.1250
6	1.025	1.847	54.2	60.8	56.9	57.3	6.00	1.20	10.0	0.1252
LIQUID RATE IS 0.2 U.S.G.P.M.										
7	0.142	0.256	61.2	42.4	0.0	51.8	1.10	0.80	1.0	0.1255
8	0.173	0.312	81.5	81.5	79.0	80.7	1.60	1.20	3.0	0.1250
9	0.325	0.588	81.7	75.9	77.6	78.4	1.60	1.00	3.0	0.1264
10	0.540	0.978	82.0	83.3	80.0	81.8	2.80	1.20	4.0	0.1265
11	0.644	1.171	78.2	79.7	78.1	78.7	3.80	1.50	6.0	0.1275
12	0.820	1.488	86.5	76.8	80.9	81.4	5.20	1.80	8.0	0.1269
13	0.960	1.742	75.9	87.5	80.0	81.1	6.50	1.70	9.0	0.1270
LIQUID RATE IS 0.5 U.S.G.P.M.										
14	0.099	0.179	61.6	46.1	0.0	53.8	1.30	0.50	1.0	0.1262
15	0.170	0.308	84.1	82.3	87.7	84.7	1.60	1.30	4.0	0.1263
16	0.194	0.351	84.2	83.1	81.8	83.0	1.70	1.50	5.0	0.1261
17	0.295	0.533	83.6	84.0	83.6	83.7	1.70	1.20	5.0	0.1259
18	0.430	0.779	84.5	88.7	86.0	86.4	2.40	1.50	5.0	0.1264
19	0.492	0.888	85.4	88.2	90.7	88.1	2.90	1.70	6.0	0.1255
20	0.590	1.068	82.3	81.1	85.9	83.1	3.10	1.60	8.0	0.1263
21	0.695	1.258	87.7	89.1	85.4	87.4	4.80	2.50	9.0	0.1264
22	0.800	1.454	77.2	84.3	88.3	83.3	5.55	2.40	12.0	0.1273

TABLE 2 (continued)

EXPERIMENTAL RESULTS FOR WATER-CARBON DIOXIDE USING 0.125 INCH DIAMETER HOLES

POINT	Q	F	EFF1	EFF2	EFF3	AEFF	PPD	ZC	ZF	DENCO2
LIQUID RATE IS 1.0 U.S.G.P.M.										
23	0.096	0.175	71.3	0.0	0.0	71.3	1.80	1.60	4.0	0.1280
24	0.180	0.327	75.1	78.3	79.9	77.8	2.20	2.00	5.0	0.1273
25	0.215	0.391	78.6	81.7	80.8	80.4	2.60	2.20	6.0	0.1277
26	0.271	0.492	83.0	84.2	0.0	83.6	2.60	2.10	6.0	0.1269
27	0.310	0.563	86.5	83.5	85.0	85.0	3.20	2.50	8.0	0.1273
28	0.370	0.668	83.0	83.2	84.2	83.5	3.60	2.80	8.0	0.1257
29	0.420	0.763	81.0	85.1	85.2	83.8	3.80	2.60	9.5	0.1273
30	0.520	0.943	84.4	90.8	91.6	88.9	5.00	3.60	18.5	0.1269
31	0.585	1.061	86.4	85.2	87.4	86.3	6.20	4.50	18.5	0.1268
LIQUID RATE IS 2.0 U.S.G.P.M.										
32	0.102	0.183	46.9	0.0	0.0	46.9	2.40	2.30	3.0	0.1240
33	0.142	0.257	66.0	0.0	0.0	66.0	2.55	2.30	5.0	0.1259
34	0.194	0.350	76.2	76.0	76.0	76.1	3.00	2.70	7.5	0.1255
35	0.222	0.401	81.8	79.4	76.7	79.3	3.40	3.00	9.0	0.1259
36	0.250	0.456	82.2	81.2	82.2	81.9	3.70	3.20	11.0	0.1282
37	0.330	0.595	80.8	77.7	85.2	81.2	4.80	4.20	14.0	0.1255
38	0.370	0.673	81.7	85.0	89.0	85.2	7.20	6.40	18.5	0.1277
39	0.420	0.759	83.8	83.2	87.7	84.9	7.60	6.50	18.5	0.1258
40	0.450	0.810	86.2	83.7	86.7	85.5	7.00	6.00	18.5	0.1249

TABLE 2 (continued)

EXPERIMENTAL RESULTS FOR WATER-CARBON DIOXIDE USING 0.125 INCH DIAMETER HOLES

POINT	Q	F	EFF1	EFF2	EFF3	AEFF	PPD	ZC	ZF	DENCO2
LIQUID RATE IS 3.0 U.S.G.P.M.										
41	0.160	0.286	65.6	59.9	62.3	62.6	3.60	2.80	7.0	0.1235
42	0.240	0.434	78.7	83.3	82.3	81.4	9.70	9.00	18.5	0.1263
LIQUID RATE IS 4.0 U.S.G.P.M.										
44	0.170	0.308	60.9	59.8	61.0	60.6	6.00	5.80	13.0	0.1263
43	0.175	0.313	61.1	56.3	61.2	59.5	4.60	4.00	10.0	0.1235
45	0.183	0.331	73.2	71.6	68.7	71.2	10.60	10.00	18.5	0.1265
46	0.198	0.357	69.3	68.2	72.0	69.8	9.50	9.00	18.5	0.1253

TABLE 3

EXPERIMENTAL RESULTS FOR WATER-CARBON DIOXIDE USING 0.250 INCH DIAMETER HOLES

POINT	Q	F	EFF1	EFF2	EFF3	AEFF	PPD	ZC	ZF	DENCO2
LIQUID RATE IS 0.1 U.S.G.P.M.										
47	0.187	0.336	0.0	0.0	0.0	0.0	0.60	0.35	1.0	0.1244
48	0.320	0.575	41.2	46.2	41.5	43.0	1.20	0.50	3.0	0.1245
49	0.360	0.647	40.2	51.3	0.0	45.7	1.30	0.50	2.5	0.1247
50	0.520	0.936	30.7	34.7	24.7	30.0	1.40	0.60	3.5	0.1249
51	0.580	1.044	23.7	29.3	17.3	23.4	1.55	0.50	4.0	0.1249
52	0.670	1.208	38.2	35.3	26.3	33.3	2.40	0.60	6.0	0.1253
53	0.795	1.436	58.3	49.5	0.0	53.9	2.60	0.60	7.5	0.1257
54	0.920	1.665	47.2	56.7	61.4	55.1	4.00	1.00	8.0	0.1262
55	1.050	1.897	7.9	15.4	8.1	10.5	4.90	1.20	11.0	0.1258
LIQUID RATE IS 0.2 U.S.G.P.M.										
56	0.173	0.312	0.0	0.0	0.0	0.0	0.50	0.30	1.0	0.1256
57	0.262	0.473	77.9	77.7	78.2	77.9	1.20	0.75	3.0	0.1259
58	0.505	0.913	74.4	75.2	80.4	76.7	1.60	0.65	4.0	0.1260
59	0.670	1.209	77.2	79.5	74.7	77.1	2.30	1.00	7.0	0.1255
60	0.820	1.483	66.9	69.3	67.2	67.8	3.45	1.10	8.0	0.1261
61	0.940	1.701	66.8	66.8	65.9	66.5	4.35	1.10	10.0	0.1263
62	1.010	1.826	66.6	62.9	66.8	65.4	4.90	1.40	11.0	0.1260
63	1.020	1.840	66.6	66.8	67.4	66.9	4.90	1.50	12.0	0.1255

TABLE 3 (continued)

EXPERIMENTAL RESULTS FOR WATER-CARBON DIOXIDE USING 0.250 INCH DIAMETER HOLES

POINT	Q	F	EFF1	EFF2	EFF3	AEFF	PPD	ZC	ZF	DENCO2
LIQUID RATE IS 0.5 U.S.G.P.M.										
64	0.138	0.249	71.3	63.7	0.0	67.5	0.65	0.50	1.0	0.1260
65	0.173	0.313	76.3	74.8	76.6	75.9	1.00	0.80	3.0	0.1261
66	0.242	0.436	81.4	82.3	81.7	81.8	1.45	1.10	4.5	0.1252
67	0.295	0.535	83.0	79.2	0.0	81.1	1.35	1.00	4.5	0.1268
68	0.375	0.676	81.4	82.1	82.8	82.1	1.55	1.00	4.5	0.1251
69	0.495	0.890	85.7	84.6	83.2	84.5	1.85	1.20	5.5	0.1246
70	0.590	1.064	75.2	81.8	84.7	80.6	2.60	1.50	8.0	0.1254
71	0.620	1.134	84.7	85.7	86.8	85.7	2.90	1.20	9.0	0.1290
72	0.825	1.499	80.6	0.0	0.0	80.6	4.40	2.00	13.0	0.1272
73	0.825	1.499	79.6	0.0	0.0	79.6	4.40	2.00	13.0	0.1273
LIQUID RATE IS 1.0 U.S.G.P.M.										
74	0.096	0.174	54.3	0.0	0.0	54.3	0.50	0.40	1.0	0.1271
75	0.136	0.247	64.3	0.0	0.0	64.3	1.45	1.30	3.0	0.1275
76	0.190	0.346	78.9	77.3	0.0	78.1	2.05	1.70	5.0	0.1278
193	0.273	0.493	0.0	0.0	0.0	0.0	2.40	1.90	6.0	0.1257
77	0.290	0.526	85.3	0.0	0.0	85.3	2.60	2.20	6.0	0.1270
206	0.295	0.535	87.1	0.0	0.0	87.1	2.30	2.00	5.0	0.1266
78	0.310	0.560	84.4	0.0	0.0	84.4	2.70	2.30	6.0	0.1259
196	0.340	0.612	0.0	0.0	0.0	0.0	3.00	2.50	5.5	0.1249
197	0.340	0.612	0.0	0.0	0.0	0.0	2.90	2.50	6.5	0.1249
79	0.415	0.753	93.2	0.0	0.0	93.2	3.50	2.70	8.0	0.1268
80	0.445	0.806	92.9	99.6	0.0	96.2	3.90	3.10	9.0	0.1264
195	0.490	0.885	0.0	0.0	0.0	0.0	4.15	3.50	10.0	0.1257
207	0.510	0.927	86.4	0.0	0.0	86.4	4.60	4.00	12.0	0.1273
198	0.545	0.981	0.0	0.0	0.0	0.0	4.40	3.50	13.0	0.1249
194	0.610	1.101	0.0	0.0	0.0	0.0	6.70	4.60	13.0	0.1257
81	0.620	1.134	81.9	83.6	0.0	82.7	6.65	5.25	16.0	0.1289
82	0.685	1.244	86.1	0.0	0.0	86.1	6.70	5.00	16.0	0.1271

TABLE 3 (continued)

EXPERIMENTAL RESULTS FOR WATER-CARBON DIOXIDE USING 0.250 INCH DIAMETER HOLES

POINT	Q	F	EFF1	EFF2	EFF3	AFFF	PPD	ZC	ZF	DENCO2
LIQUID RATE IS 2.0 U.S.G.P.M.										
83	0.114	0.210	31.2	0.0	0.0	31.2	1.00	0.90	2.5	0.1303
84	0.192	0.350	76.7	72.4	78.3	75.8	2.30	2.10	5.5	0.1281
208	0.315	0.567	83.1	0.0	0.0	83.1	4.80	4.50	12.0	0.1248
85	0.320	0.584	80.6	80.7	82.8	81.4	4.70	4.20	12.5	0.1284
86	0.420	0.764	78.1	82.1	80.7	80.3	6.90	6.10	18.5	0.1277
LIQUID RATE IS 3.0 U.S.G.P.M.										
87	0.305	0.556	84.6	84.7	0.0	84.6	7.20	6.80	18.5	0.1281
LIQUID RATE IS 4.0 U.S.G.P.M.										
209	0.196	0.355	39.2	37.8	0.0	38.5	2.50	2.00	5.0	0.1262
88	0.215	0.390	73.7	0.0	0.0	73.7	7.70	7.30	18.5	0.1269

TABLE 4

EXPERIMENTAL RESULTS FOR WATER-CARBON DIOXIDE USING 0.500 INCH DIAMETER HOLES

POINT	Q	F	EFF1	EFF2	EFF3	AEFF	PPD	ZC	ZF	DENCO2
LIQUID RATE IS 0.1 U.S.G.P.M.										
89	0.172	0.310	80.7	78.4	0.0	79.5	1.60	0.80	2.0	0.1253
90	0.285	0.513	75.8	79.2	75.7	76.9	1.80	0.60	3.0	0.1249
91	0.590	1.063	74.4	70.4	74.8	73.2	2.95	1.00	4.0	0.1251
92	0.700	1.260	60.2	57.4	64.2	60.6	5.00	1.40	7.0	0.1250
93	0.880	1.587	51.4	60.4	50.8	54.2	7.40	2.00	11.0	0.1254
LIQUID RATE IS 0.2 U.S.G.P.M.										
94	0.142	0.256	85.7	82.3	0.0	84.0	1.65	1.00	2.5	0.1256
95	0.243	0.439	84.2	81.8	82.3	82.8	1.90	1.00	3.5	0.1258
96	0.400	0.724	78.1	84.7	80.3	81.0	2.55	1.30	4.0	0.1262
97	0.620	1.126	76.2	83.9	82.4	80.8	4.60	1.70	7.0	0.1271
98	0.730	1.317	68.7	70.7	0.0	69.7	5.60	1.90	8.5	0.1255
99	0.840	1.528	68.4	65.7	71.8	68.6	7.35	2.20	12.0	0.1275
LIQUID RATE IS 0.5 U.S.G.P.M.										
180	0.100	0.180	0.0	0.0	0.0	0.0	1.50	1.00	2.0	0.1256
176	0.158	0.285	0.0	0.0	0.0	0.0	1.90	1.60	3.0	0.1257
100	0.184	0.333	76.9	80.2	79.9	79.0	2.15	1.70	4.0	0.1265
101	0.286	0.518	80.1	80.1	81.7	80.6	2.35	1.50	4.0	0.1267
177	0.320	0.578	0.0	0.0	0.0	0.0	2.20	1.45	4.0	0.1256
102	0.439	0.796	78.3	79.4	80.5	79.4	3.20	1.80	5.0	0.1267
178	0.460	0.828	0.0	0.0	0.0	0.0	2.80	1.50	5.0	0.1250
103	0.540	0.984	81.2	78.1	83.5	80.9	4.30	2.10	7.5	0.1280
179	0.580	1.048	0.0	0.0	0.0	0.0	4.50	1.80	7.0	0.1258
104	0.710	1.290	80.3	82.3	84.5	82.4	6.60	3.20	12.0	0.1272

TABLE 4 (continued)

EXPERIMENTAL RESULTS FOR WATER-CARBON DIOXIDE USING 0.500 INCH DIAMETER HOLES

POINT	Q	F	EFF1	EFF2	EFF3	AEFF	PPD	ZC	ZF	DENCO2
LIQUID RATE IS 1.0 U.S.G.P.M.										
105	0.098	0.178	64.9	60.1	0.0	62.5	1.30	1.00	2.0	0.1265
106	0.140	0.252	72.6	73.8	75.6	74.0	2.00	1.50	4.0	0.1253
183	0.158	0.286	0.0	0.0	0.0	0.0	2.05	1.50	4.0	0.1264
107	0.198	0.357	77.0	76.0	0.0	76.5	2.30	1.70	4.5	0.1252
182	0.245	0.442	0.0	0.0	0.0	0.0	2.30	1.70	5.0	0.1256
108	0.315	0.569	78.9	80.5	80.5	80.0	2.80	2.00	6.0	0.1256
181	0.315	0.569	0.0	0.0	0.0	0.0	2.80	2.10	5.5	0.1257
109	0.400	0.719	77.8	81.6	82.5	80.6	3.90	2.70	8.0	0.1245
111	0.450	0.816	83.2	85.3	83.1	83.9	4.00	2.80	7.5	0.1267
110	0.455	0.824	83.2	85.5	0.0	84.3	4.20	2.70	14.0	0.1263
112	0.460	0.832	85.0	88.1	86.9	86.7	4.50	3.50	11.0	0.1260
113	0.510	0.917	78.5	79.6	82.5	80.2	6.80	5.20	18.5	0.1247
114	0.540	0.977	74.9	76.6	0.0	75.7	7.20	5.70	18.5	0.1262
LIQUID RATE IS 2.0 U.S.G.P.M.										
115	0.096	0.174	47.4	51.2	0.0	49.3	1.70	1.60	4.0	0.1270
116	0.148	0.268	58.1	63.4	60.4	60.6	2.25	2.10	5.0	0.1261
117	0.197	0.356	65.8	67.2	69.8	67.6	3.05	2.60	6.5	0.1262
118	0.280	0.507	77.0	77.7	81.5	78.7	4.20	3.50	9.0	0.1263
189	0.310	0.559	0.0	0.0	0.0	0.0	4.60	3.80	10.0	0.1253
119	0.355	0.642	81.9	84.1	0.0	83.0	5.90	4.50	12.0	0.1261
188	0.380	0.685	0.0	0.0	0.0	0.0	5.75	5.00	14.0	0.1253
120	0.395	0.715	85.1	85.9	84.2	85.1	7.50	6.50	18.5	0.1263
190	0.420	0.757	0.0	0.0	0.0	0.0	7.20	5.00	18.5	0.1253
187	0.440	0.793	0.0	0.0	0.0	0.0	8.00	6.50	18.5	0.1253
191	0.440	0.793	0.0	0.0	0.0	0.0	7.80	6.70	18.5	0.1253
192	0.470	0.847	0.0	0.0	0.0	0.0	7.50	6.50	18.5	0.1253

TABLE 4 (continued)

EXPERIMENTAL RESULTS FOR WATER-CARBON DIOXIDE USING 0.500 INCH DIAMETER HOLES

POINT	Q	F	EFF1	EFF2	EFF3	AEFF	PPD	ZC	ZF	DENCO2
LIQUID RATE IS 3.0 U.S.G.P.M.										
185	0.145	0.261	0.0	0.0	0.0	0.0	3.85	3.20	8.0	0.1250
184	0.200	0.360	0.0	0.0	0.0	0.0	5.95	5.50	14.0	0.1248
121	0.214	0.390	70.5	75.2	0.0	72.8	9.00	8.50	18.5	0.1283
186	0.225	0.405	0.0	0.0	0.0	0.0	9.00	8.00	18.5	0.1252
122	0.243	0.438	64.0	66.4	0.0	65.2	9.70	9.20	18.5	0.1253
LIQUID RATE IS 4.0 U.S.G.P.M.										
123	0.136	0.247	44.6	50.2	0.0	47.4	4.50	3.80	9.0	0.1272
124	0.140	0.253	52.5	50.0	0.0	51.2	3.80	3.20	9.0	0.1263
125	0.180	0.323	63.7	60.1	61.9	61.9	10.00	9.50	18.5	0.1240

TABLE 5

EXPERIMENTAL RESULTS FOR WATER-CARBON DIOXIDE USING 1.000 INCH DIAMETER HOLES

POINT	Q	F	EFF1	EFF2	EFF3	AEFF	PPD	ZC	ZF	DENCO2
LIQUID RATE IS 0.1 U.S.G.P.M.										
126	0.173	0.311	0.0	0.0	0.0	0.0	0.45	0.20	1.0	0.1247
127	0.220	0.398	74.7	77.8	81.7	78.1	1.40	1.00	2.0	0.1263
128	0.295	0.532	70.1	75.4	72.9	72.8	1.80	1.20	3.0	0.1252
129	0.450	0.812	80.5	83.7	79.2	81.1	2.50	1.20	4.0	0.1254
130	0.640	1.151	72.3	70.2	71.8	71.4	3.40	1.30	6.0	0.1246
LIQUID RATE IS 0.2 U.S.G.P.M.										
131	0.174	0.314	77.6	75.2	73.4	75.4	0.80	0.50	2.0	0.1253
132	0.224	0.402	74.4	80.1	76.7	77.1	1.25	1.00	3.0	0.1241
133	0.345	0.620	84.3	90.4	81.7	82.1	1.60	1.00	3.0	0.1245
134	0.420	0.758	84.7	0.0	0.0	84.7	2.00	1.10	4.5	0.1255
135	0.435	0.785	83.2	89.0	85.7	86.0	2.00	1.00	5.0	0.1255
136	0.445	0.800	83.1	83.9	85.7	84.2	2.20	1.20	3.0	0.1246
137	0.660	1.191	79.2	72.4	75.1	75.6	3.70	1.20	7.0	0.1256
LIQUID RATE IS 0.5 U.S.G.P.M.										
168	0.100	0.181	0.0	0.0	0.0	0.0	0.50	0.50	1.0	0.1270
167	0.140	0.253	0.0	0.0	0.0	0.0	1.20	1.00	1.0	0.1261
138	0.173	0.313	77.7	76.8	0.0	77.2	1.50	1.20	2.0	0.1263
139	0.198	0.357	71.4	75.7	70.7	72.6	1.80	1.40	2.0	0.1251
166	0.210	0.380	0.0	0.0	0.0	0.0	2.00	1.40	2.0	0.1261
140	0.298	0.537	75.7	78.4	76.2	76.8	2.40	1.70	3.0	0.1254
165	0.320	0.579	0.0	0.0	0.0	0.0	2.15	1.50	3.0	0.1260
141	0.385	0.695	81.0	83.3	84.2	82.8	2.50	1.50	5.0	0.1256
142	0.445	0.804	82.2	78.9	0.0	80.5	2.80	1.60	5.0	0.1258
143	0.540	0.975	81.4	80.8	83.6	81.9	3.30	1.50	5.0	0.1256
164	0.565	1.020	0.0	0.0	0.0	0.0	3.50	1.40	7.0	0.1257
163	0.640	1.157	0.0	0.0	0.0	0.0	3.70	1.50	8.0	0.1260
144	0.670	1.207	81.1	80.7	82.3	81.4	4.40	2.00	8.0	0.1252

TABLE 5 (continued)

EXPERIMENTAL RESULTS FOR WATER-CARBON DIOXIDE USING 1.000 INCH DIAMETER HOLES

POINT	Q	F	EFF1	EFF2	EFF3	AEFF	PPD	ZC	ZF	DENCO2
	LIQUID RATE IS 1.0 U.S.G.P.M.									
174	0.078	0.141	0.0	0.0	0.0	0.0	0.30	0.25	1.0	0.1264
175	0.110	0.199	0.0	0.0	0.0	0.0	1.00	0.80	2.0	0.1264
145	0.128	0.232	63.1	63.2	63.8	63.4	1.70	1.50	2.5	0.1270
173	0.150	0.271	0.0	0.0	0.0	0.0	1.70	1.50	2.0	0.1262
146	0.200	0.360	76.1	76.1	81.9	78.0	2.20	1.80	3.0	0.1246
172	0.210	0.380	0.0	0.0	0.0	0.0	2.25	2.00	3.0	0.1263
147	0.300	0.540	80.0	81.1	85.7	82.3	2.60	2.00	4.0	0.1247
171	0.340	0.616	0.0	0.0	0.0	0.0	2.70	2.00	5.0	0.1264
148	0.360	0.653	82.4	79.6	81.8	81.3	2.60	1.80	6.0	0.1268
170	0.450	0.815	0.0	0.0	0.0	0.0	3.30	2.50	8.0	0.1265
150	0.485	0.880	85.3	84.1	85.9	85.1	4.10	2.60	9.0	0.1270
149	0.490	0.882	90.1	89.4	0.0	89.7	3.90	2.40	9.5	0.1249
169	0.620	1.122	0.0	0.0	0.0	0.0	6.50	4.50	15.0	0.1263
151	0.630	1.133	87.2	88.3	0.0	87.7	7.30	5.00	14.0	0.1248
	LIQUID RATE IS 2.0 U.S.G.P.M.									
152	0.184	0.332	60.6	59.1	57.4	59.0	2.30	2.10	4.0	0.1258
153	0.275	0.496	73.4	74.2	72.2	73.3	3.20	2.70	8.0	0.1254
154	0.297	0.536	68.2	73.9	72.9	71.7	3.20	2.60	7.0	0.1256
155	0.420	0.756	81.2	84.7	77.4	81.1	4.60	3.50	11.5	0.1250
156	0.430	0.776	79.6	80.7	79.9	80.1	4.40	3.20	9.0	0.1255
157	0.600	1.080	79.9	84.4	86.6	83.6	7.00	5.30	18.5	0.1249

TABLE 5 (continued)

EXPERIMENTAL RESULTS FOR WATER-CARBON DIOXIDE USING 1.000 INCH DIAMETER HOLES

POINT	Q	F	EFF1	EFF2	EFF3	AEFF	PPD	ZC	ZF	DENCO2
LIQUID RATE IS 3.0 U.S.G.P.M.										
202	0.110	0.199	0.0	0.0	0.0	0.0	2.50	1.40	2.0	0.1257
201	0.183	0.330	0.0	0.0	0.0	0.0	3.00	2.50	4.0	0.1257
158	0.198	0.358	57.6	59.8	58.4	58.6	3.40	3.00	6.0	0.1262
199	0.245	0.442	0.0	0.0	0.0	0.0	4.30	3.80	9.0	0.1257
200	0.275	0.497	0.0	0.0	0.0	0.0	7.10	6.30	13.0	0.1257
159	0.280	0.507	73.6	71.6	74.6	73.3	8.00	7.50	18.5	0.1262
LIQUID RATE IS 4.0 U.S.G.P.M.										
160	0.141	0.253	38.4	41.3	0.0	39.8	2.00	1.80	4.0	0.1246
204	0.152	0.274	0.0	0.0	0.0	0.0	3.00	2.50	8.0	0.1254
205	0.152	0.274	0.0	0.0	0.0	0.0	2.50	1.50	4.0	0.1254
161	0.172	0.309	54.1	0.0	0.0	54.1	2.80	2.50	6.0	0.1246
203	0.183	0.330	0.0	0.0	0.0	0.0	6.00	4.50	11.0	0.1254
162	0.197	0.355	70.2	70.1	72.8	71.0	9.50	9.20	18.5	0.1255

TABLE 6

EXPERIMENTAL RESULTS FOR GLYCOL - CARBON DIOXIDE USING 0.250 INCH DIAMETER HOLES

POINT	Q	F	EFF1	EFF2	EFF3	AEFF	PPD	ZC	ZF	DENCO2
LIQUID RATE IS 0.5 U.S.G.P.M.										
1	0.200	0.362	53.0	55.0	0.0	54.0	1.86	1.70	3.5	0.1263
2	0.315	0.571	60.5	61.8	0.0	61.1	2.35	1.90	4.5	0.1266
3	0.365	0.658	60.1	60.3	60.4	60.3	2.40	1.70	5.0	0.1254
4	0.445	0.804	64.4	61.5	0.0	62.9	2.70	1.90	5.0	0.1258
5	0.570	1.030	65.2	67.9	0.0	66.5	3.00	2.00	6.5	0.1258
6	0.640	1.156	71.3	65.6	0.0	68.4	3.70	2.00	8.0	0.1258
7	0.800	1.444	71.0	70.9	0.0	70.9	5.00	2.50	12.0	0.1256
8	0.940	1.694	70.2	74.3	69.5	71.3	6.80	3.50	15.5	0.1252
LIQUID RATE IS 1.0 U.S.G.P.M.										
9	0.200	0.361	41.2	39.0	40.1	40.1	2.20	2.00	3.5	0.1256
10	0.315	0.569	53.6	52.4	53.4	53.1	2.60	2.20	5.5	0.1258
11	0.440	0.799	57.1	0.0	0.0	57.1	2.90	2.00	6.5	0.1270
12	0.380	0.686	54.1	55.0	0.0	54.5	2.80	2.50	6.0	0.1258
13	0.445	0.802	58.9	55.3	57.9	57.4	3.10	2.20	6.5	0.1252
14	0.570	1.030	62.0	61.0	65.4	62.8	4.20	2.70	8.5	0.1258
15	0.615	1.106	65.9	63.0	64.5	64.5	4.40	2.90	10.0	0.1247
16	0.700	1.261	65.3	0.0	0.0	65.3	6.00	3.50	12.0	0.1252
17	0.760	1.365	67.2	65.7	64.4	65.8	6.40	4.40	15.5	0.1243
LIQUID RATE IS 2.0 U.S.G.P.M.										
18	0.196	0.355	31.5	28.3	0.0	29.9	2.75	2.70	5.5	0.1262
19	0.295	0.531	37.0	0.0	0.0	37.0	3.00	2.80	6.5	0.1250
20	0.330	0.594	42.2	41.2	41.3	41.6	3.55	3.00	7.0	0.1251
21	0.390	0.683	46.0	46.8	0.0	46.4	4.00	5.00	10.0	0.1246
22	0.445	0.803	52.0	57.1	53.4	54.2	9.60	8.90	20.0	0.1256

2. Dry Plate Pressure Drop Data.

The dry plate pressure drop data given in Tables 7 to 10 were obtained using sealed downcomers (20,45). The dry plate pressure drop coefficient, K, was calculated from experimental data using equation 19 and compared with the value obtained with equation 20. An empirical correlation based on the F-factor (equation 15) is also given.

TABLE 7

DRY PLATE PRESSURE DROP DATA FOR 0.125-INCH DIAMETER HOLES

Q	ρ_G	F-factor	h_D
1.140	0.1250	2.053	6.30
1.130	0.1254	2.038	6.30
1.080	0.1252	1.946	5.70
1.070	0.1254	1.930	5.50
0.990	0.1250	1.783	4.70
0.960	0.1253	1.731	4.45
0.910	0.1252	1.640	4.00
0.870	0.1247	1.565	3.60
0.830	0.1251	1.495	3.30
0.790	0.1254	1.425	2.95
0.730	0.1250	1.314	2.60
0.700	0.1251	1.261	2.30
0.630	0.1247	1.133	1.90
0.555	0.1251	1.000	1.50
0.460	0.1247	0.827	1.00
0.430	0.1250	0.744	0.80
0.356	0.1242	0.639	0.60
0.283	0.1252	0.512	0.35
0.265	0.1249	0.477	0.38
0.183	0.1250	0.330	0.10
0.150	0.1251	0.270	0.10
0.110	0.1250	0.198	0.05

TABLE 8

DRY PLATE PRESSURE DROP DATA FOR 0.250-INCH DIAMETER HOLES

Q	ρ_G	F-factor	h_D
1.170	0.1231	2.091	5.80
1.170	0.1243	2.101	5.00
1.100	0.1230	1.965	4.50
1.020	0.1241	1.830	3.40
0.970	0.1227	1.730	3.10
0.920	0.1239	1.649	3.00
0.850	0.1230	1.518	2.30
0.820	0.1237	1.469	2.10
0.730	0.1222	1.300	1.50
0.700	0.1237	1.254	1.50
0.640	0.1236	1.146	1.20
0.545	0.1234	0.975	0.90
0.460	0.1234	0.823	0.70
0.420	0.1234	0.751	0.50
0.325	0.1234	0.581	0.35
0.255	0.1234	0.456	0.20
0.184	0.1232	0.329	0.10

TABLE 9

DRY PLATE PRESSURE DROP DATA FOR 0.500-INCH DIAMETER HOLES

Q	ρ_G	F-factor	h_D
1.090	0.1257	1.968	7.70
1.080	0.1267	1.958	7.70
1.050	0.1266	1.902	7.35
1.020	0.1255	1.842	6.45
0.960	0.1265	1.739	5.80
0.920	0.1254	1.659	5.20
0.910	0.1265	1.648	5.00
0.850	0.1262	1.537	4.30
0.790	0.1263	1.430	3.50
0.700	0.1262	1.266	2.85
0.670	0.1259	1.211	2.75
0.550	0.1256	0.993	1.80
0.500	0.1260	0.904	1.50
0.367	0.1260	0.663	0.80
0.355	0.1260	0.642	0.70
0.273	0.1260	0.494	0.40
0.223	0.1261	0.403	0.20
0.178	0.1262	0.322	0.15
0.150	0.1260	0.271	0.10
0.110	0.1261	0.199	0.05

TABLE 10

DRY PLATE PRESSURE DROP DATA FOR 1.000-INCH DIAMETER HOLES

Q	ρ_G	F-factor	h_D
1.100	0.1272	1.998	6.65
1.100	0.1269	1.996	7.00
1.080	0.1285	1.972	6.40
1.020	0.1265	1.848	5.90
1.010	0.1267	1.829	5.90
0.960	0.1264	1.738	5.30
0.920	0.1267	1.668	5.00
0.850	0.1265	1.540	4.50
0.819	0.1263	1.482	4.15
0.750	0.1260	1.356	3.30
0.710	0.1263	1.285	2.90
0.630	0.1252	1.135	2.20
0.570	0.1261	1.031	1.85
0.450	0.1256	0.812	1.10
0.394	0.1261	0.713	0.80
0.325	0.1261	0.588	0.50
0.263	0.1261	0.476	0.30
0.233	0.1261	0.421	0.20
0.210	0.1262	0.380	0.15
0.184	0.1260	0.333	0.10
0.110	0.1261	0.199	0.05

TABLE 11

DRY PLATE PRESSURE DROP CORRELATIONS

D_h	T/D_h	K	K	F-factor
inches	-	eq'n. 20	expt.	
0.125	2.512	0.866	0.95	$h_D = 1.430\ F^{2.088}$
0.250	1.380	0.997	0.85	$h_D = 0.997\ F^{2.106}$
0.500	0.512	1.290	1.40	$h_D = 1.745\ F^{2.184}$
1.000	0.306	1.459	1.35	$h_D = 1.563\ F^{2.251}$

3. Concentration Profile Data.

The following tables, 12 to 17, give the data obtained from the concentration profile studies. The tables give a point data number, its position in the test section above the tray, the point concentration, and the point efficiency. The position is given by three coordinates. The vertical coordinate, h, is measured in inches from the tray floor. The horizontal coordinates, x and y, are measured in inches and conform to the coordinate system in the following diagram.

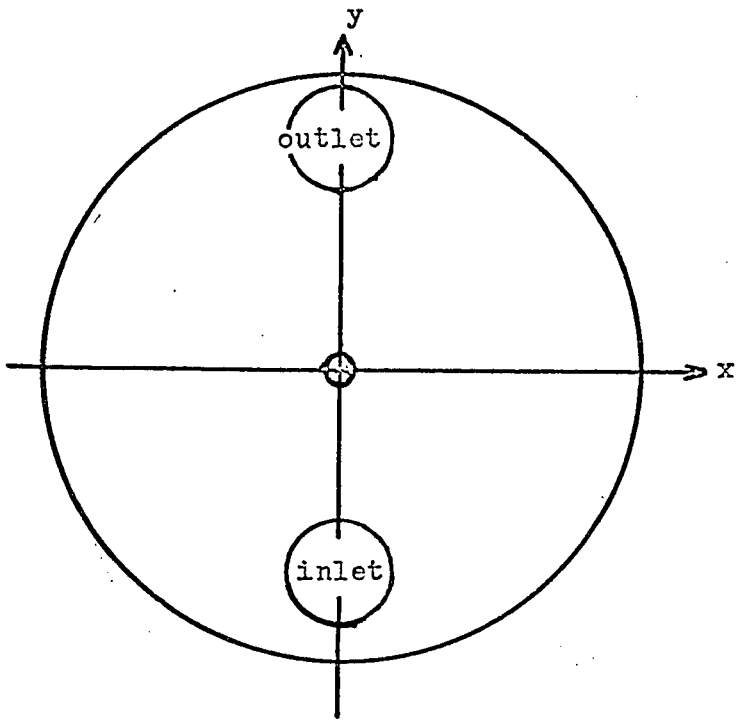

TABLE 12

CONCENTRATION PROFILE FOR WATER-CARBON DIOXIDE

Liquid flow rate: 1.0 gpm.

Gas flow rate: 0.295 cu. ft./sec.

Overall efficiency: 87.1 %

Point	x	y	h	Conc.	Eff. (%)
1	1.0	-3.0	0.125	0.00706	16.7
2	1.0	-2.5	0.125	0.01165	24.3
3	1.0	-2.0	0.125	0.01426	37.8
4	1.0	-1.0	0.125	0.02172	59.6
5	1.0	-2.0	0.125	0.02095	57,4
6	1.0	-1.0	0.125	0.02070	56.6
7	1.0	0.0	0.125	0.02354	64.9
8	1.0	1.0	0.125	0.02227	61.7
9	1.0	2.0	0.125	0.02197	60.4
10	1.0	2.5	0.125	0.02146	58.9
11	-3.0	0.0	0.125	0.01292	32.8
12	-2.0	0.0	0.125	0.01779	47.3
13	-1.0	0.0	0.125	0.01564	41.0
14	0.0	0.0	0.125	0.01360	34.9
15	1.0	0.0	0.125	0.01706	45.2
16	2.0	0.0	0.125	0.01727	45.8
17	3.0	0.0	0.125	0.01570	41.1
18	-3.0	0.0	0.375	0.01482	39.4
19	-1.5	0.0	0.375	0.02116	58.0
20	0.0	0.0	0.375	0.02511	69.5
21	1.5	0.0	0.375	0.02151	59.0
22	-1.5	0.0	1.0	0.02878	80.0
23	0.0	0.0	1.0	0.03067	85.6
24	1.5	0.0	1.0	0.02789	77.4
25	1.5	-2.5	1.0	0.02758	76.4
26	1.5	2.5	1.0	0.02685	74.3
27	0.0	-1.7	1.0	0,02297	62.7
28	0.0	1.7	1.0	0.02679	74.1
29	-1.5	2.5	1.0	0.02774	76.9
30	-1.5	-2.5	1.0	0.02753	76.3
31	0.0	0.0	1.0	0.02658	73.4
32	-1.5	0.0	4.0	0.03030	84.5
33	1.5	0,0	4.0	0.03098	86.5
34	1.5	-2.5	4.0	0.03114	87.0
35	1.5	2.5	4.0	0.03124	84.3
36	-1.5	-2.5	4.0	0.03114	87.0
37	-1.5	2.5	4.0	0.02978	83.0

TABLE 13

CONCENTRATION PROFILE FOR WATER-CARBON DIOXIDE

Liquid flow rate: 1.0 gpm.

Gas flow rate: 0.51 cu. ft./sec.

Overall efficiency: 86.4 %

Point	x	y	h	Conc.	Eff. (%)
38	1.0	-2.75	0.125	0.00524	11.3
39	1.0	-2.25	0.125	0.01426	37.8
40	1.0	-1.75	0.125	0.01482	39.4
41	1.0	-0.75	0.125	0.01862	50.5
42	1.0	0.25	0.125	0.02460	68.0
43	1.0	1.25	0.125	0.02339	64.5
44	1.0	2.25	0.125	0.02237	61.5
45	1.0	2.75	0.125	0.02318	63.9
46	-3.0	0.0	0.125	0.01601	42.8
47	-2.0	0.0	0.125	0.01543	41.1
48	-1.0	0.0	0.125	0.01617	43.2
49	0.0	0.0	0.125	0.01606	42.9
50	1.0	0.0	0.125	0.01339	35.1
51	2.0	0.0	0.125	0.01921	52.2
52	3.0	0.0	0.125	0.01664	44.6
53	-3.0	0.0	0.375	0.02141	58.7
54	-2.0	0.0	0.375	0.02116	58.6
55	-1.0	0.0	0.375	0.02371	65.7
56	0.0	0.0	0.375	0.02395	66.1
57	1.0	0.0	0.375	0.02217	60.9
58	2.0	0.0	0.375	0.02075	56.8
59	0.0	0.0	1.5	0.02978	83.2
60	1.0	0.0	1.5	0.03077	86.1
61	2.0	0.0	1.5	0.03114	87.2
62	3.0	0.0	1.5	0.02412	66.0
63	0.0	-1.7	1.5	0.03355	94.3
64	0.0	1.7	1.5	0.03308	92.9
65	1.0	-2.0	1.5	0.02847	79.4
66	1.0	2.0	1.5	0.03145	88.1
67	2.0	-2.0	1.5	0.02972	83.0

TABLE 13 (cont.)

CONCENTRATION PROFILE FOR WATER-CARBON DIOXIDE

Liquid flow rate: 1.0 gpm.

Gas flow rate: 0.51 cu. ft./sec.

Overall efficiency: 86.4 %

Point	x	y	h	Conc.	Eff. (%)
68	-2.0	0.0	3.0	0.02978	83.2
69	0.0	0.0	3.0	0.03103	86.7
70	2.0	0.0	3.0	0.02976	83.1
71	-1.0	-2.5	3.0	0.03014	84.3
72	-1.0	2.0	3.0	0.03072	86.0
73	2.0	-2.0	3.0	0.02931	81.8
74	2.0	2.0	3.0	0.02920	81.5
75	0.0	-1.7	3.0	0.02925	81.7
76	0.0	1.7	3.0	0.03376	94.9
77	-2.0	0.0	6.0	0.02836	79.0
78	0.0	0.0	6.0	0.03082	86.3
79	1.5	0.0	6.0	0.03151	88.2
80	1.5	-2.5	6.0	0.03014	84.3
81	1.5	2.5	6.0	0.02836	79.0
82	0.0	-1.7	6.0	0.02805	78.1
83	0.0	3.0	6.0	0.02920	81.5
84	-1.0	-2.7	6.0	0.02821	78.6
85	-1.0	0.0	6.0	0.02815	78.4
86	1.0	-2.7	6.0	0.02800	78.0
87	1.5	0.0	6.0	0.02910	81.2
88	-3.0	0.0	9.0	0.02831	78.9
89	0.0	0.0	9.0	0.02716	75.5
90	1.5	2.5	9.0	0.02779	77.4
91	1.5	-2.5	9.0	0.02857	79.7
92	-0.5	-3.0	9.0	0.02894	80.7
93	-1.5	2.5	9.0	0.02976	83.1

TABLE 14

CONCENTRATION PROFILE FOR WATER-CARBON DIOXIDE

Liquid flow rate: 2.0 gpm.

Gas flow rate: 0.315 cu. ft./sec.

Overall efficiency: 83.1 %

Point	x	y	h	Conc.	Eff. (%)
94	1.0	-2.75	0.125	0.00473	5.3
95	1.0	-2.25	0.125	0.01112	25.2
96	1.0	-1.75	0.125	0.01264	29.9
97	1.0	-0.75	0.125	0.01710	43.7
98	1.0	0.25	0.125	0.01629	41.2
99	1.0	1.25	0.125	0.02283	61.5
100	1.0	1.75	0.125	0.02511	68.8
101	-3.0	0.0	0.125	0.01507	39.4
102	-2.0	0.0	0.125	0.01810	44.3
103	-1.0	0.0	0.125	0.01659	39.6
104	0.0	0.0	0.125	0.01501	34.7
105	1.0	0.0	0.125	0.02098	53.1
106	2.0	0.0	0.125	0.01711	41.2
107	3.0	0.0	0.125	0.01716	41.4
108	-3.0	0.0	0.375	0.01965	51.6
109	-1.5	0.0	0.375	0.02055	54.4
110	0.0	0.0	0.375	0.02253	60.6
111	1.5	0.0	0.375	0.02283	61.5
112	-2.0	0.0	1.0	0.02831	75.7
113	1.0	0.0	1.0	0.02842	76.0
114	1.0	-2.5	1.0	0.02726	72.5
115	1.0	2.0	1.0	0.02805	74.9
116	0.0	-1.7	1.0	0.02569	67.6
117	0.0	1.7	1.0	0.02795	74.6
118	-3.0	0.0	3.0	0.02899	77.8
119	1.0	-2.5	3.0	0.02878	77.1
120	1.0	2.0	3.0	0.02899	77.8
121	0.0	0.0	9.0	0.02772	73.7
122	-1.5	0.0	9.0	0.02716	70.2
123	-1.5	-2.5	9.0	0.02872	75.4

TABLE 15

CONCENTRATION PROFILE FOR WATER-CARBON DIOXIDE

Liquid flow rate: 4.0 gpm.

Gas flow rate: 0.196 cu. ft./sec.

Overall efficiency: 39.2 %

Point	x	y	h	Conc.	Eff. (%)
131	-3.0	0.0	0.125	0.00664	6.0
132	-2.0	0.0	0.125	0.01344	27.6
133	-1.0	0.0	0.125	0.01606	36.0
134	0.0	0.0	0.125	0.01365	28.2
135	1.0	0.0	0.125	0.01292	25.9
136	2.0	0.0	0.125	0.00978	15.7
137	3.0	0.0	0.125	0.00805	10.1
142	-1.5	0.0	1.0	0.02240	56.5
143	1.5	0.0	1.0	0.02282	57.9
144	1.5	-2.5	1.0	0.02125	52.8
145	1.5	2.5	1.0	0.02334	59.6
146	0.0	-1.7	1.0	0.01989	48.4
147	0.0	1.7	1.0	0.02224	56.0
148	-3.0	0.0	4.0	0.02219	55.9
149	-1.5	0.0	4.0	0.02224	56.0
150	0.0	0.0	4.0	0.02287	58.0

TABLE 16

CONCENTRATION PROFILE FOR WATER-CARBON DIOXIDE

Liquid flow rate: 4.0 gpm.

Gas flow rate: 0.246 cu. ft./sec.

Overall efficiency: 58.0 %

Point	x	y	h	Conc.	Eff. (%)
124	1.0	-2.75	0.125	0.00524	6.8
125	1.0	-2.25	0.125	0.01107	25.0
126	1.0	-1.75	0.125	0.01320	31.6
127	1.0	-0.75	0.125	0.01776	45.8
128	1.0	0.25	0.125	0.01923	50.3
129	1.0	1.25	0.125	0.01872	48.8
130	1.0	2.75	0.125	0.02283	61.5
138	-3.0	0.0	0.375	0.01675	42.6
139	-1.5	0.0	0.375	0.01923	50.3
140	0.0	0.0	0.375	0.02055	54.4
141	1.5	0.0	0.375	0.01964	51.6

TABLE 17

CONCENTRATION PROFILE FOR GLYCOL-CARBON DIOXIDE

Liquid flow rate: 1.0 gpm.

Gas flow rate: 0.44 cu. ft./sec.

Overall efficiency: 57.1 %

Point	x	y	h	Conc.	Eff. (%)
1	1.0	-2.75	0.125	0.01700	25.0
2	1.0	-1.25	0.125	0.02191	42.5
3	1.0	0.25	0.125	0.02410	50.3
4	1.0	2.25	0.125	0.02910	68.4
5	3.0	0.0	1.5	0.03070	73.9
6	0.0	0.0	1.5	0.02990	71.1
7	0.0	-1.7	1.5	0.02800	64.2
8	1,0	0.0	4.0	0.02800	64.2
9	-1.5	0.0	4.0	0.02911	68.4
10	0.0	-1.7	4.0	0.02679	60.0

4. Calculated Results for N_{tL}, k_La, and h_L.

Tables 18 to 22 contain the calculated values of N_{tL}, k_La, and h_L for the four hole sizes and glycol. For the water-carbon dioxide system, the number of transfer units, N_{tL}, were calculated by means of equation 9. For the glycol-carbon dioxide system, the number of transfer units were calculated by means of equation 37. The mass transfer coefficients, k_La, were calculated using equation 8. The lengths of transfer units were calculated by means of equation 12.

TABLE 18

CALCULATED RESULTS FOR WATER - CARBON DIOXIDE USING 0.125 INCH DIAMETER HOLES

POINT	NUMBER OF TRANSFER UNITS			MASS TRANSFER COEFFICIENT			LENGTH OF TRANSFER UNIT		
LIQUID RATE IS 0.1 U.S.G.P.M.									
2	0.986	1.013	1.103	289.9	297.9	324.2	0.5070	0.4934	0.4535
3	1.217	1.181	1.419	214.7	208.3	250.3	0.4107	0.4234	0.3524
4	1.297	1.294	1.523	227.1	226.5	268.7	0.3884	0.3895	0.3282
5	0.919	0.830	1.053	135.1	122.0	154.7	0.5442	0.6023	0.4750
6	0.781	0.936	0.842	114.8	137.7	123.7	0.6403	0.5339	0.5941
LIQUID RATE IS 0.2 U.S.G.P.M.									
7	0.947	0.552	0.0	417.5	243.3	0.0	0.5281	0.9064	0.0
8	1.687	1.687	1.561	496.1	496.1	458.8	0.2963	0.2963	0.3204
9	1.698	1.423	1.496	599.1	502.0	527.8	0.2944	0.3514	0.3342
10	1.715	1.799	1.609	504.2	526.2	473.2	0.2916	0.2794	0.3107
11	1.523	1.595	1.519	358.3	375.0	357.2	0.3282	0.3136	0.3292
12	2.002	1.461	1.655	392.5	286.4	324.5	0.2497	0.3422	0.3020
13	1.423	2.079	1.609	295.3	431.5	334.0	0.3514	0.2404	0.3107
LIQUID RATE IS 0.5 U.S.G.P.M.									
14	0.957	0.618	0.0	1688.3	1090.2	0.0	0.5224	0.8090	0.0
15	1.839	1.732	2.096	1247.6	1174.8	1421.8	0.2719	0.2887	0.2386
16	1.845	1.778	1.704	1085.0	1045.4	1001.8	0.2710	0.2812	0.2935
17	1.808	1.833	1.808	1328.8	1346.9	1328.8	0.2766	0.2729	0.2766
18	1.864	2.180	1.966	1096.2	1282.1	1156.1	0.2682	0.2293	0.2543
19	1.924	2.137	2.375	998.3	1108.8	1232.3	0.2599	0.2340	0.2105
20	1.732	1.666	1.959	954.5	918.4	1079.9	0.2887	0.3001	0.2552
21	2.006	2.216	1.924	739.3	781.9	678.8	0.2386	0.2256	0.2599
22	1.478	1.952	2.146	543.3	690.4	788.5	0.3382	0.2701	0.2330

TABLE 18 (continued)

CALCULATED RESULTS FOR WATER - CARBON DIOXIDE USING 0.125 INCH DIAMETER HOLES

POINT	NUMBER OF TRANSFER UNITS			MASS TRANSFER COEFFICIENT			LENGTH OF TRANSFER UNIT		
	LIQUID RATE IS 1.0 U.S.G.P.M.								
23	1.248	0.0	0.0	1376.2	0.0	0.0	0.4006	0.0	0.0
24	1.390	1.528	1.604	1226.2	1347.6	1415.1	0.3596	0.3273	0.3116
25	1.542	1.698	1.650	1236.2	1361.7	1323.2	0.3243	0.2944	0.3030
26	1.772	1.945	0.0	1488.4	1549.9	0.0	0.2822	0.2710	0.0
27	2.002	1.802	1.897	1412.9	1271.4	1338.6	0.2497	0.2775	0.2636
28	1.772	1.784	1.845	1116.3	1123.8	1162.5	0.2822	0.2803	0.2710
29	1.661	1.904	1.911	1126.7	1291.7	1296.2	0.3011	0.2626	0.2617
30	1.858	2.386	2.477	919.4	1169.1	1213.7	0.2691	0.2096	0.2019
31	1.995	1.911	2.071	782.1	748.9	812.0	0.2506	0.2617	0.2414
	LIQUID RATE IS 2.0 U.S.G.P.M.								
32	0.633	0.0	0.0	971.0	0.0	0.0	0.7899	0.0	0.0
33	1.079	0.0	0.0	1654.8	0.0	0.0	0.4635	0.0	0.0
34	1.435	1.427	1.427	1875.7	1864.8	1864.8	0.3483	0.3504	0.3504
35	1.704	1.580	1.457	2003.6	1857.9	1713.1	0.2935	0.3165	0.3432
36	1.726	1.671	1.726	1902.9	1842.6	1902.9	0.2897	0.2992	0.2897
37	1.650	1.501	1.911	1306.2	1260.5	1604.9	0.3030	0.3332	0.2617
38	1.698	1.897	2.207	936.2	1045.8	1216.8	0.2944	0.2636	0.2265
39	1.920	1.784	2.096	987.9	968.2	1137.4	0.2747	0.2803	0.2386
40	1.981	1.814	2.017	1164.5	1066.6	1186.2	0.2525	0.2756	0.2478
	LIQUID RATE IS 3.0 U.S.G.P.M.								
41	1.067	0.914	0.976	2016.8	1727.1	1843.7	0.4686	0.5472	0.5126
42	1.546	1.790	1.732	909.3	1052.4	1018.2	0.3233	0.2794	0.2887

TABLE 18 (continued)

CALCULATED RESULTS FOR WATER – CARBON DIOXIDE USING 0.125 INCH DIAMETER HOLES

POINT	NUMBER OF TRANSFER UNITS			MASS TRANSFER COEFFICIENT			LENGTH OF TRANSFER UNIT		
	LIQUID RATE IS 4.0 U.S.G.P.M.								
44	0.939	0.911	0.942	1142.4	1108.6	1145.5	0.5325	0.5487	0.5310
43	0.944	0.928	0.947	1665.5	1460.3	1670.1	0.5296	0.6040	0.5281
45	1.317	1.259	1.162	929.1	888.2	819.6	0.3797	0.3972	0.4305
46	1.181	1.146	1.273	825.8	858.2	999.0	0.4234	0.4364	0.3928

TABLE 19

CALCULATED RESULTS FOR WATER - CARBON DIOXIDE USING 0.250 INCH DIAMETER HOLES

POINT	NUMBER OF TRANSFER UNITS			MASS TRANSFER COEFFICIENT			LENGTH OF TRANSFER UNIT		
LIQUID RATE IS 0.1 U.S.G.P.M.									
48	0.531	0.620	0.536	187.3	218.7	189.2	0.9416	0.8066	0.9326
49	0.514	0.719	0.0	181.4	253.8	0.0	0.9725	0.6949	0.0
50	0.367	0.426	0.294	107.8	125.3	83.4	1.3634	1.1732	1.7625
51	0.270	0.347	0.190	95.4	122.3	67.0	1.8484	1.4421	2.6323
52	0.481	0.435	0.305	141.5	128.0	89.7	1.0389	1.1483	1.6384
53	0.875	0.683	0.0	257.2	200.9	0.0	0.5716	0.7319	0.0
54	0.639	0.837	0.952	112.7	147.6	167.9	0.7829	0.5974	0.5253
55	0.082	0.167	0.094	12.1	24.6	12.4	6.0757	2.9898	5.9193
LIQUID RATE IS 0.2 U.S.G.P.M.									
57	1.510	1.501	1.523	710.1	705.9	716.5	0.3312	0.3332	0.3282
58	1.363	1.394	1.630	739.6	756.8	884.5	0.3670	0.3586	0.3068
59	1.478	1.585	1.374	521.6	559.1	484.9	0.3382	0.3155	0.3638
60	1.106	1.181	1.115	354.6	378.7	357.5	0.4522	0.4234	0.4485
61	1.103	1.103	1.076	353.6	353.6	345.1	0.4535	0.4535	0.4647
62	1.097	0.992	1.103	276.3	249.9	277.9	0.4559	0.5043	0.4535
63	1.097	1.103	1.121	257.9	259.3	263.6	0.4559	0.4535	0.4461

TABLE 19 (continued)

CALCULATED RESULTS FOR WATER - CARBON DIOXIDE USING 0.250 INCH DIAMETER HOLES

POINT	NUMBER OF TRANSFER UNITS			MASS TRANSFER COEFFICIENT			LENGTH OF TRANSFER UNIT		
LIQUID RATE IS 0.5 U.S.G.P.M.									
64	1.248	1.013	0.0	2202.0	1787.6	0.0	0.4006	0.4934	0.0
65	1.440	1.378	1.452	1587.3	1519.6	1601.3	0.3473	0.3628	0.3442
66	1.682	1.732	1.698	1348.7	1389.4	1361.7	0.2973	0.2887	0.2944
67	1.772	1.570	0.0	1562.9	1384.9	0.0	0.2822	0.3184	0.0
68	1.682	1.720	1.760	1483.5	1517.4	1552.5	0.2973	0.2906	0.2840
69	1.945	1.871	1.784	1429.5	1375.0	1311.1	0.2571	0.2673	0.2803
70	1.394	1.704	1.877	919.9	1001.8	1103.9	0.3586	0.2935	0.2663
71	1.877	1.945	2.025	1379.8	1429.5	1488.3	0.2663	0.2571	0.2469
72	1.640	0.0	0.0	723.2	0.0	0.0	0.3049	0.0	0.0
73	1.590	0.0	0.0	701.0	0.0	0.0	0.3145	0.0	0.0
LIQUID RATE IS 1.0 U.S.G.P.M.									
74	0.783	0.0	0.0	3453.3	0.0	0.0	0.6385	0.0	0.0
75	1.030	0.0	0.0	1397.7	0.0	0.0	0.4854	0.0	0.0
76	1.556	1.483	0.0	1614.5	1538.6	0.0	0.3214	0.3372	0.0
77	1.917	0.0	0.0	1537.3	0.0	0.0	0.2608	0.0	0.0
206	2.049	0.0	0.0	1806.3	0.0	0.0	0.2441	0.0	0.0
78	1.858	0.0	0.0	1424.9	0.0	0.0	0.2691	0.0	0.0
79	2.688	0.0	0.0	1756.3	0.0	0.0	0.1860	0.0	0.0
80	2.645	5.521	0.0	1505.1	3141.9	0.0	0.1890	0.0906	0.0
207	1.995	0.0	0.0	879.8	0.0	0.0	0.2506	0.0	0.0
81	1.709	1.809	0.0	574.3	607.5	0.0	0.2925	0.2766	0.0
82	1.973	0.0	0.0	696.2	0.0	0.0	0.2534	0.0	0.0

TABLE 19 (continued)

CALCULATED RESULTS FOR WATER - CARBON DIOXIDE USING 0.250 INCH DIAMETER HOLES

POINT	NUMBER OF TRANSFER UNITS			MASS TRANSFER COEFFICIENT			LENGTH OF TRANSFER UNIT		
	LIQUID RATE IS 2.0 U.S.G.P.M.								
83	0.374	0.0	0.0	1465.9	0.0	0.0	1.3370	0.0	0.0
84	1.457	1.287	1.529	2447.3	2162.8	2566.8	0.3432	0.3884	0.3273
208	1.778	0.0	0.0	1393.8	0.0	0.0	0.2812	0.0	0.0
85	1.640	1.645	1.760	1377.5	1381.9	1478.6	0.3049	0.3039	0.2840
86	1.519	1.720	1.645	878.3	995.0	951.4	0.3292	0.2906	0.3039
	LIQUID RATE IS 3.0 U.S.G.P.M.								
87	1.871	1.877	0.0	1455.9	1461.0	0.0	0.2673	0.2663	0.0
	LIQUID RATE IS 4.0 U.S.G.P.M.								
209	0.498	0.475	0.0	1755.5	1675.1	0.0	1.0049	1.0530	0.0
88	1.336	0.0	0.0	1291.0	0.0	0.0	0.3744	0.0	0.0

TABLE 20

CALCULATED RESULTS FOR WATER - CARBON DIOXIDE USING 0.500 INCH DIAMETER HOLES

POINT	NUMBER OF TRANSFER UNITS			MASS TRANSFER COEFFICIENT			LENGTH OF TRANSFER UNIT		
	LIQUID RATE IS 0.1 U.S.G.P.M.								
89	1.645	1.532	0.0	362.7	337.9	0.0	0.3039	0.3263	0.0
90	1.419	1.570	1.415	417.1	461.6	415.9	0.3524	0.3184	0.3534
91	1.363	1.217	1.378	240.4	214.7	243.1	0.3670	0.4107	0.3628
92	0.921	0.853	1.027	116.1	107.5	129.4	0.5427	0.5859	0.4867
93	0.722	0.926	0.709	63.6	81.7	62.6	0.6930	0.5398	0.7049
	LIQUID RATE IS 0.2 U.S.G.P.M.								
94	1.945	1.732	0.0	686.2	610.9	0.0	0.2571	0.2887	0.0
95	1.845	1.704	1.732	651.0	601.1	610.9	0.2710	0.2935	0.2887
96	1.519	1.877	1.625	412.1	509.5	440.9	0.3292	0.2663	0.3078
97	1.435	1.826	1.737	287.9	379.0	360.5	0.3483	0.2738	0.2878
98	1.162	1.229	0.0	215.7	227.9	0.0	0.4305	0.4073	0.0
99	1.152	1.070	1.266	184.7	171.6	203.0	0.4340	0.4673	0.3950
	LIQUID RATE IS 0.5 U.S.G.P.M.								
100	1.465	1.619	1.604	760.3	840.2	832.4	0.3412	0.3087	0.3116
101	1.614	1.614	1.698	949.3	949.3	998.6	0.3097	0.3097	0.2944
102	1.528	1.580	1.635	748.6	774.1	801.0	0.3273	0.3165	0.3059
103	1.671	1.519	1.802	702.0	637.8	756.8	0.2992	0.3292	0.2775
104	1.625	1.732	1.864	447.8	477.3	513.9	0.3078	0.2887	0.2682

TABLE 20 (continued)

CALCULATED RESULTS FOR WATER - CARBON DIOXIDE USING 0.500 INCH DIAMETER HOLES

POINT	NUMBER OF TRANSFER UNITS			MASS TRANSFER COEFFICIENT			LENGTH OF TRANSFER UNIT		
LIQUID RATE IS 1.0 U.S.G.P.M.									
105	1.047	0.919	0.0	1846.9	1620.8	0.0	0.4776	0.5442	0.0
106	1.295	1.339	1.411	1522.5	1575.1	1658.8	0.3862	0.3733	0.3545
107	1.470	1.427	0.0	1525.0	1480.8	0.0	0.3402	0.3504	0.0
108	1.556	1.635	1.635	1372.3	1441.9	1441.9	0.3214	0.3059	0.3059
109	1.505	1.693	1.743	983.3	1106.0	1138.7	0.3322	0.2954	0.2869
111	1.784	1.917	1.778	1123.8	1207.9	1120.0	0.2803	0.2608	0.2812
110	1.784	1.931	0.0	1165.4	1261.6	0.0	0.2803	0.2589	0.0
112	1.897	2.139	2.033	956.1	1072.8	1024.4	0.2636	0.2349	0.2460
113	1.537	1.590	1.743	521.4	539.3	591.3	0.3253	0.3145	0.2869
114	1.382	1.452	0.0	427.8	449.5	0.0	0.3617	0.3442	0.0
LIQUID RATE IS 2.0 U.S.G.P.M.									
115	0.642	0.717	0.0	1416.6	1582.0	0.0	0.7783	0.6969	0.0
116	0.870	1.005	0.926	1461.4	1688.6	1556.3	0.5748	0.4975	0.5398
117	1.073	1.115	1.197	1455.9	1512.6	1624.7	0.4660	0.4485	0.4176
118	1.470	1.501	1.687	1481.4	1512.6	1700.9	0.3402	0.3332	0.2963
119	1.709	1.939	0.0	1340.1	1441.7	0.0	0.2925	0.2719	0.0
120	1.904	1.959	1.845	1033.3	1063.3	1001.5	0.2626	0.2552	0.2710

TABLE 20 (continued)

CALCULATED RESULTS FOR WATER – CARBON DIOXIDE USING 0.500 INCH DIAMETER HOLES

POINT	NUMBER OF TRANSFER UNITS			MASS TRANSFER COEFFICIENT			LENGTH OF TRANSFER UNIT		
LIQUID RATE IS 3.0 U.S.G.P.M.									
121	1.221	1.394	0.0	760.0	868.1	0.0	0.4096	0.3586	0.0
122	1.022	1.091	0.0	587.7	627.4	0.0	0.4894	0.4584	0.0
LIQUID RATE IS 4.0 U.S.G.P.M.									
123	0.591	0.697	0.0	1096.6	1294.5	0.0	0.8466	0.7172	0.0
124	0.744	0.693	0.0	1641.5	1528.4	0.0	0.6716	0.7213	0.0
125	1.013	0.919	0.965	752.7	682.4	716.7	0.4934	0.5442	0.5182

TABLE 21

CALCULATED RESULTS FOR WATER - CARBON DIOXIDE USING 1.000 INCH DIAMETER HOLES

POINT	NUMBER OF TRANSFER UNITS			MASS TRANSFER COEFFICIENT			LENGTH OF TRANSFER UNIT		
	LIQUID RATE IS 0.1 U.S.G.P.M.								
127	1.374	1.505	1.698	242.4	265.5	299.6	0.3638	0.3322	0.2944
128	1.207	1.402	1.306	177.5	206.2	191.9	0.4141	0.3565	0.3830
129	1.635	1.814	1.570	240.3	266.7	230.8	0.3059	0.2756	0.3184
130	1.284	1.211	1.266	174.2	164.3	171.8	0.3895	0.4130	0.3950
	LIQUID RATE IS 0.2 U.S.G.P.M.								
131	1.496	1.394	1.324	1055.7	983.8	934.4	0.3342	0.3586	0.3776
132	1.363	1.614	1.457	480.7	569.6	513.9	0.3670	0.3097	0.3432
133	1.852	1.630	1.698	653.2	574.9	599.1	0.2701	0.3068	0.2944
134	1.877	0.0	0.0	602.1	0.0	0.0	0.2663	0.0	0.0
135	1.784	2.207	1.945	629.3	778.7	686.2	0.2803	0.2265	0.2571
136	1.778	1.826	1.945	522.7	536.9	571.8	0.2812	0.2738	0.2571
137	1.570	1.287	1.390	461.6	378.5	408.7	0.3184	0.3884	0.3596
	LIQUID RATE IS 0.5 U.S.G.P.M.								
138	1.501	1.461	0.0	1102.9	1073.8	0.0	0.3332	0.3422	0.0
139	1.252	1.415	1.228	798.6	901.3	773.4	0.3994	0.3534	0.4073
140	1.415	1.532	1.435	734.0	795.1	744.8	0.3534	0.3263	0.3483
141	1.661	1.799	1.845	976.5	1052.4	1085.0	0.3011	0.2794	0.2710
142	1.726	1.556	0.0	951.4	857.7	0.0	0.2897	0.3214	0.0
143	1.692	1.650	1.908	989.0	970.4	1063.0	0.2973	0.3030	0.2766
144	1.666	1.645	1.732	734.7	725.5	763.6	0.3001	0.3039	0.2887

TABLE 21 (continued)

CALCULATED RESULTS FOR WATER - CARBON DIOXIDE USING 1.000 INCH DIAMETER HOLES

POINT	NUMBER OF TRANSFER UNITS			MASS TRANSFER COEFFICIENT			LENGTH OF TRANSFER UNIT		
	LIQUID RATE IS 1.0 U.S.G.P.M.								
145	0.997	1.000	1.016	1172.4	1175.6	1194.9	0.5015	0.5002	0.4921
146	1.431	1.431	1.709	1402.7	1402.7	1675.1	0.3493	0.3493	0.2925
147	1.609	1.666	1.945	1419.5	1469.4	1715.4	0.3107	0.3001	0.2571
148	1.737	1.590	1.704	1702.5	1557.8	1669.7	0.2878	0.3145	0.2935
150	1.917	1.839	1.959	1200.8	1247.6	1329.1	0.2608	0.2719	0.2552
149	2.313	2.244	0.0	1699.8	1649.6	0.0	0.2162	0.2228	0.0
151	2.056	2.146	0.0	725.3	757.0	0.0	0.2432	0.2330	0.0
	LIQUID RATE IS 2.0 U.S.G.P.M.								
152	0.931	0.894	0.853	1564.8	1502.0	1433.6	0.5368	0.5593	0.5859
153	1.324	1.355	1.280	1730.4	1770.3	1672.7	0.3776	0.3691	0.3906
154	1.146	1.343	1.306	1554.6	1822.7	1771.6	0.4364	0.3722	0.3830
155	1.671	1.877	1.487	1684.7	1892.3	1499.1	0.2992	0.2663	0.3362
156	1.599	1.645	1.604	1752.6	1803.7	1768.9	0.3145	0.3039	0.3116
157	1.604	1.958	2.010	1068.0	1236.7	1337.9	0.3116	0.2691	0.2488
	LIQUID RATE IS 3.0 U.S.G.P.M.								
158	0.858	0.911	0.977	1513.5	1607.5	1547.2	0.5827	0.5487	0.5701
159	1.332	1.259	1.370	939.7	888.2	967.0	0.3754	0.3972	0.3649

TABLE 21 (continued)

CALCULATED RESULTS FOR WATER - CARBON DIOXIDE USING 1.000 INCH DIAMETER HOLES

POINT	NUMBER OF TRANSFER UNITS			MASS TRANSFER COEFFICIENT			LENGTH OF TRANSFER UNIT		
LIQUID RATE IS 4.0 U.S.G.P.M.									
160	0.485	0.533	0.0	1899.3	2088.3	0.0	1.0320	0.9386	0.0
161	0.779	0.0	0.0	2197.8	0.0	0.0	0.6421	0.0	0.0
162	1.211	1.207	1.302	928.5	926.0	998.5	0.4130	0.4141	0.3840

TABLE 22

CALCULATED RESULTS FOR GLYCOL-CARBON DIOXIDE USING 0.250 INCH DIAMETER HOLES

POINT	NUMBER OF TRANSFER UNITS			MASS TRANSFER COEFFICIENT			LENGTH OF TRANSFER UNIT		
	LIQUID RATE IS 0.5 U.S.G.P.M.								
1	0.885	0.944	0.0	459.3	489.6	0.0	0.5648	0.5298	0.0
2	1.123	1.170	0.0	521.4	543.3	0.0	0.4451	0.4272	0.0
3	1.109	1.116	1.120	575.5	579.1	580.9	0.4508	0.4480	0.4465
4	1.271	1.159	0.0	590.0	538.2	0.0	0.3934	0.4313	0.0
5	1.304	1.422	0.0	574.9	627.0	0.0	0.3835	0.3517	0.0
6	1.589	1.320	0.0	700.6	582.3	0.0	0.3147	0.3787	0.0
7	1.573	1.568	0.0	555.0	553.1	0.0	0.3179	0.3189	0.0
8	1.532	1.757	1.497	386.1	442.8	377.4	0.3263	0.2845	0.3339
	LIQUID RATE IS 1.0 U.S.G.P.M.								
9	0.596	0.551	0.573	526.1	486.1	505.8	0.8383	0.9073	0.8719
10	0.902	0.868	0.897	723.6	696.3	719.0	0.5540	0.5758	0.5576
11	1.009	0.0	0.0	889.7	0.0	0.0	0.4956	0.0	0.0
12	0.917	0.944	0.0	647.0	665.9	0.0	0.5453	0.5298	0.0
13	1.068	0.953	1.035	856.2	763.9	829.6	0.4682	0.5248	0.4833
14	1.178	1.141	1.312	769.5	745.5	857.2	0.4245	0.4382	0.3811
15	1.333	1.216	1.275	810.9	739.5	775.5	0.3750	0.4113	0.3922
16	1.308	0.0	0.0	659.2	0.0	0.0	0.3823	0.0	0.0
17	1.390	1.325	1.271	557.2	531.1	509.5	0.3597	0.3774	0.3934
	LIQUID RATE IS 2.0 U.S.G.P.M.								
18	0.412	0.359	0.0	538.1	468.6	0.0	1.2141	1.3942	0.0
19	0.512	0.0	0.0	644.8	0.0	0.0	0.9770	0.0	0.0
20	0.618	0.596	0.599	726.6	701.4	703.9	0.8093	0.8393	0.8353
21	0.704	0.723	0.0	496.6	510.1	0.0	0.7104	0.6916	0.0
22	0.857	1.009	0.897	339.8	399.9	355.5	0.5833	0.4956	0.5576

APPENDIX B

1. Calculation of Equilibrium Concentrations.
2. Chemical Analysis.
3. Sample Calculation of Efficiency.

1. Calculation of Equilibrium Concentrations.

A. Water

Let P be the total gas pressure in mm. of mercury. If P_w is the vapour pressure of water, then the partial pressure of carbon dioxide is $P-P_w$ assuming the carbon dioxide is saturated with water. For slightly soluble gases the equilibrium relationship can be expressed by Henry's law constant, H, over the temperature and pressure range used. Hence the mole fraction of carbon dioxide in the water is given by

$$x^* = \frac{P-P_w}{760\ H} \tag{46}$$

where x^* has the units of $\frac{\text{moles of } CO_2}{\text{moles of } CO_2 + \text{moles of water}}$

If the moles of carbon dioxide is much less than that of water one can assume that x^* = (moles of CO_2)/(moles of water) and hence the equilibrium concentration is given by

$$c^* = \frac{55.5\ (P-P_w)}{760\ H} \tag{47}$$

where the units of c^* are moles of carbon dioxide per litre of solution. If one assumes different temperatures and total pressures and using values of P_w (41) and H (32), values of c^* can be calculated. These values of c^*, temperature, and pressure are plotted in Figure 45 for easy interpolation.

B. Glycol

The saturated values of carbon dioxide in aqueous glycol were obtained at 77°F. and 760 mm. of mercury (50) and corrected by assuming the ideal gas law.

$$c_2^* = c_1^*\ (537\ P_2)/(460 + T_2)(760) \tag{48}$$

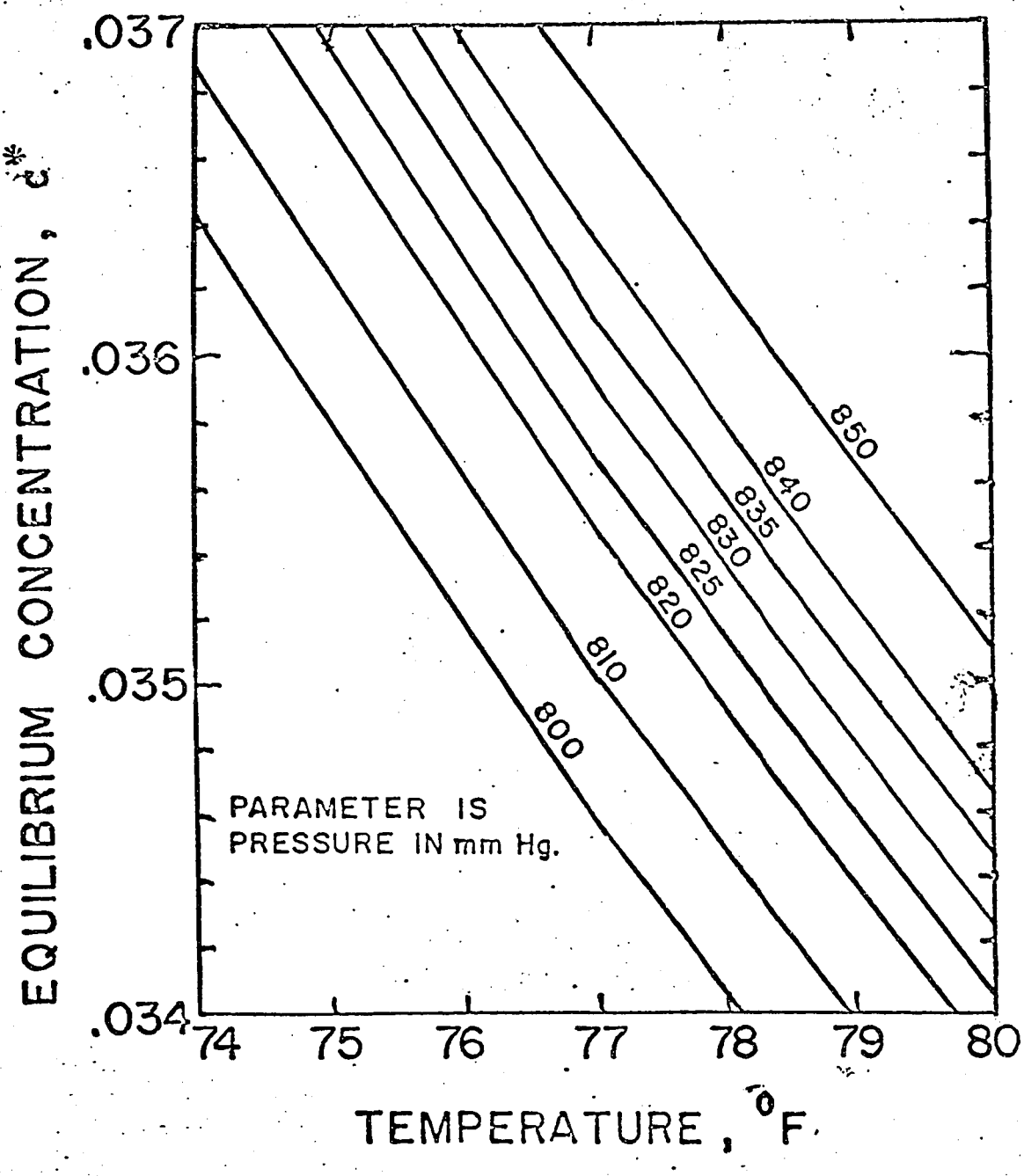

Figure 45. Equilibrium Concentrations for the Water and Carbon Dioxide System

2. Chemical Analysis.

A. Water

A known volume of sample was immediately put into a measured amount of a barium hydroxide solution. The carbon dioxide reacted with the barium hydroxide according to the reaction

$$CO_2 + Ba(OH)_2 = BaCO_3 + H_2O \qquad (49)$$

The barium carbonate immediately precipitates and the solution is covered and left to stand for 15 to 20 minutes. The excess barium hydroxide was back-titrated with hydrochloric acid to a phenolphthalein end point according to the reaction

$$Ba(OH)_2 + 2HCl = BaCl_2 + 2H_2O \qquad (50)$$

Barium chloride was added to prevent the undesirable side reaction

$$BaCO_3 + 2HCl = CO_2 + H_2O + BaCl_2 \qquad (51)$$

If one considers V_s the volume of sample of normality N_s, V_b the volume of barium hydroxide of normality N_b, and V_a the volume of hydrochloric acid of normality N_a, then from the stoichiometry of equations 49, 50, and 51 one obtains

$$N_s V_s = (N_b V_b - N_a V_a)/2 \qquad (52)$$

Since the volume of the sample was always 25 ml., then one has

$$c_{CO_2} = 0.02(N_b V_b - N_a V_a) \qquad (53)$$

where c_{CO_2} is the carbon dioxide concentration in gram moles per litre.

B. Glycol

Because of the low solubility product of barium hydroxide and barium carbonate in aqueous glycol, the barium carbonate does not precipitate in the viscous solution, and as a result sodium hydroxide was used. The analysis using sodium hydroxide was equal in accuracy to the analysis procedure using barium hydroxide. The reaction between carbon dioxide and sodium hydroxide is

$$CO_2 + 2NaOH = Na_2CO_3 + 2H_2O \qquad (54)$$

The excess hydroxide was back-titrated with hydrochloric acid according to the reactions

$$NaOH + HCl = NaCl\ H_2O \qquad (55)$$

$$Na_2CO_3 + HCl = NaHCO_3 + NaCl \qquad (56)$$

From stoichiometry

$$N_s V_s = N_b V_b - N_a V_a \qquad (57)$$

For a 25 ml. sample

$$c_{CO_2} = 0.04(N_b V_b - N_a V_a) \qquad (58)$$

3. Sample Calculation of Efficiency.

The following data is for the water-carbon dioxide system.

Temperature: 77.0°F

Total pressure: 835.1 mm. of mercury

Inlet sample: $V_s = 25.0$

$V_b = 2.0$ $N_b = 0.11884$

$V_a = 2.21$ $N_a = 0.08196$

Outlet sample: $V_s = 25.0$

$V_b = 15.0$ $N_b = 0.11884$

$V_a = 3.50$ $N_a = 0.08196$

The calculations to find the Murphree liquid efficiency are as follows;

From Figure 45, the equilibrium concentration is obtained

$c^* = 0.03615$ gram moles per litre

From equation 53, $c_{in} = 0.00113$ gram moles per litre

From equation 53, $c_{out} = 0.02991$ gram moles per litre

With these values the efficiency is obtained from equation 10;

$$E_{ML} = \frac{0.02991-0.00113}{0.03615-0.00113} x100$$

$$E_{ML} = \frac{0.02878}{0.03502} x100$$

$$E_{ML} = 82.3\ \%$$

APPENDIX C

1. Liquid rotameter calibrations.
2. Orifice plate calibration.
3. Gas flow rate calculations.
4. Equipment list.

1. Liquid rotameter calibrations.

Both high and low flow rates rotameters were calibrated by using the working fluids and measuring the mass flow rate at a known rotameter setting. One liquid was city water and the other a 92 weight percent aqueous solution of ethylene glycol. The purity of the glycol solution was determined using viscosity measurements (50). The calibration data were plotted in Figures 46 and 47 for interpolation. The data is also listed in Tables 23, 24, 25, and 26.

TABLE 23

LOW FLOW RATE ROTAMETER CALIBRATION - WATER

Rotameter Setting	ΔW lbs.	ΔT sec.	Flow Rate lbs./min.	Flow Rate gpm.
0.0	-	-	-	-
0.189	9.2	360	1.53	0.184
0.345	5.6	120	2.80	0.335
0.480	8.0	120	4.00	0.480
0.660	6.7	100	5.10	0.612
0.700	11.4	120	5.70	0.683
0.850	7.0	60	7.00	0.838
0.975	4.2	30	8.40	1.004
1.025	8.9	60	8.90	1.065

TABLE 24

HIGH FLOW RATE ROTAMETER CALIBRATION - WATER

Rotameter Setting	ΔW lbs.	ΔT sec.	Flow Rate lbs./min.	Flow Rate gpm.
0.0	-	-	-	-
0.95	7.45	60	7.45	0.894
1.54	12.70	60	12.70	1.523
2.05	17.40	60	17.40	2.090
2.52	20.80	60	20.80	2.490
3.05	20.70	50	24.80	2.970
3.80	16.00	30	32.00	3.840
4.70	19.70	30	39.40	4.720

TABLE 25

LOW FLOW RATE ROTAMETER CALIBRATION - GLYCOL

Rotameter Setting	ΔW lbs.	ΔT sec.	Flow Rate lbs./min.	Flow Rate gpm.
0.0	-	-	-	-
0.260	4.2	120	2.1	0.188
0.502	4.2	60	4.2	0.375
0.750	6.3	60	6.3	0.563
1.000	8.3	60	8.3	0.742

TABLE 26

HIGH FLOW RATE ROTAMETER CALIBRATION - GLYCOL

Rotameter Setting	ΔW lbs.	ΔT sec.	Flow Rate lbs./min.	Flow Rate gpm.
0.0	-	-	-	-
1.05	8.2	60	8.2	0.733
2.05	7.1	30	14.2	1.270
2.55	9.5	30	19.0	1.700
3.00	11.6	30	23.2	2.075
4.00	15.8	30	31.6	2.825

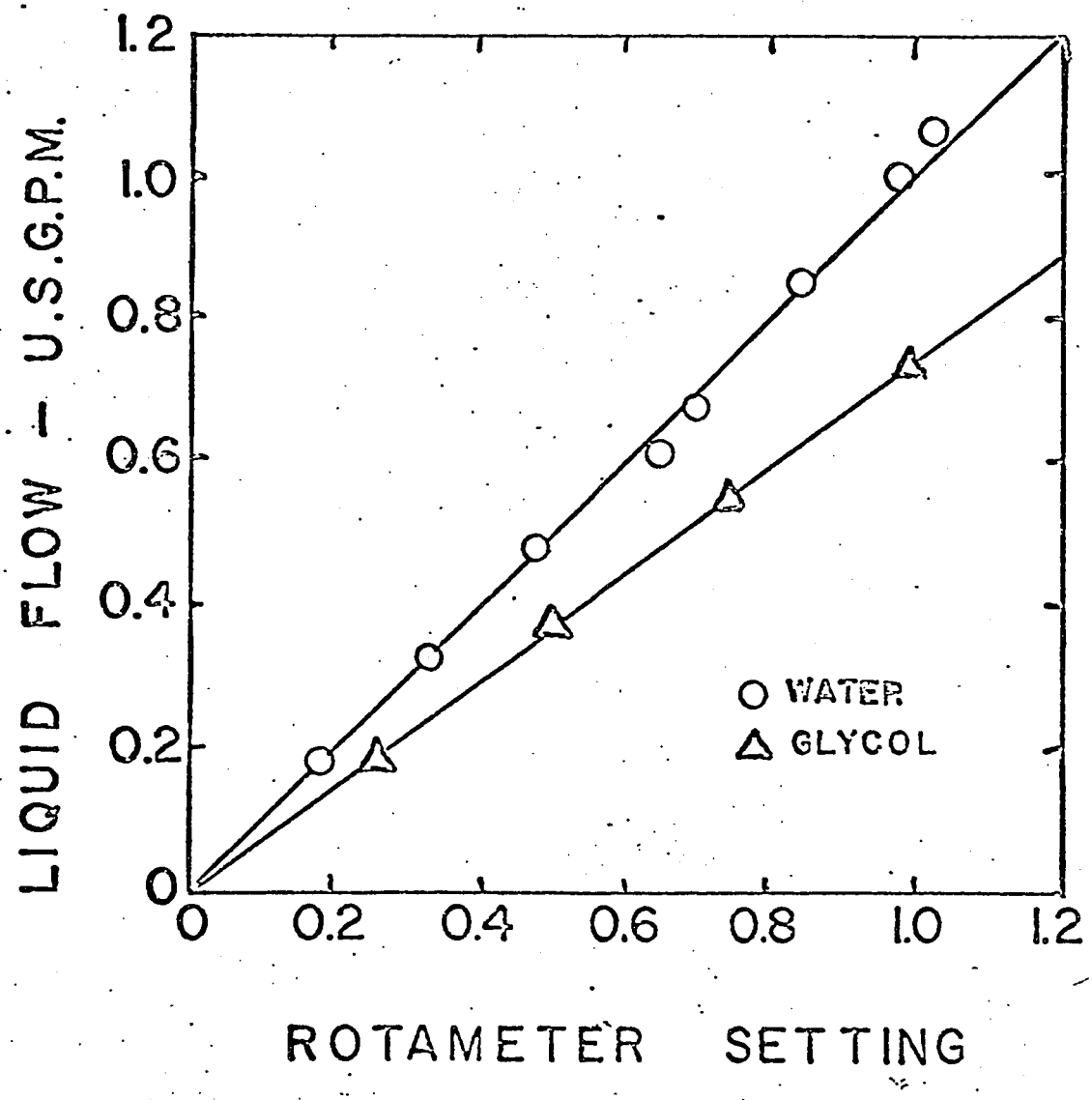

Figure 46. Low Flow Rate Rotameter Calibration

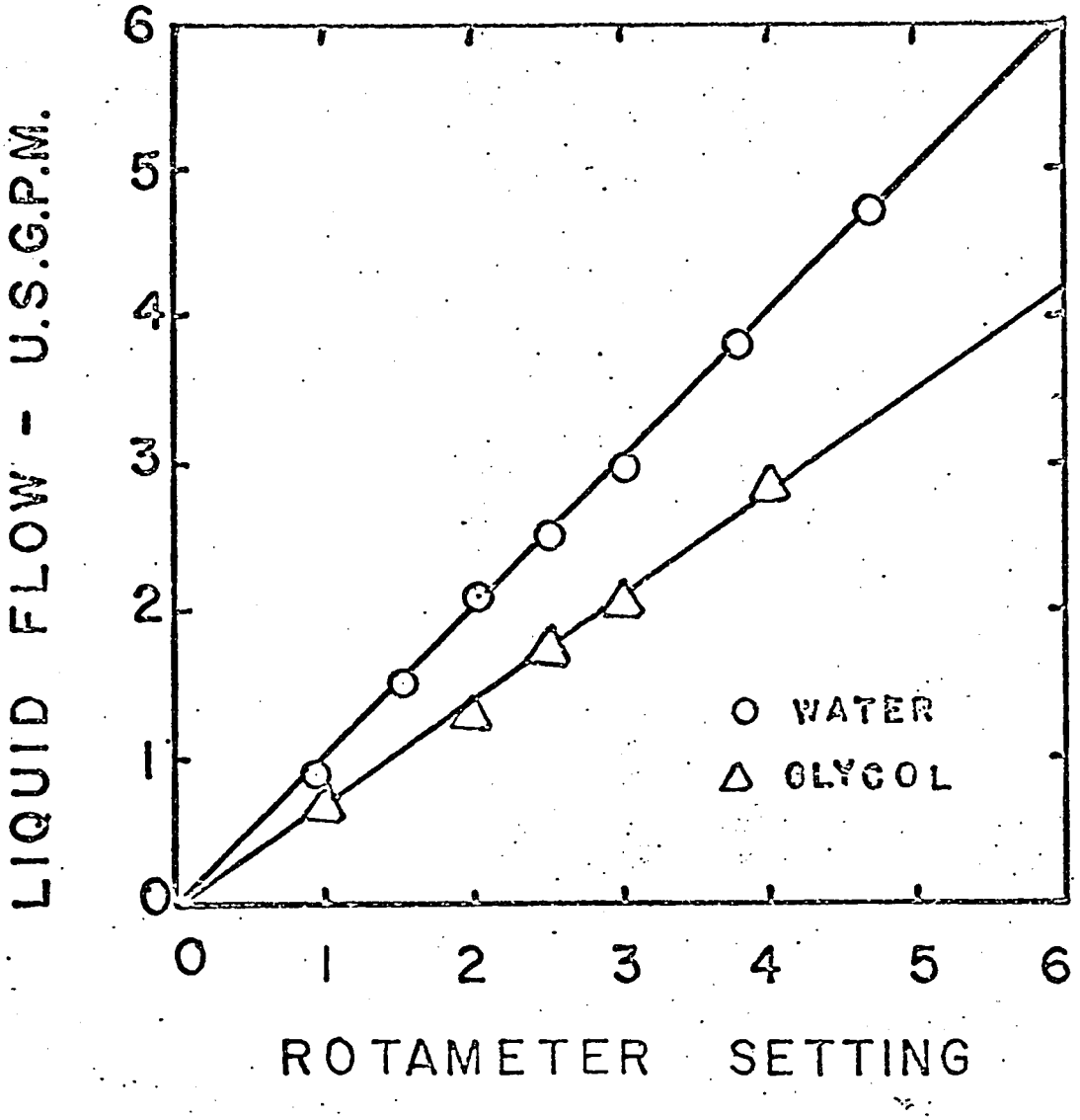

Figure 47. High Flow Rate Rotameter Calibration

2. Orifice plate calibration.

The orifice plate was calibrated by measuring the mass flow rate in the pipe and the pressure drop across the plate. The mass flow rate was obtained using water as a fluid. From the liquid flow rate and the water temperature, the Reynolds number was calculated based on the orifice diameter.

$$Re = \frac{\rho_L V_L D_O}{\mu_L} \tag{59}$$

The pressure drop was measured with water and mercury manometers and the orifice coefficient, C, calculated from the equation

$$V_L = C\,(2g\Delta h)^{\frac{1}{2}} \tag{60}$$

A dimensionless plot of Reynolds number and orifice coefficient was then constructed which holds for all fluids, both liquids and gases. Calibration data is listed in Table 27, and is plotted in Figure 48.

TABLE 27

ORIFICE PLATE CALIBRATION DATA

Δh	ΔW	ΔT	C	Re
in. water	lbs. water	sec.	-	-
0.10	17.7	60	0.718	3380
0.10	17.3	60	0.735	3500
0.20	24.8	60	0.718	4980
0.25	26.8	60	0.713	5130
0.28	14.2	30	0.710	5700
0.30	14.95	30	0.708	5920
0.33	15.5	30	0.706	6260
0.40	33.9	60	0.700	6880
0.70	22.1	30	0.688	8970
0.80	47.5	60	0.692	9050
0.60	20.6	30	0.691	9130
0.78	22.9	30	0.689	9260
0.87	24.7	30	0.688	10030
1.00	26.2	30	0.685	10920
1.20	28.8	30	0.685	11000
1.10	27.5	30	0.685	11140
1.10	27.7	30	0.688	11140
1.50	21.3	20	0.682	12980
1.80	68.4	60	0.668	13060
1.80	32.8	30	0.678	13230
1.70	22.6	20	0.674	13720
2.20	38.8	30	0.682	14820
2.10	37.2	30	0.670	15000
2.23	25.5	20	0.668	15620
2.50	40.4	30	0.666	16200
2.28	28.1	20	0.663	17230
4.05	34.1	20	0.660	18520
3.45	31.4	20	0.661	19240
4.75	36.4	20	0.655	22300
5.42	58.4	30	0.656	22310
6.55	42.8	20	0.665	23200
13.20	30.2	10	0.651	34500
13.55	60.8	20	0.647	34850
22.65	78.9	20	0.648	45200
40.70	52.8	10	0.647	60400
58.25	62.8	10	0.647	71946
73.80	70.7	10	0.646	81200
79.50	73.5	10	0.646	84200
96.30	81.2	10	0.648	92800

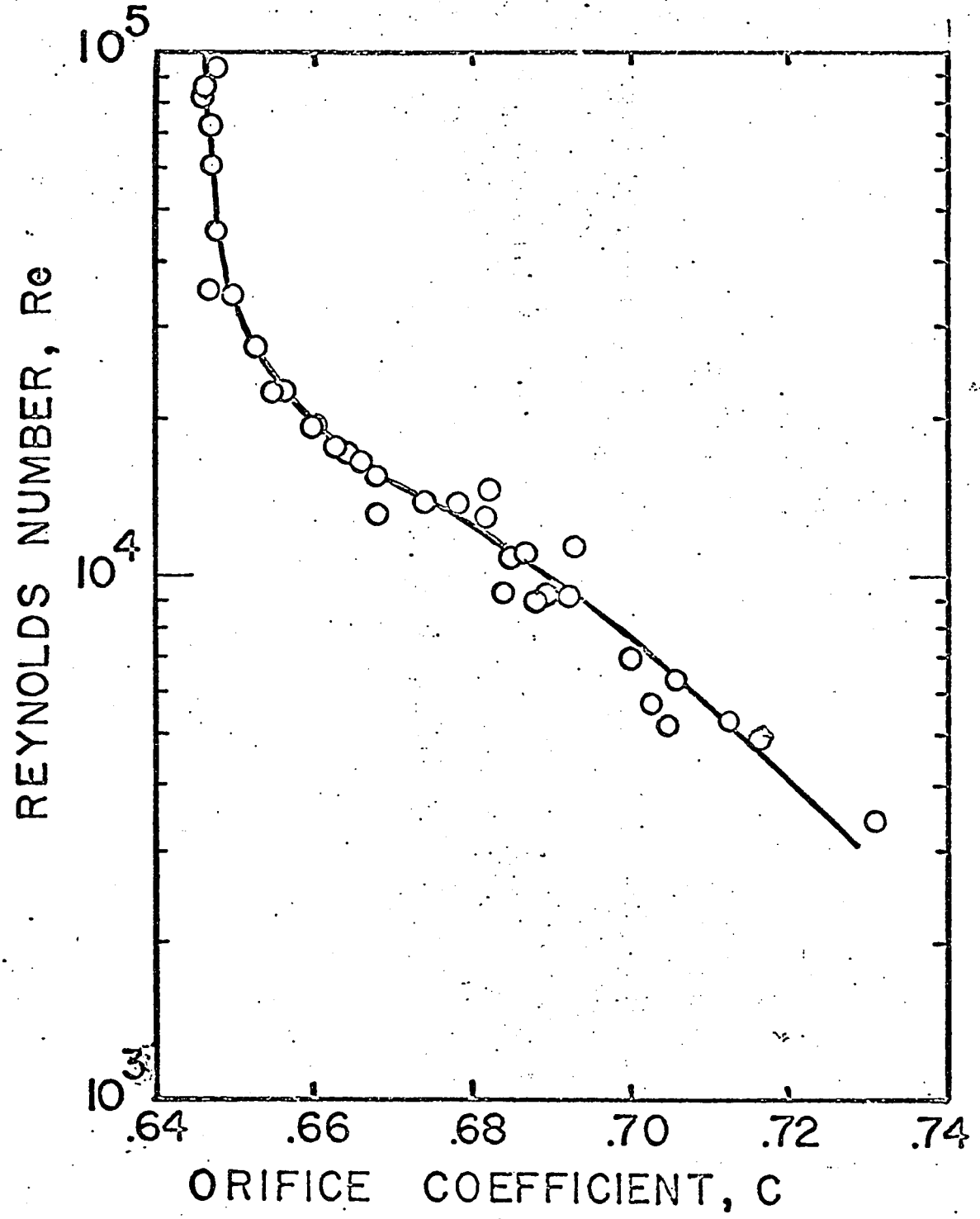

Figure 48. Orifice Plate Calibration Curve

3. Gas flow rate calculation.

Gas flow rate was measured by means of an orifice plate. The orifice plate, made of stainless steel, had an orifice diameter of 1.272 inches and the internal pipe diameter was 2.436 inches. Pressure taps were located one inch both upstream and downstream from the plate. The standard fifty upstream pipe diameters required for a uniform gas velocity profile was provided. The velocity of the gas is given by

$$V = C(2g\,\Delta h_w\,\rho_w/\rho_G)^{\frac{1}{2}} \tag{61}$$

The volumetric gas flow rate is given by

$$Q = 0.00545\ V\ D_O^2 \tag{62}$$

This is a trial and error problem. At 77°F. and 850 mm. of mercury pressure, for water saturated carbon dioxide one obtains a viscosity of 0.036018 lbs./(ft. hr.) and a density of 0.1229 lbs./(cu. ft.). From equation 59. the gas Reynolds number is

$$Re = \frac{\rho_L\ V\ D_O}{\mu_G} = 1302\ V \tag{63}$$

where V is the gas velocity in feet per second. From equation 61 one has

$$V = 57.15\ C\ \Delta h^{\frac{1}{2}} \tag{64}$$

Assuming an orifice pressure drop of 1-inch of water, one obtains from equation 64

$$V = 57.15\ C \tag{65}$$

Assume V = 40 ft./sec. and hence Re = 52200 from equation 63. From the orifice calibration curve one finds C = 0.648. This is substituted into equation 65 to obtain V = 37.1 ft./sec.. A new

Reynolds number is found to be 48400 from equation 63. A new orifice coefficient is found to be 0.648. Hence V = 37.1 ft./sec.. From equation 62, Q is 0.327 cu. ft./sec..

If the pressure drop across the orifice is assumed to be 9 inches of water, then Q would have been 0.978 cu. ft./sec.. The two values of Q and $\triangle h$ are plotted on log-log paper and joined by a straight line. Now the pressure is assumed to be 800 mm. of mercury and the process is repeated. The results are given in Table 28 and Figure 49. Pressures between 800 and 850 mm. of mercury are linearly interpolated. Small temperature changes do not effect the gas flow rate to any significant amount. Even if the carbon dioxide is assumed dry, the gas flow rate would change by only 2%. Hence, the graph was applicable to dry plate gas flow conditions. This method of finding gas flow rates is a common standard procedure (56).

TABLE 28

CALCULATION OF VOLUMETRIC GAS FLOW RATES

Δh	Total Pressure, mm of mercury	
inches of water	800	850
1.0	0.289	0.327
4.0	0.592	0.651
9.0	0.866	0.978

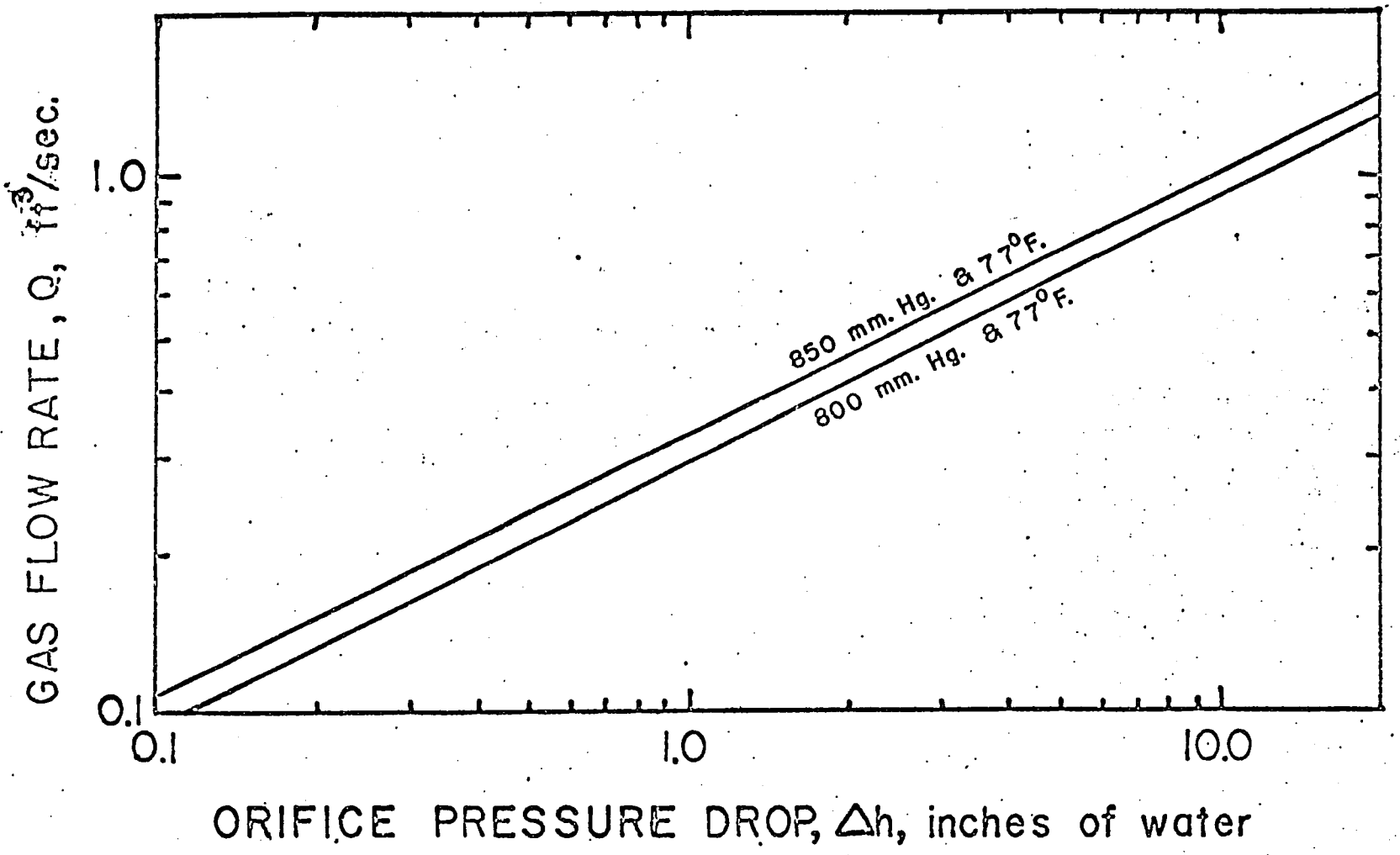

Figure 49. Gas Flow Rate versus Orifice Plate Pressure Drop

4. Equipment list.

1. Pump	Type: vacuum Manuf: Westinghouse Serial no: 14N5525 Pressure: 30 inches of water vacuum
2. Pump	Type: centrifugal Manuf: - Serial no: - Pressure: 50 psig maximum
3. Blower	Type: centrifugal Manuf: Robbins and Myers Serial no: 7D9837 Pressure: 14 inches of water maximum 3400 rpm., 1 hp.
4. Rotameter	Manuf: Brooks Instruments Tube size: R-8M 25-2 BR-½-27G10 Flow range: 0 to 1.0 gpm. S.G.=1.0
5. Rotameter	Manuf: Brooks Instruments Tube size: R-9M-25-3 Flow range: 0 to 5.0 gpm., S.G.=1.0